2003-05-08

Peptidyltransfer Reaction Catalyzed by the Ribosome and the Ribozyme: a Dissertation

Lele Sun
University of Massachusetts Medical School

PEPTIDYLTRANSFER REACTION CATALYZED BY THE RIBOSOME AND THE RIBOZYME

A Dissertation Presented

By

Lele Sun

Submitted to the Faculty of the

University of Massachusetts Graduate School of Biomedical Sciences, Worcester

In partial fulfillment of the requirements for the degree of

DOCTOR OF PHILOSOPHY

BIOCHEMISTRY AND MOLECULAR BIOLOGY

(May 8, 2003)

PEPTIDYL TRANSFER REACTION CATALYZED BY THE RIBOSOME AND THE RIBOZYME

A Dissertation Presented
By
Lele Sun

Approved as to style and content by:

_____
Dr. Tony Ip, Chair of Committee

_____
Dr. Sharon Huo, Member of Committee

_____
Dr. David Lambright, Member of Committee

_____
Dr. Craig Mello, Member of Committee

_____
Dr. Thoru Pederson, Member of Committee

_____
Dr. Biliang Zhang, Dissertation Mentor

_____
Dr. Anthony Carruthers, Dean of the Graduate School of Biomedical Sciences

Interdisciplinary Graduate Program
May 8, 2003

COPYRIGHTS

(*) These authors contribute equally to the work.

ACKNOWLEDGEMENTS

First of all, I would like to thank my mentor, Dr. Biliang Zhang for his comprehensive support and scientific instruction throughout the thesis research. I thank Dr. Zhiyong Cui for the excellent chemical synthesis of the compounds in all the experiments I have conducted. I thank Dr. Lei Zhang for his contribution to the synthesis of CCA-*NH*-Phe substrate. I thank Chunfang Li for helping me perform part of the kinetics experiments.

I thank the research advisory and defense committee for their helpful comments on my research. I thank Dr. Anna Delprato and Dr. Heather Cook for reading the whole manuscript and for their helpful comments.

Finally, I appreciate all the people that have helped me during the thesis research.

ABSTRACT

The "RNA world" hypothesis makes two predictions that RNA should have been able both to catalyze RNA replication and to direct protein synthesis. The evolution of RNA-catalyzed protein synthesis should be critical in the transition from the RNA world to the modern biological systems. Peptide bond formation is a fundamental step in modern protein biosynthesis. Although many evidence suggests that the ribosome is a ribozyme, peptide bond formation has not been achieved with ribosomal RNAs only. The goal of this thesis is to investigate whether RNA could catalyze peptide bond formation and how RNA catalyzes peptide bond formation. Two systems have been employed to approach these questions, the ribozyme system and the ribosome system. Ribozymes have been isolated by *in vitro* selection that can catalyze peptide bond formation using the aminoacyl-adenylate as the substrate. The isolation of such peptide-synthesizing ribozymes suggests that RNA of antiquity might have directed protein synthesis and bolsters the "RNA world" hypothesis. In the other approach, a novel assay has been established to probe the ribosomal peptidyltransferase reaction in the presence of intact ribosome, ribosomal subunit, or ribosomal RNA alone. Several aspects of the peptidyltransfer reaction have been examined in both systems including metal ion requirement, pH dependence and substrate specificity. The coherence between the two systems is discussed and their potential applications are explored. Although the ribozyme system might not be a reminiscence of the ribosome catalysis, it is still unique in other studies. The newly established assay for ribosomal peptidyltransferase reaction provides a good system to investigate the mechanism of ribosomal reaction and may have potential application in drug screening to search for the specific peptidyltransferase inhibitors.

TABLE OF CONTENTS

LIST OF FIGURES

LIST OF TABLES

Chapter I

Introduction

The idea that RNA might be capable of catalysis can be traced back to Woese (Woese, 1967), Crick (Crick, 1968), and Orgel (Orgel, 1968) hypothesis. Although the modern biological systems are based on DNA genomes and protein enzymes, RNA has a pervasive role in many fundamental cellular processes. RNA has remarkable features: it contains only four different "building blocks" that share similar chemical properties; it can fold into various tertiary structures that are highly tolerant of sequence variations; and it is easily soluble in water (Joyce, 2002). All these features make RNA suitable as the basis for a genetic system -- the "RNA world", in which all organisms stored genetic information in RNA, catalyzed chemical reactions with RNA, and carried out all the other necessities of life with RNA---- and RNA alone (Waldrop, 1992; Joyce, 2002). Although it may never be able to find the physical evidence of an RNA-based organism because the RNA world is likely to have been extinct for almost four billion years, the discovery of the self-splicing pre-rRNA in *Tetrahymena* and the cleavage of tRNA precursor by the RNA component within a ribonucleoprotein complex, RNase P, demonstrated the existence of modern catalytic RNAs, the *ribozymes* (Cech et al., 1981; Kruger et al., 1982; Guerrier-Takada et al., 1983). These findings greatly foster the "RNA world" hypothesis.

With the discovery of the initial catalytic RNAs, other naturally occurring ribozymes have been identified including group I intron, group II intron, hammerhead ribozyme, hairpin ribozyme, hepatitis delta virus (HDV) ribozyme, *Neuropora* Varkub

satellite ribozyme, RNase P, the ribosome and most recently, the spliceosome (Table 1-1, Doudna & Cech, 2002). Most of these ribozymes catalyze reactions at a phosphorus center (DeRose, 2002, Figure 1-1a, 1b) except the ribosome, which catalyzes peptidyltransfer reaction at a carbon center (DeRose, 2002, Figure 1-1c). Obviously, the reactions that are performed by the naturally occurring ribozymes are very limited. The catalytic capacity of RNA has been broadened by *in vitro* selection and *in vitro* evolution, which is also called the "test-tube evolution" (Ellington & Szostak, 1990; Joyce, 1989; Beaudry & Joyce, 1992).

In vitro selection and *in vitro* evolution methodology employs the integration of three processes: amplification, mutation and selection. Amplification is used to generate additional copies of the genetic information; mutagenesis is to introduce variability; and selection serves to reduce variability by excluding those molecules that do not conform to the imposed fitness criterion (Joyce, 1989). A general scheme for *in vitro* selection and *in vitro* evolution is shown in Figure 1-2. For *in vitro* selection, the initial RNA pool is *in vitro* transcribed from a pool of randomized DNA templates; then the RNA molecules are subjected to a selection for specific characteristics. A common technique used in the selection strategy as shown in Figure 1-2 is to covalently attach a biotin group on the RNA molecules with our desired features, thus such RNA molecules could be separated from others by flowing through a Neutravidin column. The selected RNA molecules are released from the column then converted to cDNA by reverse transcription. The cDNA will be amplified by PCR. At this step, DNA shuffling technique (Stemmer, 1994) or mutagenic PCR (Cadwell & Joyce, 1992) could be used to create diversity. Finally, the amplified DNA templates initiate the next selection cycle. *In vitro* evolution differs from

Table 1-1. Naturally occurring ribozymes and ribonucleoprotein enzymes

Ribozyme	Sequenced examples	Size (nt)	Activity (reaction product)
Hammerhead	11	40	Self-cleavage via transesterification (2', 3'-cyclic phosphate)
Hepatitis delta virus	2	90	
Hairpin	1	70	
Varkud satellite	1	160	
Group I intron	>1500	210	Self-splicing via transesterification (3'-OH)
Group II intron	> 700	500	
RNase P *	>500	300	Pre-tRNA processing via hydrolysis (3'-OH)
Spliceosome * (U2+U6 snRNAs)	70, 50	180, 100	RNA splicing via transesterification (3'-OH)
Ribosome * (23S rRNA)	>900	2,600	Peptidyltransfer (amide)

Number of sequenced examples is a snapshot as of 2002 and is influenced by DNA-sequencing strategies and database upkeep; it may provide a rough indication of relative abundance. RNAs in any group vary in size; the size provided here indicates the lower end of the length distribution for the natural examples. See www.rna.icmb.utexas.edu and www.jwbrown.mbio.ncsu.edu/RnaseP/.

Ribonucleoprotein enzymes. RNase P: bacterial and archaebacterial RNAs have the relevant activity in the absence of protein. Spliceosome: U2 and U6 small nuclear RNAs (snRNAs) alone show an activity related to the natural activity. Ribosome: no activity has yet been observed with protein-free, large-subunit rRNA.

Doudna, J. A. & Cech, T. R. (2002) The chemical repertoire of natural ribozymes. Nature 418, 222-228.

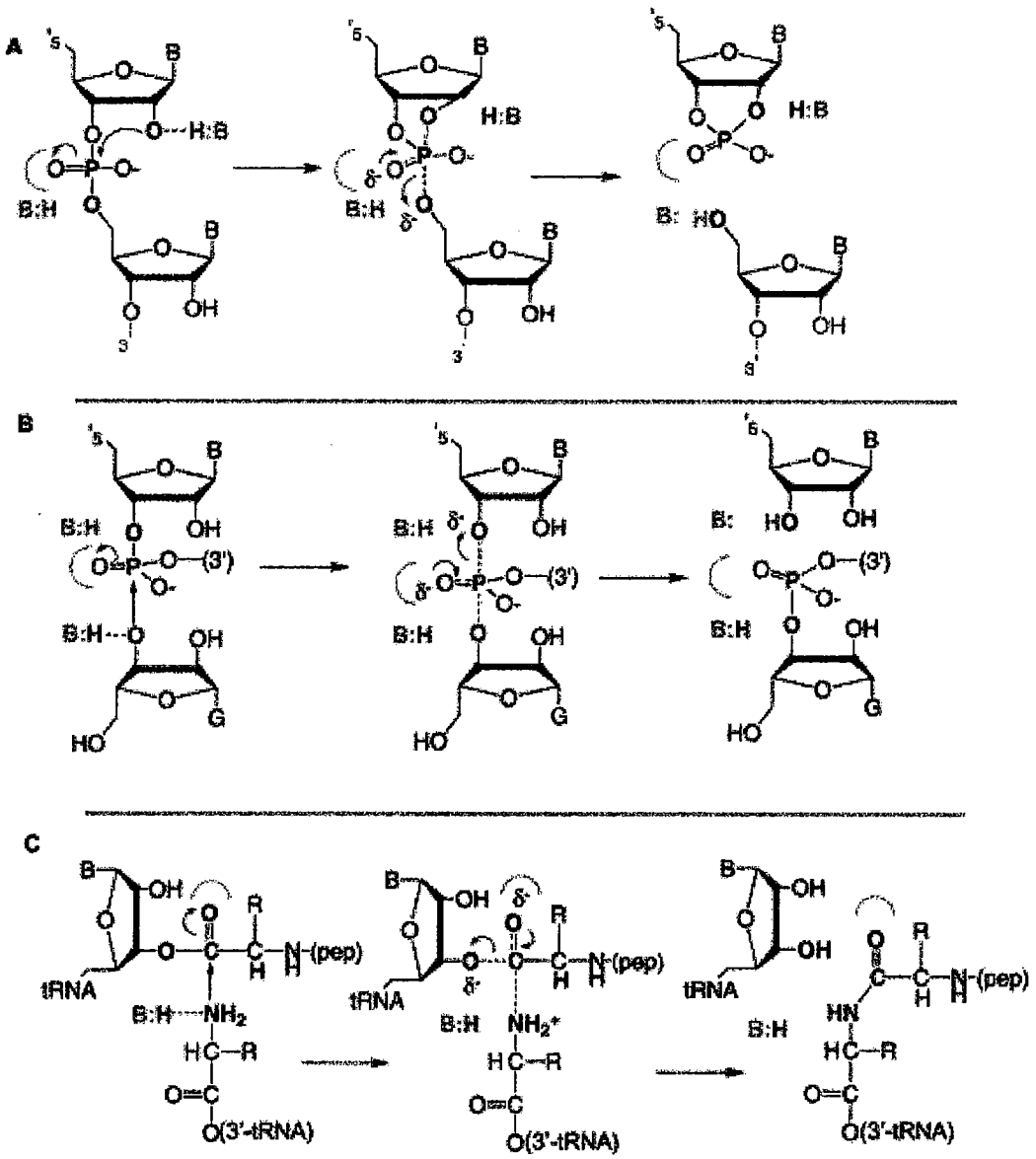

Figure 1-1. Reactions Catalyzed by Ribozymes
Reactions catalyzed by naturally occurring ribozymes require proton transfers that may be effected by general acid/base chemistry (denoted as A: or B:) or other factors established by the RNA environment (see Figure 4). Neutralization of negatively charged intermediates (pink arcs) may also be important. (a) Intramolecular phosphoryl transfer reaction catalyzed by one class of ribozymes including the hammerhead, hepatitis delta virus (HDV), hairpin, neurospora VS, and RNaseP RNAs. (b) The Group I and Group II introns catalyze attack of an extrinsic nucleophile, here shown as a guanosine, at a specific phosphodiester bond. (c) The ribosome has been proposed to contain an all-RNA active site for peptidyl transfer.

DeRose, V. J. (2002) Two Decades of RNA Catalysis. Chem. Biol. 9, 961-969.

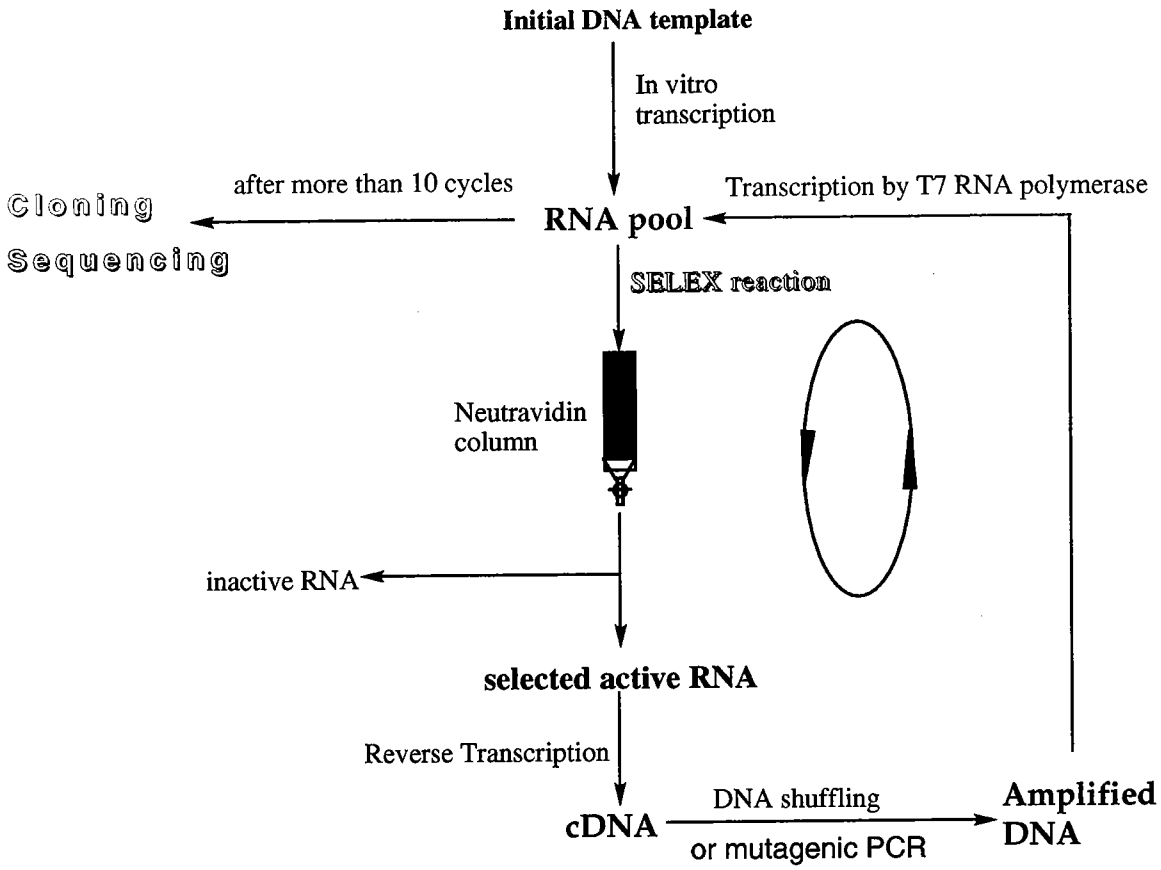

Figure 1-2. General scheme for *in vitro* selection and *in vitro* evolution. For *in vitro* selection, a pool of RNA molecules are *in vitro* transcribed from the initial DNA templates and subjected to a selection for specific characteristics. The selected RNA molecules with the desired characteristics are converted to cDNA by reversed transcription and subsequent DNA amplification is achieved by PCR. The amplified DNA templates will initiate the next selection cycle. *In vitro* evolution differs from *in vitro* selection in that it will introduce new mutations in the selection cycles. Thus, even if the desired ribozyme does not exist in the initial pools, suboptimal variants can be selected and, over the course of evolution, gain new mutations that result in the behavior of interest.

in vitro selection in that it will introduce new mutations in the selection cycles. Thus, even if the desired ribozymes does not exist in the initial pools, suboptimal variants can be selected and, over the course of evolution, gain new mutations that result in the behavior of interest (Tsang & Joyce, 1992). This method has provided powerful tools for isolating ribozymes that are capable of catalyzing various chemical and biochemical reactions in addition to those that are performed by naturally occurring ribozymes. Molecules have been isolated from pools of random RNA sequences that catalyze polynucleotide kinase activity (Lorsch et al., 1994), alkylation (Wilson et al., 1995), carbon-sulfur bond formation (Wecker et al., 1996), and the Diels-Alder reaction (Tarasow et al., 1997; Seelig et al., 1999). Aminoacyl transfer reactions can be catalyzed by ribozymes to form 3'-terminal (Illangasekare et al., 1995; 1999; Lee et al. 2000) or 2'-internal aminoacyl esters (Jenne et al., 1998), 5'-terminal esters or amide bonds (Lohse et al., 1996; Wiegand et al., 1997), and peptide bond formation (Zhang & Cech, 1997; Zhang & Cech, 1998; Sun et al., 2002). RNA can also catalyze nucleotide synthesis (Unrau et al., 1998). These findings have greatly expanded the catalytic versatility of RNA and provide support for the hypothesis that the first biological catalyst may have been an RNA molecule.

If a "RNA world" was a precursor to extant life, RNA must have been able both to catalyze RNA replication and to direct peptide synthesis (Schimmel & Henderson, 1994; Hager et al., 1996; Yarus, 1999; Joyce, 2002). Although natural ribozyme has not yet been found that could catalyze RNA polymerization, such ribozymes have been obtained by *in vitro* selection and evolution. Typical examples are the class I ligase (Bartel & Szostak, 1993; Ekland et al., 1995; Ekland & Bartel, 1996), hc ligase (Jaeger et

al., 1999; McGinness & Joyce, 2001), L1 ligase (Robertson & Ellington, 1999) and R3 ligase (Rogers & Joyce, 2001). These ribozymes could catalyze formation of 3', 5'-phosphodiester between NTPs. A recent report even described a ribozyme that catalyzes RNA polymerization by the successive addition of up to 14 nucleotides and can use any sequence of RNA as the template (Johnson et al., 2001). These findings illustrate the plausibility of RNA-catalyzed RNA replication.

Another important issue regarding RNA-based life is RNA-catalyzed protein synthesis. The evolution of RNA-catalyzed protein synthesis would have been a critical step in the transition from the RNA world to modern biological systems (Benner et al., 1989; Schimmel et al., 1993). In all living cells, the ribosome is the site where protein synthesis occurs, although non-ribosomal protein synthesis pathways also exist in some microorganisms (Marahiel et al., 1997; Von Dohren et al., 1997; Marahiel, 1997: Stachelhaus et al., 1998). Peptide bond formation is a fundamental step in protein synthesis. Accumulating biochemical, genetic, and crystal structural evidence suggest that the ribosomal peptidyltransfer reaction is catalyzed by the 23S rRNA within the large subunit of the ribosome. Depletion of most of the proteins in the 50S subunit didn't eliminate the peptidyltransferase activity (Noller et al., 1992), suggesting that the peptidyltransferase activity might reside in the ribosomal RNA. Mutations at conserved nucleotides in the central part region of domain V within 23S rRNA conferred antibiotic resistance to peptidyltransferase inhibitors (Rodriguez-Fonseca et al., 1995; Triman, 1999). Cross-linking and chemical footprinting experiments also indicate that 23S rRNA is the peptidyltransferase center where tRNA substrates bind and peptide bond formation occurs (Steiner et al., 1988; Moazed & Noller, 1989; Moazed & Noller, 1989). More

importantly, it is those wonderful ribosome crystal structures that provide views of what the peptidyltransferase center looks like and reveal the fact that the ribosome is a ribozyme (Yusupov et al., 2001; Ban et al., 2000; Cate et al., 1999; Ban et al., 1998; Blanchard & Puglisi, 2001; Harms et al., 2001). In one of the crystal structures of the large ribosomal subunit (Ban et al., 2000), the peptidyltransferase center is totally surrounded by the ribosomal RNAs (Figure 1-3a) and the closest protein atom is in 18 Å from the synthesized peptide bond (Figure 1-3b). Therefore, even in modern ribosome, RNA is the enzyme in promoting peptide bond formation.

However, unlike RNase P whose activity has been obtained in the presence of RNAs only (Guerrier-Takada et al., 1983), the ribosomal peptidyltransferase activity has not been achieved with protein free ribosomal RNAs. Researchers have shown peptidyltransferase activity with *in vitro* transcribed 23S rRNA domains (Nitta et al., 1998), however, further studies indicate that the formation of peptide bond was caused by the introduced alcohol in the reaction system (Khaitovich et al., 1999b; Nitta et al., 1999). Therefore, until now, no one has been able to acquire the ribosomal peptidyltransferase activity with ribosomal RNAs only. This phenomenon illustrates that although the ribosome is a ribozyme, it requires proteins to help the ribosomal RNAs to achieve the peptidyltransferase activity in the modern protein biosynthesis.

Although modern ribosomal RNAs do require proteins to achieve activity, RNAs in the ancient world might have existed to direct protein synthesis in a protein-free system. In exploring this possibility, ribozymes have been isolated *in vitro* from a randomized pool that can catalyze peptide bond formation in a protein-free system (Zhang & Cech, 1997). Peptide bond was formed between a phenylalanine tethered to

a

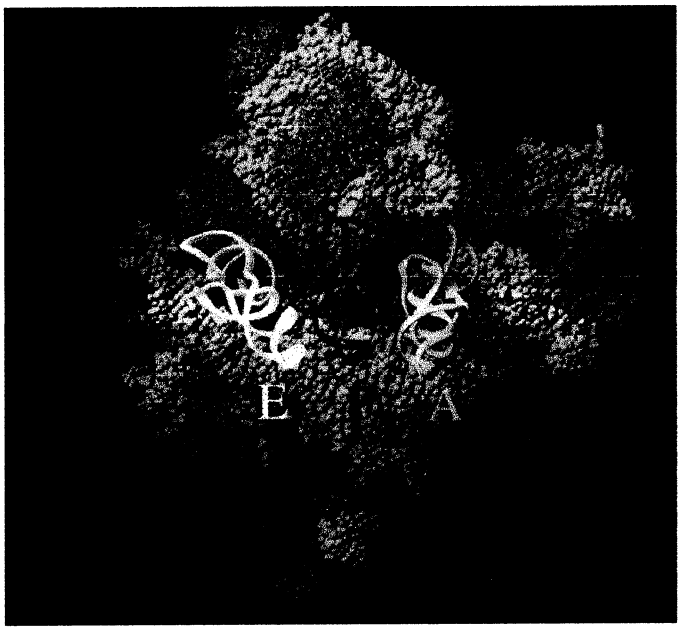

b

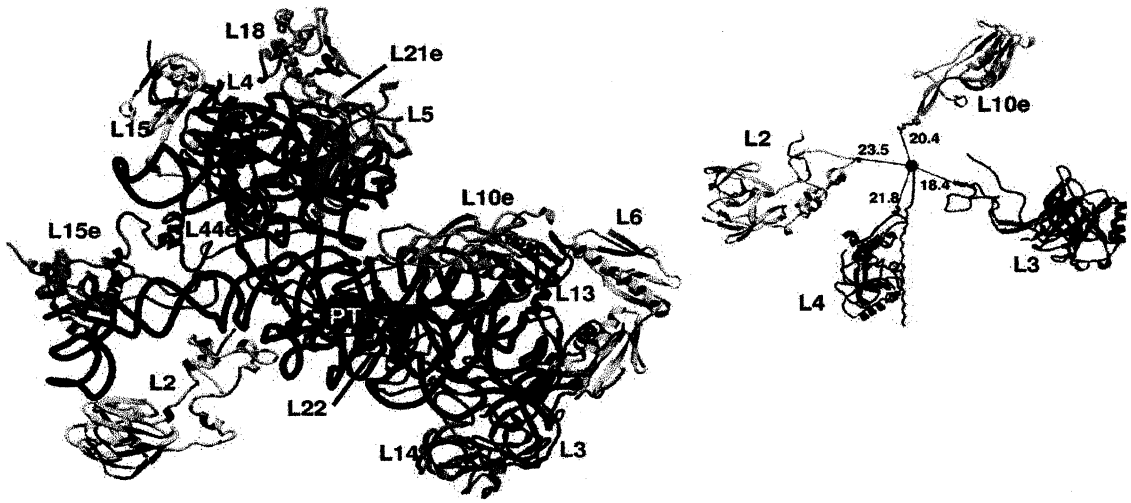

Figure 1-3. (a) A space-filling representations of the 50S ribosomal subunit with the 3 tRNA molecules. The proteins are in pink and the rRNA in blue. A backbone ribbon representation of the A-, P-, and E-sites are shown in yellow, red and white, respectively. (b) The closest approach of polypeptides to the peptidyltransferase active site marked by the Yarus inhibitor, CcdA-p-Puro. The left panel includes a coil representation of domain V RNA backbone in red, with the Yarus inhibitor in magenta in space-filling representation, and a ribbon backbone representation of 14 proteins that interact with that domain. Right panel is a view of the active site with the RNA removed.

Nissen et al. (2002) The structural basis of ribosome activity in peptide bond synthesis. Science 289, 920-930.

the 5' end of the ribozyme and a substrate mixture containing predominant *N*-biotinyl-methionyl-2'(3')-*O*-AMP. Characterization of this peptide bond-forming ribozyme has provided useful insights into the ribosomal peptidyltransferase reaction (Zhang & Cech, 1998). The isolation of the peptide bond-forming ribozyme not only fosters the RNA world hypothesis but also provides a good model itself for investigating the ribosomal peptidyltransferase activity.

In this work, I present the isolation and characterization of a new family of peptide bond-forming ribozyme. This ribozyme family is isolated by a similar strategy used for the previous isolation (Zhang & Cech, 1997), but employs a different substrate, *N*-biotinyl-methionyl-5'-adenylate. The significance of utilizing the aminoacyl-5'-adenylate as the substrate for peptide bond formation is evolutionary. Aminoacyl-adenylate is a universal intermediate for both ribosomal and nonribosomal processes of peptide biosynthesis (Bodley, 1988; Von et al., 1997; Marahiel et al., 1997). The isolation of such ribozymes suggests that RNA of antiquity might have existed in directing uncoded protein synthesis using aminoacyl-5'-adenylate and bolsters the "RNA world" hypothesis. Chapter III and Chapter IV describe the isolation of the new family of peptide-synthesizing ribozymes using the aminoacyl-5'-adenylate as the substrate, study of the secondary structure, and investigation of one family member (the R180 ribozyme) for its amino acid specificity, metal ion requirement and pH dependence. A mechanism is proposed in addressing how the peptide bond formation might occur in the R180-catalyzed reaction. Interestingly, a peptide-synthesizing ribozyme isolated from the previous selection (the C25 ribozyme, Zhang & Cech, 1997, 1998) can also utilize the

aminoacyl-5'-adenylate as the substrate in catalyzing peptide bond formation. Therefore, in Chapter III, the R180 ribozyme is compared with the C25 ribozyme for their specificity in substrate binding and their ability in catalyzing long peptide synthesis.

Another part of this work (Chapter V) is seemingly independent of but intrinsically related to the above chapters. Although peptide bond formation could be achieved by *in vitro* selected ribozymes, it is our ultimate goal to study the mechanism of peptidyltransfer reaction in the ribosome. Investigation of the ribosomal peptidyltransfer reaction has been hampered by technical problems associated with the complexity of the ribosome and its substrates (see details in Chapter V). Conventional assays in characterizing the ribosomal peptidyltransferase activity have many disadvantages. To overcome these obstacles and gain a better understanding of the mechanistic aspects of the ribosomal peptidyltransfer reaction, I have established a more convenient yet more specific assay in probing the ribosomal peptidyltransferase activity. Using this system, several important aspects of the ribosomal peptidyltransferase activity are examined including metal ion requirement, pH dependence, P-site substrate specificity and antibiotic inhibition.

Finally, Chapter II describes a new method in introducing a free thiol group into the 5' end of RNA. Many chemical entities containing thiol-reactive groups, such as fluorophores, proteins, nucleic acids, can be attached to the 5' end of RNA molecules by this method. This technique may have potential application in analysis and detection of RNA, mapping RNA-protein interactions, *in vitro* selection of novel catalytic RNAs and even gene array technology.

Chapter II

5'-Sulfhydryl-Modification of RNA

An Application in Studying RNA Structure and Function

RNA molecules play important roles in cellular processes including regulation, protein biosynthesis, RNA splicing, and retroviral replication. Site-specific substitution and derivatization provide powerful tools for studying RNA structure and function (Favre, 1990; Uhlmann and Peyman, 1990; Sontheimer and Steitz, 1993; Griffin et al., 1995; Cech and Herschlag, 1996; Dewey et al., 1996; Thomson et al., 1996; Allerson et al., 1997; Sontheimer, et al., 1997; Strobel and Shetty, 1997). Although solid phase chemical synthesis can be used to introduce functional groups at any specific position of oligonucleotides shorter than approximately 40 nucleotides (Gait et al., 1998), investigations of larger RNA molecules face a limited number of methodologies for site-specific modification and substitution. Several 5'-modifications of RNA molecules have been shown to have broad applications in studying RNA structures, mapping RNA-protein interactions, and in the *in vitro* selection of catalytic RNAs.

In vitro transcription reactions are widely used to synthesize RNA from recombinant DNA templates. RNA generated *in vitro* has been used for many applications, for example, RNA processing, translation, RNA-protein interactions, and the generation of ribozymes. Most of the *in vitro* selection methodologies employed the use of 5'-end-modified RNA transcripts. The inclusion of a disulfide bond is a desirable feature of many of these 5'-end modifications. A key functional group required for the selection scheme may be tethered distal to the disulfide bond. Following the isolations of

the desired RNA, reduction of the disulfide bond may be used to affect the liberation of the selected RNA in a soluble form suitable for reverse-transcription.

Phosphorothioate modification is one of the most popular methods for functionalizing the 5' terminus of RNA by a transcription or kinase reaction (Burgin & Pace, 1990; Joseph & Noller, 1996; Zhang & Cech, 1997). Fluorophores are the most attractive probes for RNA structure (Qin & Pyle, 1999) but only a low efficiency of conjugating terminal phosphorothioates with fluorophores has been achieved (Czworkowski et al., 1991). The sulfhydryl group is another special reactive group that can be incorporated into nucleic acids (Fidanaza et al., 1994; Musier-Forsyth & Schimmel, 1994; Sun et al., 1996; Cohen & Cech, 1997) as an alternative to the use of phosphorothioates. The thiol-reactive functional groups are primarily alkylating reagents, including haloacetamides, maleimides, benzylic halides, and bromomethylketones (Haugland, 1996). The thiol group demonstrates a unique property; that is, the thiol-disulfide exchange reaction. A pyridyl disulfide group is the most popular type of thiol-disulfide exchange functional group used in the construction of cross-linkers or modification reagents. A pyridyl disulfide will readily undergo an interchange reaction with a free sulfhydryl to yield a single mixed-disulfide product. Once a disulfide linkage is formed, it may be cleaved subsequently using disulfide reducing agents. Although 5'-phosphorothioate-RNA (5'-GMPS-RNA) can react with pyridyl disulfide to form a phosphorothioate sulfide compound (R-S-SPO_3-RNA) (Lorsch & Szostak, 1994; Macosko et al. 1999), a limitation of the thiophosphate disulfide product is the relative lability (Goody & Eckstein, 1971; Sengle et al., 2000). A free thiol group can be

introduced into the 5'-termini of RNA chemically using carbodiimide and cysteamine, but the phosphoramidate linkage is not very stable (Chu et al., 1986; Chu & Orgel, 1988).

To overcome these limitations, we have developed a method to introduce a 5'-terminal sulfhydryl group into the 5'-termini of RNA molecules by *in vitro* transcription. We have reported that a thiol group could be indirectly introduced into 5'-termini of RNA with an initiator, 5'-deoxy-5'-thioguanosine-5'-monophophorothioate (GSMP), by T7 RNA polymerase (Zhang et al., 2001a). The method requires an additional step of dephosphorylation of 5'-GSMP-RNA to produce 5'-HS-G-RNA. Herein, we report two new 5'-modified guanosines as initiator for T7 RNA polymerase to directly incorporate a free thiol to 5'-termini of RNA by *in vitro* transcription. The new initiators are *O*-[ω-sulfhydryl-bis(ethylene glycol)]-*O*-(5'-guanosine) monophosphate (5'-HS-PEG_2-GMP), and *O*-[ω-sulfhydryl-tetra(ethylene glycol)]-*O*-(5'-guanosine) monophosphate (5'-HS-PEG_4-GMP). These initiators are not only to introduce directly a free thiol into 5'-end of RNA, but also provide a flexible polyethylene glycol (PEG) linker between HS group and RNA, which is important for some bioconjugation applications. Three thiol-reactive biotin agents have been tested to couple with 5'-thiol of RNA molecules. The bioconjugation of maleimide-activated horseradish peroxidase with the 5'-sulfhydryl of RNA was also studied.

Experimental Procedures

Preparation of 5'-HS-PEG_2-GMP-RNA, 5'-HS-PEG_4-GMP-RNA, and 5'-HS-G-RNA. The 5'-GTP-RNA, 5'-GSMP-RNA, and 5'-HS-PEG-GMP-RNA were prepared

by run-off transcription in the presence of the four ribonucleotides or the four ribonucleotides supplemented with GSMP or HS-PEG_2-GMP or HS-PEG_4-GMP. In general, the 222-bp DNA template for *in vitro* transcription was generated by PCR from pC25 plasmid DNA (Zhang & Cech, 1997). Transcription reactions were carried out with 4 µl of T7 RNA polymerase in the presence of 2 mM each NTP, 7.2 µg of DNA template, 10 µCi α-^{32}P-ATP, 4 mM spermidine, 0.05% Triton X-100, 12 mM $MgCl_2$, 20 mM DTT, and 40 mM Tris buffer (pH 7.5) in a total 200 µl reaction at 37 ^{0}C for 3 hours. A 4 µl aliquot of 0.5 M EDTA (pH 7.4) was added to dissolve the white Mg^{2+}-pyrophosphate precipitate and 80 µl of formamide dye was added, and then loaded on an 8% polyacrylamide gel. RNA was purified through an 8% polyacrylamide [29:1 acrylamide : bis(acrylamide)]/8 M urea gel. RNA was visualized by UV shadowing and excised from the gel. The gel slice was crushed and soaked overnight in TE buffer (10 mM Tris-HCl, pH 7.5, 1 mM EDTA, and 250 mM NaCl) at 4 °C to elute the RNA. After filtering the soaking solution, RNA was recovered by ethanol precipitation and the pellet was dissolved in 10-50 µl of ddH_2O.

To prepare 5'-HS-PEG_n-GMP-RNA (where n = 2 or 4), 5'-HS-PEG_n-GMP was added into the transcription reaction with a ratio of 5'-HS-PEG_n-GMP to GTP of 1:1, 4:1, 8:1 or 16:1. A 20 µl aliquot of 0.5 M EDTA (pH 7.4) was added to dissolve the white precipitate before adding formamide-loading dye. The RNA transcript was purified as described above.

To prepare 5'-HS-G-RNA, 5'-GSMP-RNA was synthesized by runoff transcription in the presence of GSMP with a ratio of GSMP:GTP:ATP:CTP:UTP = 8:1:1:1:1 mM. The 5'-GSMP-RNA was dephosphorylated by Calf Intestinal alkaline

phosphatase (New England Biolabs) in NEBuffer 3 (50 mM Tris-HCl, 10 mM $MgCl_2$, 100 mM NaCl, 1mM dithiothreitol, pH 7.9) at 37 ^{0}C for 3 hours to generate 5'-HS-G-RNA. The reaction was stopped by the addition of 10 µl of 200mM EGTA and incubation at 65 ^{0}C for 10 min. The 5'-HS-G-RNA was recovered and resuspended as described above.

Conjugation of thiol-reactive agents with 5'-HS-G-RNA and 5'-HS-PEG_n-RNA. The 5'-GTP-RNA, 5'-HS-G-RNA, and 5'-HS-PEG_n-RNAs were incubated with Biotin-PEG_3-iodoacetamide, Biotin-HPDP, and Biotin-PEG_3-Maleimide, in 10 mM HEPES (pH 7.8), 300 mM NaCl, and 1 mM EDTA at room temperature for 2 hr. The reaction mixtures were extracted with phenol/chloroform/ isoamyl alcohol (25:24:1) (pH 6.7) once and chloroform once, and precipitated with ethanol. The RNA pellets were resuspended in 20 µl of pure water and stored at –20 °C. A 2 µl aliquot of each of the biotinylated RNAs was incubated with 15 µg of streptavidin in the binding buffer (20 mM HEPES, pH 7.4, 5.0 mM EDTA, and 1.0 M NaCl) at room temperature for 20 min prior to mixing with 0.25 volumes of formamide loading buffer (90% formamide; 0.01% bromophenol blue and 0.025% xylene cyanol). The biotinylated RNA products were resolved by electrophoresis through 7.5 M urea polyacrylamide gels. The biotinylated RNA can complex with streptavidin and the mobility of the 5'-biotin-RNA::streptavidin complex through the gel will be retarded relative to unbiotinylated RNA. The fraction of product formation relative to total RNA at each lane was quantitated with a Molecular Dynamics PhosphorImager.

For conjugation with maleimide-activated horseradish peroxidase (HRP), a 1.0 µl aliquot of 5'-GTP-RNA or 5'-HS-PEG_n-GMP-RNA was incubated with 10 µg of HRP in

maleimide conjugation buffer (100 mM sodium phosphate, 5 mM EDTA, pH 7.6) at room temperature for one hour. The HRP-conjugated RNA was then resolved by electrophoresis through an 7.5 M urea/8% polyacrylamide gel. Detection of the HRP-maleimide-RNA conjugate was based on the electrophoretic mobility change of the conjugated RNA that obviated the need to assay for HRP's enzymatic activity. The mobility of HRP labeled RNA will be slower than unmodified RNA on 7.5 M urea/8% polyacrylamide gel.

Results

Conjugation of 5'-HS-PEG$_n$-GMP-RNA with maleimide-activated HRP

Horseradish peroxidase (HRP, MW 40 kD) is one of the most common enzymes used for immunoassay detection systems. Ordinarily the enzyme is detectable because it can, under appropriate conditions, form soluble color responses, color precipitates, or generate the chemical emission of light. One commercially available version of horseradish peroxidase contains a thiol-reactive maleimide group enabling the HRP to be introduced efficiently into the 5'-end of the thiol-modified RNA. The change in mass may be detected by an electrophoretic mobility change, thus obviating the need for the bioassay based on HRP's enzymatic activity.

We synthesized two new 5'-modified guanosines, *O*-[ω-sulfhydryl-bis(ethylene glycol)]-*O*-(5'-guanosine) monophosphate (5'-HS-PEG$_2$-GMP), and *O*-[ω-sulfhydryl-tetra(ethylene glycol)]-*O*-(5'-guanosine) monophosphate (5'-HS-PEG$_4$-GMP). The structures of 5'-HS-PEG$_2$-GMP, 5'-HS-PEG$_4$-GMP and GSMP were shown in Figure 2-1.

The results of conjugating 5'-HS-PEG_n-GMP-RNA with the maleimide-activated HRP are demonstrated in Figure 2-2. The 5'-HS-PEG_n-GMP-RNA was incubated with maleimide-activated HRP and detected as an RNA band-shift (Figure 2-2, lanes 2 and 5), which is the 5'-HRP-S-PEG_n-GMP-RNA. The overall yield of 5'-HRP-S-PEG_n-GMP-RNA was 55% with 5'-HS-PEG_4-GMP and 61% with 5'-HS-PEG_2-GMP. Neither 5'-HS-PEG_2-GMP-RNA nor 5'-HS-PEG_4-GMP-RNA demonstrated a retarded band in the absence of the maleimide-activated HRP treatment (Figure 2-2, lanes 1 and 4). The 5'-GTP-capped-RNA served as a negative control (Figure 2-2, lane 3). When 5'-GTP-RNA was treated with the maleimide activated HRP, no retarded band was detected (Figure 2-2, lane 3). The results suggest that the HRP protein was linked to the 5'-terminal thiol of RNA, not to other functional groups present in RNA. These data also imply that 5'-HS-PEG_2-GMP is a better substrate than 5'-HS-PEG_4-GMP, although both can serve as effective initiators for T7 RNA polymerase. The major advantage of the di- and tetra-ethylene glycol derivatives are that they provide flexible spacers between the RNA and the thiol group, and this flexibility may be crucial for some bioconjugation applications and immobilized binding studies.

Next, we explored the efficiency of incorporation of 5'-HS-PEG_2-GMP during *in vitro* transcription reactions performed with varying molar ratios of GTP to 5'-HS-PEG_2-GMP (Figure 2-3). The molar ratio of GTP to HS-PEG_2-GMP was adjusted by maintaining a consistent concentration of 1 mM GTP while varying the concentration of HS-PEG_2-GMP in the transcription reactions. The thiol-containing RNAs generated by the transcription reactions were conjugated to maleimide-activated HRP during a subsequent incubation step. Assuming that the thiol-maleimide reaction was quantitative,

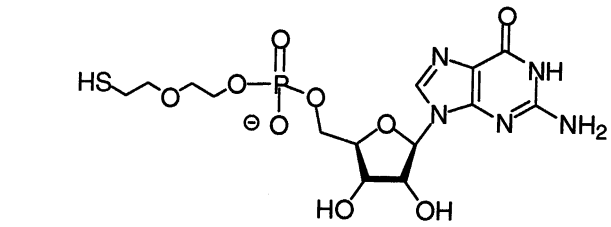

HS-PEG$_2$-GMP

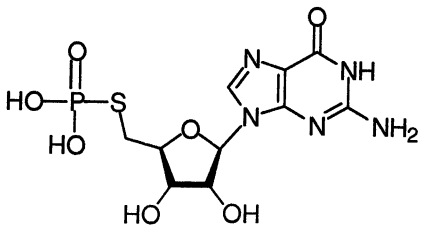

GSMP

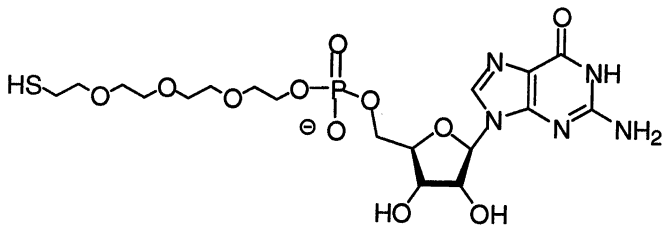

HS-PEG$_4$-GMP

Figure 2-1. Chemical structures of HS-PEG$_2$-GMP, HS-PEG$_4$-GMP, and GSMP.

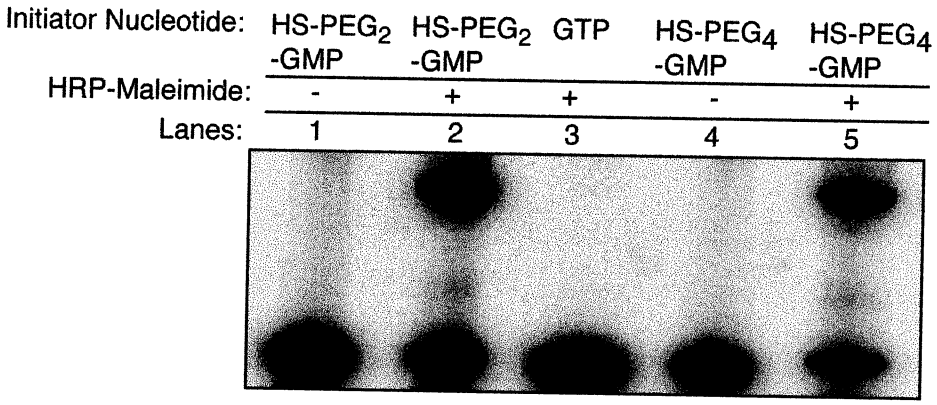

Figure 2-2. Autoradiogram of RNAs transcribed in the presence and absence of 5'-HS-PEG$_n$-GMP as initiator nucleotides and incubated with maleimide-activated horseradish peroxidase (HRP) prior to electrophoresis. The top band represents the RNA-HRP complex, and the low band is the ^{32}P labeled RNA.

a

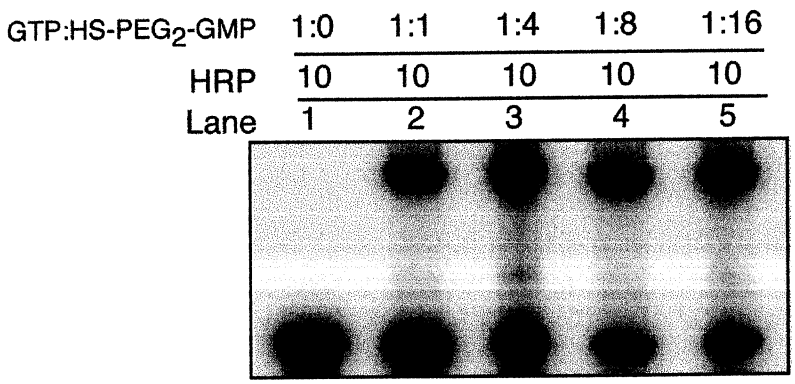

b

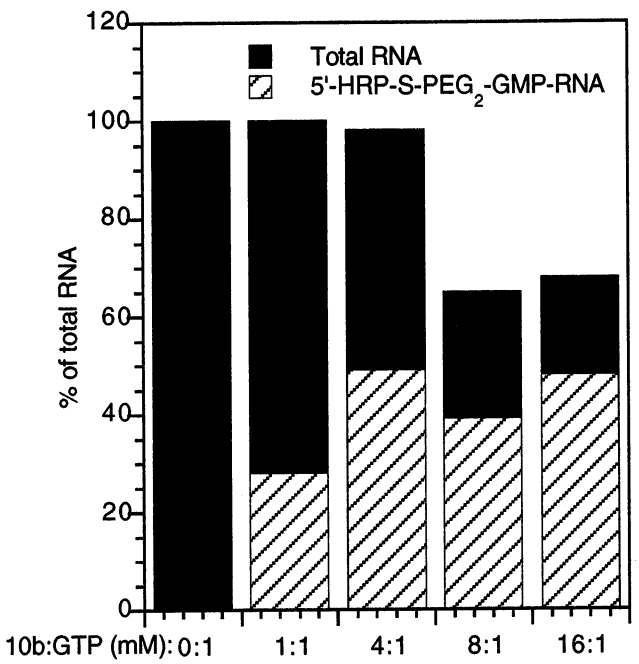

Figure 2-3. (a) The autoradiogram of RNAs transcribed using various ratios of GTP : 5'-HS-PEG_2-GMP and incubated with maleimide activated horseradish peroxidase prior to electrophoresis. The top band represents the RNA-HRP complex, and the low band is the ^{32}P labeled RNA. (b) Quantitative analysis of transcription yield and incorporation efficiency of 5'-HS-PEG_2-GMP using maleimide-activated horseradish peroxidase to detect 5'-HS-PEG_2-GMP-initiated RNA. The total RNA was quantitated using a Varian UV spectrometer (260 nm); the height of the bars represents the total RNA yield after the gel purification of each RNA transcript. The shaded portions are the fraction of the 5'-HS-PEG_2-GMP-initiated RNA. Percentage values are normalized to an *in vitro* transcription reaction with each NTP at 1.0 mM without the 5'-HS-PEG_2-GMP initiator nucleotide.

resolution of the 5'-HRP-S-PEG_2-GMP-RNA from the unconjugated RNA allowed us to determine the percent of RNA transcripts that successfully employed HS-PEG_2-GMP as the initiator nucleotide in lieu of GTP. No 5'-HRP-RNA was formed when HS-PEG_2-GMP was absent from the transcription reaction (Figure 2-3a, lane 1) confirming that the conjugation of the maleimide-activated HRP with the RNA was dependent upon the use of the thiol-containing initiator nucleotide.

The efficiency of incorporation of HS-PEG_2-GMP may be dissected in terms of both relative and absolute yields (i.e. what fraction of the total transcripts were initiated with HS-PEG_2-GMP, and how many moles of transcripts were produced). This is an important distinction since the absolute yield from the transcription reactions decreased at the highest concentrations of HS-PEG_2-GMP tested (Figure 2-3b). When the ratio of GTP : HS-PEG_2-GMP was 1 : 1, approximately 28% of the nascent transcripts were initiated with HS-PEG_2-GMP. The percent of transcripts initiated with HS-PEG_2-GMP increased to 51%, 60%, and 72% as the GTP : HS-PEG_2-GMP ratio was varied from 1 : 4, 1 : 8 , and 1 : 16 mM, respectively. Interestingly, the fraction of 5'-HRP-S-PEG_2-GMP-RNA increased significantly over this interval but the absolute yield of 5'-HRP-S-PEG_2-GMP-RNA remained relatively constant as the absolute total transcription yield (including GTP-initiated transcripts) decreased (Figure 2-3b). When the concentration of HS-PEG_2-GMP reached 8 mM, it appeared to slightly inhibit transcription by T7 RNA polymerase. Normalizing the absolute yield of total RNA to 100% when the ratio of GTP to 5'-HS-PEG_2-GMP was 1 mM : 0 mM, the yield decreased to 98% for 1 mM : 4 mM, 65% for 1 mM : 8 mM, and 68% for 1 mM : 16 mM transcription reactions.

A comparison of these incorporation efficiencies with published reports using similar initiator nucleotides is complicated by the facts that each laboratory prefers slightly different transcription conditions and that the nucleotide concentrations frequently vary among studies. In spite of these differences, our yields compare favorably with the yields reported by Sengle et al (2000) in which transcription reactions employing a 1 mM : 4 mM ratio of GTP to their biotinylated-GMP analog resulted in 25% of their transcripts initiating with their analog. Under similar GTP : GMP analog conditions, we observed that 51 % of the transcripts initiated with our thiol-containing GMP-analog HS-PEG_2-GMP. Interestingly, Sengle and his colleagues reported that GMPS at low concentrations appeared to enhance the absolute total transcription yield and then began to decrease the total yield as the GMPS concentration was raised further. In contrast the addition of AMP and GMP decreased the transcription yields in a concentration-dependent manner. We find that our HS-PEG_2-GMP nucleotide behaves more similar to the effect reported for AMP and GMP addition, specifically a concentration-dependent decrease in yields from transcription reactions utilizing T7 RNA polymerase.

We chose to use PEG linkers because the flexibility that they provide enables their future use in applications in which steric hindrance may be an issue. In light of the finding that PEG-containing GMP nucleotides are incorporated less efficiently as initiator nucleotides as the length of the PEG linker increases (Seelig & Jäschke, 1999a), we sought to balance the competing demands of linker flexibility with incorporation efficiency. The results from Figure 2-3b suggest that we have found an acceptable balance; the initiator nucleotide HS-PEG_2-GMP, containing two PEG subunits, decreased

the absolute total transcription yield when present at a GTP : HS-PEG_2-GMP ratio at 1 mM : 8-16 mM but without significantly lowering the absolute yield of the desired HS-PEG_2-GMP -capped-RNA.

Thiol-reactive biotin conjugation with 5'-HS-PEG_2-GMP-RNA

The reactivity of 5'-HS-PEG_2-GMP-RNA was tested with three thiol-reactive biotin reagents, Biotin-PEG_3-iodoacetamide, Biotin-HPDP, and Biotin-PEG_3-Maleimide (from Moleuclar Biosciences, Boulder, CO, Figure 2-4). The streptavidin gel-shift results of 5'-HS-PEG_2-GMP-RNA with these biotinylated thiol-reactive reagents are shown in Figure 2-5. When 5'-HS-PEG_2-GMP-RNA was reacted with Biotin-PEG_3-iodoacetamide, Biotin-HPDP, and Biotin-PEG_3-Maleimide, the thiol-modified RNA molecules were biotinylated and detected as band-shifts in the presence of streptavidin upon gel electrophoresis that represented streptavidin::RNA complexes (Figure 2-5, lanes 4, 6, and 7), no retarded band was detected without streptavidin (Figure 2-5, lane 8). When 5'-GTP-capped-RNA was treated with Biotin-PEG_3-iodoacetamide, Biotin-HPDP, and Biotin-PEG_3-Maleimide, no biotinylated RNA was detected in the presence of streptavidin (Figure 2-5, lanes 1, 2, and 3, respectively). The retarded band disappeared after treatment with DTT (Figure 2-5, lane 5), which reduced the product of the thiol-disulfide exchange reaction between 5'-HS-RNA and Biotin-HPDP Biotin-HPDP. The overall fraction of biotinylated RNA was 39% after reaction with Biotin-HPDP, 45% with Biotin-PEG_3-Maleimide, and 23% with Biotin-PEG_3-iodoacetamide for 5'-HS-PEG_2-GMP (Figure 2-5, lanes 4, 6, and 7, respectively).

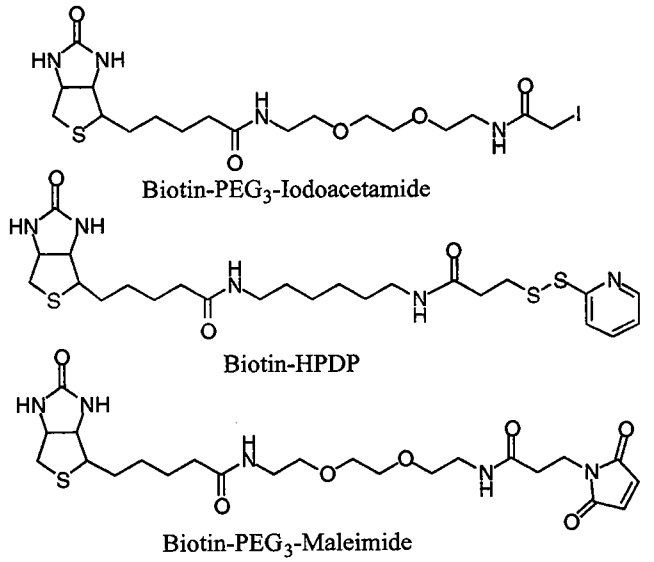

Figure 2-4. Chemical structures of thiol-reactive agents.

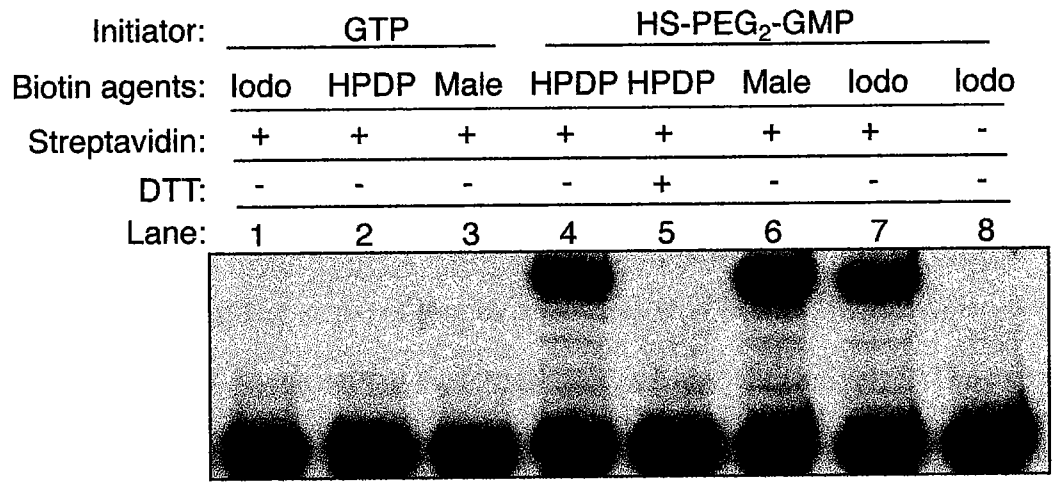

Figure 2-5. The autoradiogram of the streptavidin gel-shift analysis of transcription products (5'-GTP-RNA and 5'-HS-PEG_2-RNA) following incubation with Biotin-PEG_3-iodoacetamide (Iodo), Biotin-HPDP (HPDP), and Biotin-PEG_3-Maleimide (Male). Lane 1-3: 5'-GTP-RNA; lane 4-8: 5'-HS-PEG_2-RNA. The top band corresponds to the 5'-biotin-RNA::streptavidin complex, and the low band represents the RNA.

Thiol-reactive biotin conjugation with 5'-HS-G-RNA

The bridging phosphorothioate 5'-GSMP-RNA was dephosphorylated by alkaline phosphatase to generate 5'-HS-G-RNA (i.e. RNA containing a 5' thiol instead of a 5'-hydroxyl group) (Zhang et al., 2001a). The streptavidin gel-shift results of 5'-HS-G-RNA following reaction with Biotin-PEG_3-iodoacetamide, Biotin-HPDP, and Biotin-PEG_3-Maleimide are shown in Figure 2-6. When 5'-HS-RNA was reacted with Biotin-PEG_3-iodoacetamide, Biotin-HPDP, and Biotin-PEG_3-Maleimide, the thiol-modified RNA molecules were biotinylated and detected as band-shifts in the presence of streptavidin (lanes 4, 6, and 9, respectively); no retarded band was detected without streptavidin (lanes 5, 7, and 10) nor when 5'-GTP-capped-RNA was treated with Biotin-PEG_3-iodoacetamide, Biotin-HPDP, and Biotin-PEG_3-Maleimide (lanes 1, 2, and 3, respectively). The retarded band disappeared after treatment with DTT (lane 8), which reduced the product of the thiol-disulfide exchange reaction between 5'-HS-RNA and Biotin-HPDP Biotin-HPDP. These results suggest that the biotin group was transferred to the terminal thiol of the 5'-HS-RNA, not to other nucleophilic groups of RNA. The overall yield (three steps) of biotinylated RNA is 57% with Biotin-PEG_3-iodoacetamide and 60% with Biotin-HPDP for GSMP (lane 6 and 9, respectively). The experiments demonstrated that GSMP can serve as a better initiator nucleotide for transcription by T7 RNA polymerase than HS-PEG_2-GMP and HS-PEG_4-GMP for the purpose of introducing a sulfhydryl group at the 5'-end of RNA.

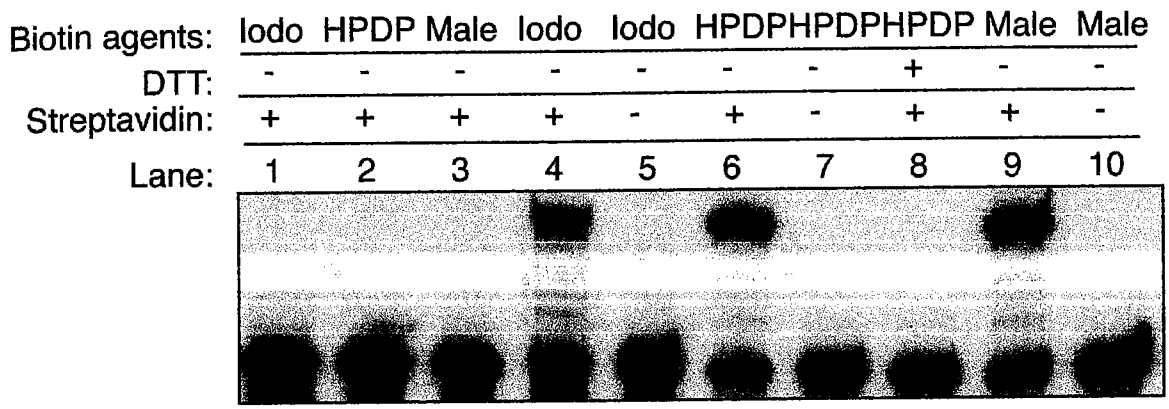

Figure 2-6. The autoradiogram of the streptavidin gel-shift analysis of transcription products (5'-GTP-RNA and 5'-GSMP-RNA) following incubation with Biotin-PEG_3-iodoacetamide (Iodo), Biotin-HPDP (HPDP), and Biotin-PEG_3-Maleimide (Male). Lane 1-3: 5'-GTP-RNA; lane 4-10: 5'-HS-G-RNA. The top band corresponds to the 5'-biotin-RNA::streptavidin complex, and the low band represents the RNA.

Conclusion

We have developed a general method to introduce a single thiol group tethered to the 5'-end of RNA via spacers of various lengths. Our results demonstrate that GSMP and 5'-HS-PEG_n-GMP can serve as initiator nucleotides for T7 RNA polymerase thus introducing a sulfhydryl group into the 5'-end of RNA. Fluorophores, biotinylated compounds, peptides, proteins, DNAs, RNAs, enzymes, and other chemical entities containing thiol-reactive functional groups can be attached to the thiol-modified RNA molecules using the techniques described here. These methods may have potential applications in analysis and detection of RNA, mapping RNA-protein interactions, *in vitro* selection of novel catalytic RNAs and even gene array technologies.

Chapter III

Peptide-Synthesizing Ribozymes Using the Aminoacyl-Adenylate As the Substrate

The aminoacyl-adenylate is a universal intermediate for both ribosomal and nonribosomal processes of peptide biosynthesis in modern biological systems (Bodley, 1988; Von et al., 1997; Marahiel et al., 1997). In coded peptide synthesis, the specific amino acid is activated as its aminoacyl-5'-adenylate en route to the formation of the appropriate 3'(2')-aminoacyl-tRNA. The tRNA provides the amino acid with a nucleic acid "tag", although such a tag would not be required by uncoded peptide-synthesizing machines. Non-ribosomal polypeptide biosynthesis requires a minimum of three successive steps: (1) amino acid adenylation (aa-AMP), (2) aminoacylation of holo-PCP (Peptide Carrier Protein) by the formation of a thioester, and (3) peptide bond formation. Thus, the aminoacyl-adenylate is the key activated intermediate for both types of polypeptide biosynthesis.

Before the emergence of coded peptide synthesis, how were peptides made? What biological molecule was the first catalyst for peptide synthesis? From the demonstration that RNA can form an aminoacyl-5'-guanylate-RNA (Kumar & Yarus, 2001), we can make the feasible extrapolation that the biologically relevant aminoacyl-5'-adenylates could have been present in a hypothesized primordial RNA world in which ribozymes were a major catalytic force. Using the aminoacyl-adenylate as substrate, self-aminoacylating ribozymes have been isolated from combinatorial RNA libraries (Illangasekare et al., 1995; Illangasekare & Yarus, 1999a; Illangasekare & Yarus, 1999b).

Furthermore, RNAs capable of catalyzing amide bond formation have been isolated by employing biotinyl-5'-AMP phosphoanhydride (Wiegand et al., 1997) or a nucleotide-aminoacyl ester as a substrate (Lohse et al., 1996).

Acknowledging the key role of the aminoacyl-adenylate in peptide synthesis, I carried out a selection in seeking of the ribozymes that are capable of utilizing aminoacyl-adenylate as the substrate to catalyze peptide bond formation.

This chapter reports the identification of peptide-synthesizing ribozymes that use *N*- biotin-aminoacyl-5'-adenylate as a substrate for peptide bond formation. One highly active ribozyme family (the R180 family) has been identified that can catalyze dipeptide synthesis using six different aminoacyl-5'-adenylates and five different RNA-tethered amino acids, in which the amino acids used in the selection are replaced with other standard amino acids. This new system bolsters the case that RNAs of antiquity could have catalyzed uncoded protein synthesis using aminoacyl-5'-adenylates, compounds which persist as intermediates for both uncoded and coded peptide synthesis in biology today.

During the investigation of the R180 ribozyme, I found that a previously isolated ribozyme, the C25 ribozyme, could also utilize the aminoacyl-adenylate in catalyzing peptide bond formation. The C25 ribozyme was isolated in catalyzing peptide bond formation using a substrate of predominantly *N*-blocked-methionyl-3'(2')-AMP esters (Zhang & Cech, 1997). It is surprising that two ribozymes isolated from two different selections could both utilize the aminoacyl-5'-adenylate in catalyzing peptide bond formation. This finding further suggests that the aminoacyl-5'-adenylate might play a role in mediating uncoded protein synthesis in an ancient world. The specificity of

substrate binding was compared between the R180 and C25 ribozymes. These two ribozymes were also examined for their ability in catalyzing long peptide synthesis.

Experimental Procedures

***In vitro* selection.** The initial RNA pool used the 10^{th} generation from previous study (Zhang & Cech, 1997). RNAs were prepared from PCR-amplified DNA by *in vitro* transcription in the presence of GMPS : GTP = 8:1 as described previously (Zhang & Cech, 1997). The 5'-GMPS-RNA was purified by PAGE and then reacted with *N*-bromoacetyl-*N'*-phenylalanyl-cystamine. The selection conditions were as follows: the 1-4 μM 5'-Phe-SS-RNA was incubated with 0.1-8.0 mM biotinoyl-amidocaproyl-methionyl-5'-AMP anhydride in the presence of 100 mM $MgCl_2$, 300 mM KCl and 50 mM Hepes buffer (pH 7.4) at 25 °C. The active 5'-Phe-SS-RNA molecules were converted to 5'-biotin-Met-Phe-SS-GMPS-RNA, re-isolated by streptavidin-agarose, and used as RT-PCR templates for the next cycle of selection. The first three cycles of selection to use biotin-Met-5'-AMP employed mutagenic PCR to introduce variants. After six cycles of selection, the final pool was cloned and sequenced to identify the most active ribozymes.

Ribozyme preparations. Both C25 ribozyme and R180 ribozyme were prepared by runoff transcription. Reactions were carried out in 40 mM Tris•HCl (pH 7.4), 12 mM $MgCl_2$, 40 mM DTT, 4 mM spermidine, and 0.08% TritonX-100 with 5 μg of corresponding DNA templates per 100 μl reaction at 37 °C. Ribozymes were synthesized in the presence of 5 μCi/100μl reaction of α-^{32}P-ATP, 2 mM each ATP/GTP/CTP/UTP,

and 32 mM guanosine-5'-monophosphorothioate (GMPS). The 5'-^{32}P-GMPS-ribozymes were then were purified by 8%/7.5 M Urea denaturing polyacrylamide gel electrophoresis and detected by UV absorbance. The gel containing the ribozymes was cut out, squeezed by syringe, and soaked in TE buffer at 4 °C overnight. The soaking solution was separated from the gel by filtration and centrifugation. And ribozymes were precipitated by 250 mM NaCl and cold ethanol in dry ice. To prepare 5'-aminoacyl'-SS-GMPS-RNAs, 5'-GMPS-RNAs were first linked with 2 mM *N, N'*-bis (bromoacetyl) – cystamine in the presence of chemical linkage buffer (CLB, 40 mM HEPES, pH 7.8, 150 mM NaCl and 10 mM EDTA). Reactions were performed by rotating at room temperature for 2 hours. After treatment with DTT, the resulted 5'-cysteamine-GMPS-RNAs were precipitated by cold ethanol and dissolved in degassed distilled water. Second linkage was performed between 5'-cysteamine-GMPS-RNA and 10 mM aminoacyl' (Phe, Lys, Leu, Trp, Gln, Phe-Cys) - pyridyldithioethyl amide in CLB buffer at room temperature for another 2 hours. After phenol/chloroform extraction, 5'-aminoacyl'-SS-GMPS-RNAs were precipitated by cold ethanol, dissolved in degassed distilled water and stored at -20 °C.

Nuclease digestion. The enzymatic digestion reactions were carried out with 5' or 3'-labeled R180 RNA in the presence of the reaction buffer (20 mM Tris-HCl [pH 7.5], 100 mM KCl, and 50 mM $MgCl_2$) at 37 °C. A total of 2 µl of 5' or 3'-labeled RNA (~10^6 CPM) solution was incubated with the reaction buffer for 10 min at 50 °C, slowly cooled down to room temperature, and then incubated with 1 µl of the appropriate diluted RNase solution (Nuclease S1 and RNase T1 from Roche; RNase T2 from Sigma; RNase V1

from Pharmacia Biotech). The digestion products were resolved by subjecting them to electrophoresis through 20% polyacrylamide / 7.5 M urea denaturing gels.

Kinetics assays. A 0.3-6.0 μM solution of the R180 ribozyme was preincubated with 100 mM $MgCl_2$ and 300 mM KCl, and 50 mM HEPES buffer (pH 7.4) for 10 min at 50 °C. The reactions were initiated by adding 2.0 μL aliquots of 0.1 to 5.0 mM biotin-Met-AMP in deionized H_2O. Aliquots (1.0-2.0 μL) of the reaction mixture were removed at specific time intervals, quenched with 2.5 μL of 50 mM HEPES, pH 7.4, 25 mM EDTA, 90% formamide dye, and stored in dry ice. Each sample was incubated with 7.5 μg of streptavidin for 20 min at room temperature and then loaded on a 7.5 M urea/8% polyacrylamide gel. The fraction of product formation relative to total substrate and product at each time point was quantitated using a Molecular Dynamics PhosphorImager.

Leaving group substitution. In order to reveal the binding site of the substrate, C25 ribozyme and R180 ribozyme were tested for their activity with various substrate derivatives. Eight kinds of anhydride substrates were prepared with four nucleotide-leaving groups (Bio-Met-AMP/GMP/CMP/UMP) and four non-nucleotide leaving groups (Bio-Met-IMI/PNP/NHS/CME). Reaction were performed with 0.5 μM 5'-Phe-SS-RNA (C25 or R180), 50 μM Biotin-Met-X in the presence of 100 mM $MgCl_2$, 300 mM KCl and 50 mM HEPES (pH 7.4) at 25 °C. 2 μl aliquots of the reaction mixture was removed at specific time points, quenched with 2 μl of quench buffer (50 mM HEPES, pH 7.5, 25 mM EDTA, and 90% formamide dye), and stored in dry ice. Each sample was incubated with 10 μg of streptavidin at room temperature for 15~20 minutes prior to

loading on 8%/7.5 M urea denaturing polyacrylamide gel. Reaction product was analyzed and the observed rate constants were obtained as described above.

Amino acid specificity assays. To examine amino acid specificity, six kinds of biotin-aminoacyl-AMP anhydrides (Phe, Leu, Gln, Met, Arg, and Ala) and five 5'-aminoacyl'-SS-GMPS-RNAs (Phe, Leu, Gln, Trp, and Lys) were prepared. Reaction were performed with 0.5 μM 5'-Phe-SS-RNA, 50 μM Biotin-aminoacyl-5'-AMP in the presence of 100 mM $MgCl_2$, 300 mM KCl and 50 mM HEPES (pH 7.4) at 25 °C. Products were analyzed as described in the substrate specificity section.

Results

In Vitro Selection of the R180 Family

Our previously isolated ribozymes used a substrate of predominantly *N*-biotinyl-amidocaproyl-methionyl-3'(2')-AMP esters (Biotin-Met-2'[3']-AMP monoester, Zhang & Cech, 1997). We performed a new selection beginning with the 10^{th} generation RNA pool from the above selection (Zhang & Cech, 1997). In the new selection, six additional cycles were carried out by switching the selection substrate to pure *N*-biotinyl-amidocaproyl-methionyl-5'-adenylate (Bio-Met-5'-AMP anhydride, synthesized as described for its congeners in Lacey et al. 1990 with modification).

The selection strategy of 5'-Phe-SS-GMPS-RNA with Bio-Met-5'-AMP is outlined in Figure 3-1. The initial 5'-GMPS-RNA pool transcribed from the 10^{th} generation DNA templates was reacted with *N*-bromoacetyl-*N'*-phenylalanyl-cystamine to produce 5'-phenylalanyl-cystaminyl-acetamidyl-GMPS-RNA (5'-Phe-SS-GMPS-

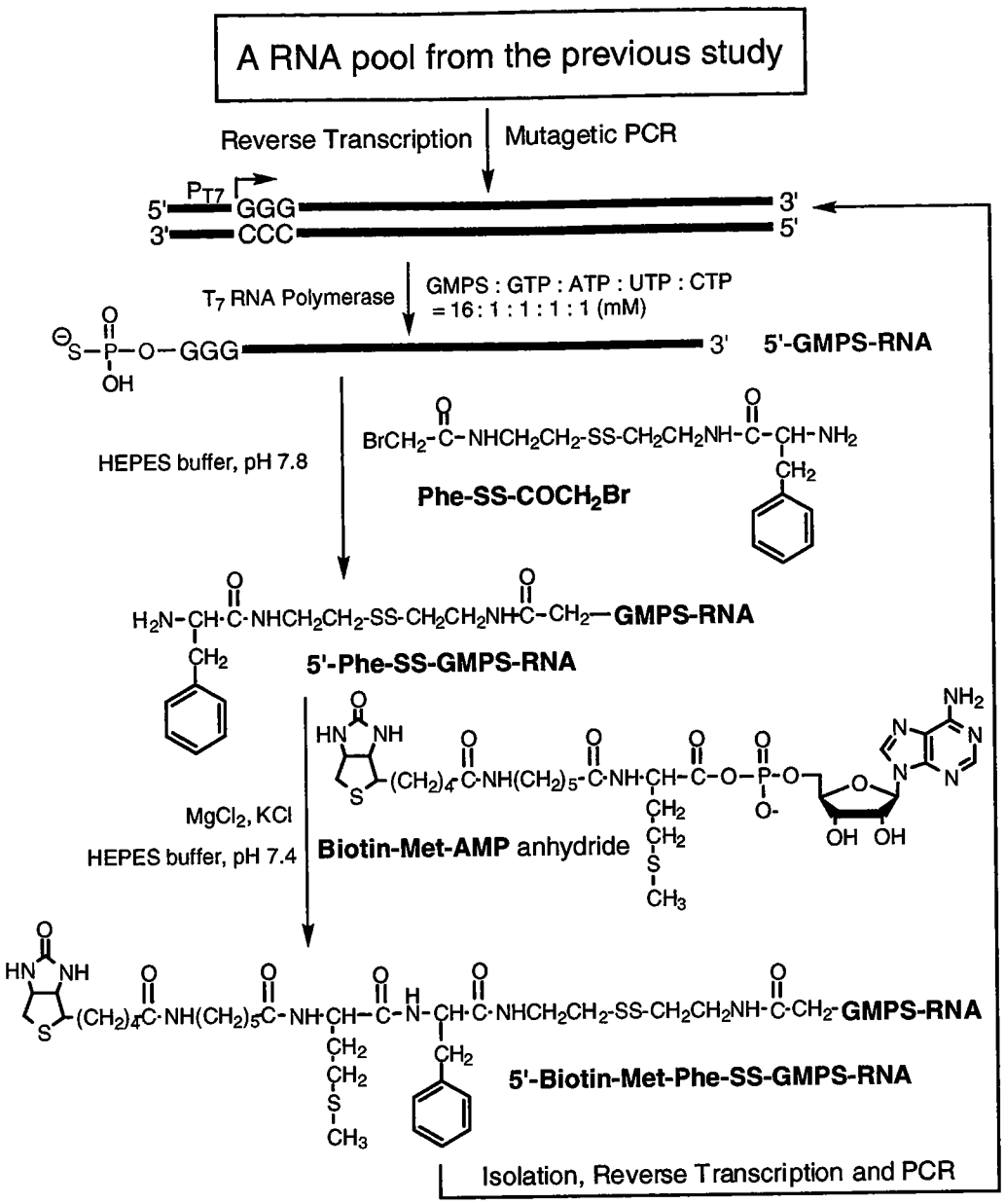

Figure 3-1. Initial RNA pool construction and *in vitro* selection. The starting RNA pool was from the 10th generation of the previous work [21]. The RNA pool was prepared from PCR amplified DNA by *in vitro* transcription in the presence of GMPS :GTP = 8:1. The 5'-GMPS-RNA was purified by PAGE and then reacted with *N*-bromoacetyl-*N'*-phenylalanyl-cystamine. The 5'-Phe-SS-RNA was incubated with Biotin-Met-AMP in the presence of $MgCl_2$, KCl and Hepes buffer and the reacted 5'-Biotin-Met-Phe-SS-RNA molecules were isolated by collecting them on streptavidin-agarose, washed in the presence of urea, and resolubilized by the addition of DTT. The collected RNA was used as RT-PCR templates for input into the next cycle of selection.

RNA), and incubated with Biotin-Met-5'-AMP anhydride in 100 mM $MgCl_2$, 300 mM KCl and 50 mM HEPES buffer (pH 7.4) at 25 °C. The active RNA molecules were isolated by streptavidin-agarose, washed extensively in the presence of urea, and subsequently resolubilized as described before (Zhang & Cech, 1997). Reverse-transcription and amplification by mutagenic PCR was performed for the first three cycles of the selection that used Biotin-Met-5'-AMP. After six cycles of selection with Biotin-Met-5'-AMP, the final pool was cloned and sequenced.

A highly active ribozyme family was identified by assaying individual clones coupled with sequence alignment analysis. This family comprised six RNA members: R180, R182, R185, R186, R193, and R202. Fortuitously, we also found eight more family members that emerged from the background of a separate selection that was intended to isolate variants of the distinct clone 16 and 25 ribozyme families (Zhang & Cech, 1997). The sequences of fourteen ribozymes are shown in Figure 3-2a. The sequence between G25 to G127 was a highly conserved region. The region after U128 of the family has significantly divergent sequence (pink color box, Figure 3-2a). These data suggest that within the internal sequence of the ribozyme, the 5'-proximal-portion is more critical for activity than the distal sequence; unfortunately, the relative importance of the 5'- and 3'-termini could not be assessed by comparative sequence analysis because they were constrained to form primer-binding sites.

Secondary Structure Model

The sequences of six RNAs were analyzed by the RNA Mfold program (Zuker et al., 1999) to predict their secondary structures. The best secondary structural model of

a

```
          21        30        40        50        60        70        80        90       100
R180      -AAGCGAGUGUGCAGACACGAUACUUCUGCCCGCCGGUGGAUUCGUAAGAAUUGCUAGGGCUUGGCCUUGUGAGCAACGACUUAC
R182      -AAGCGAGUGUGCAGACACGAUACUUCUGCCCGCCGGUGGAUUCGUAAGAAUUGCUAGGGCUUGGCCacGUGAGCAACaACUUAC
R185      -AAGCGAGUGUGCAGACACGAUACUUCUGCCCGCCGGUGGAUUCGUAAGAAUcGCUAGGGCUUGGCCaUGUGAGCAACGACUUAC
R186      -AAGCGAGUGUGCAGACACGAUACUUCUGCCCGCCGGUGGAUUCGUAAGAAUUGCUAGGGCUUGGCCaUGUaAGCAACGACUUAC
R193      -AAGCGAGUGUGCAGACACGAUACUUCUGCCCGCCGGUGGAUUCGUAAGAAUUGCUAGGGCUUGGCCcUGUGAGCAACGACUUAC
R202      -AAaCGAGUGUGCAGACACGAUACUUCUGCCCGCCGGUGGAUUCGUAAGAAUUGCUAGGGCUUGGCCaUGUGAGCAACGACUUAC
C25#40    -cAaCGAGUGUGCAGACACGAUACUUCUGCCCGCCGGUGGAUUuGUAAGAAUUGCUAGGGCUUaGCCaUGcGAGCAACGACUUAC
E25#92    -AAGuGAGUGUGCAGACACGAUACUUCUGCCCGCCGGUGGAUUCGUAAGAAUUGCUAGGGCUUGGCCUUGUGAGCAACGACUUAC
E25#95    -AAGCGAGUGUGCAGACACGAUACUUCUGCCCGCCGGUGGAUUCGUAAGAAUUGCUAGGGCUUGGCCcUGUGAGCAACaACUUAC
E25#96    -cAaCGAGUGUGCAGACACGAUACUUCUGCCCGCCGGUGGAUUCGUAAGAAUUGCUAGGGCUUGGCCcUGUGAGCAACGACUUAC
E25#98    -AAGCGAGUGUGCAGACACGAUACUUCUGCCCGCCGGUGGAUUuGUAAGAAUUGCUAGGGCUUGGCCUUGcGAaCAACGACUUAC
E25#107   -AAGCGAGUGUGCAGACACGAUACUUCUGCCCGCCGGUGGgUUCGUAAGAAUUGCUAGGGCUUGGCCaUGUGAGCAAuGACUUAC
E16#64    -AAGCGAGUGUGCAGACACGAUACUUCUGCCCGCCGGUGGAUUCGUAAGAAUcGCUAGGGCUUGGCCaUGUGAGCAACGACUUAC
E16#67    -AAGCGAGUGUGCAGACACGAUACUUCU-CCuGCCGGUGGAcUCGUAAGAAUUGCUAGGGCUUGGCCaUGUGAGCAACGACUUAC
            *  ********************** ** ********  * ******** ********** ***  *  *  **  ******

          110       120       130       140       150       160
                                                    CCGUGCGCC----------------------
                                                    CAGUUCGGCCC--------------------
                                                    UUAGUCACCCGCCCC----------------
                                                    UUAGUCACCCGCCCC----------------
                                                    GGAGUCUAUUCCGGUCACCGUACGA-------
                                                    UUCUCACAACAAGCCCAGGGAUUGGCGUUGAC
                                                    CGGCACCACUGCUCU----------------
                                                    GACCGACACUUGCUCC---------------
                                                    CGGCACCACUGCGCU----------------
                                                    GAGUCUAUUCCGGUCACCGUACGA-------
                                                    GACCGACACUUGCUCC---------------
                                                    CCCGUCUCCAACUUCCGCC------------
                                                    UUAGUCACCCGCCCCA---------------
                                                    CGGCACCACUGCUCU----------------
          ********** ***** ***
```

b

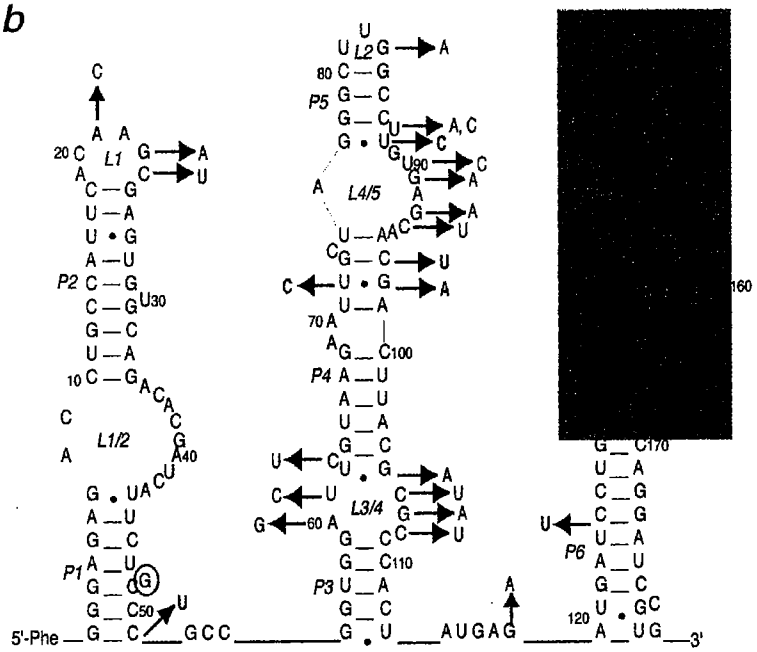

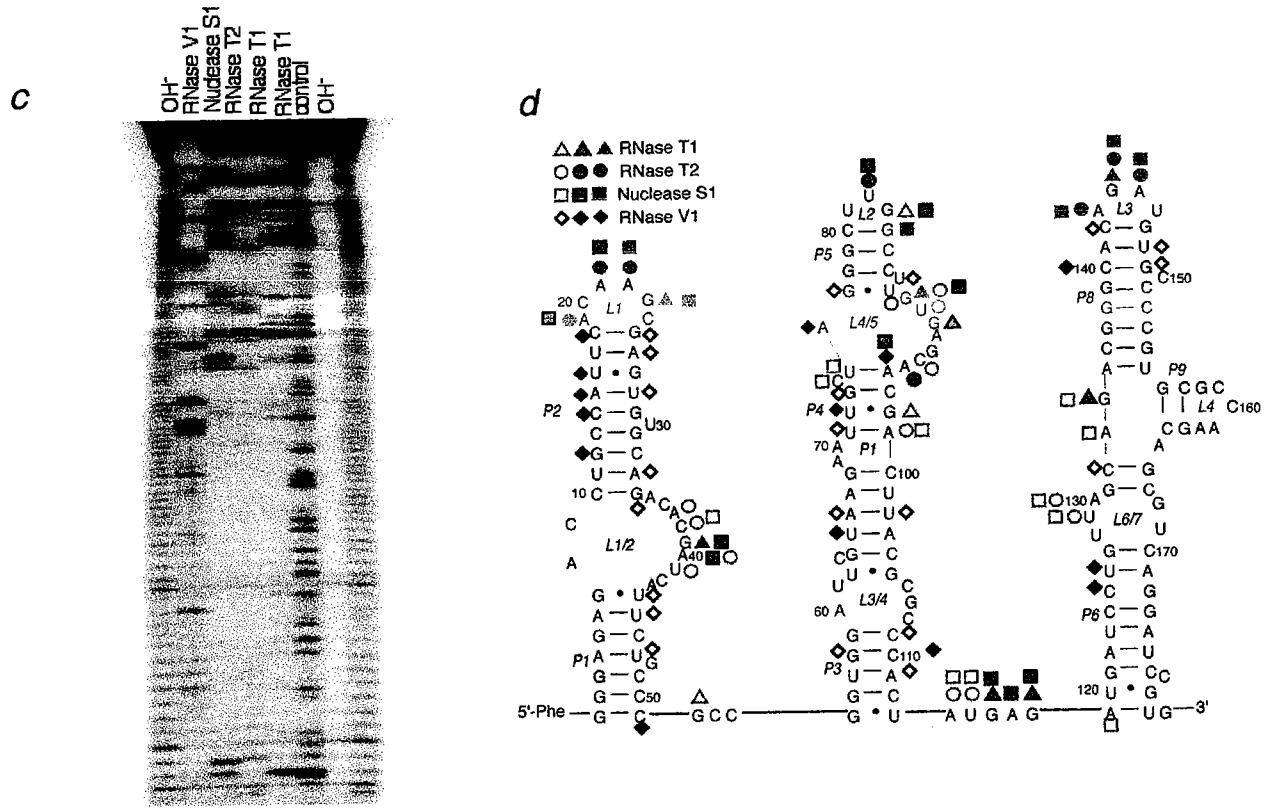

Figure 3-2. (a) Sequence alignment of the R180 ribozyme family. The flanking fixed primer sequences are not shown. Differences in individual clones from the consensus sequence (top sequence) are in lower case and red colored letters. The pink box indicates the region of structural divergence within the family. (b) Secondary structural model of the R180 ribozyme and its phylogenetic family. A deleted nucleotide is encircled. The single-nucleotide variations that fall within predicted loops (red) and base-paired regions (blue) in the phylogenetically conserved regions are highlighted. (c) Gel electrophoresis of nuclease digestion. (d) Enzymatic probing of the secondary structure of R180 ribozyme. The shaped symbols superimposed on the structure show positions cleaved by specific nucleases: RNase T1 (triangle), RNase T2 (circle), Nuclease S1 (square), and RNase V1 (diamond); solid color, filled color, and open symbols represent strong, medium, and weak enzymatic cleavage, respectively.

the R180 ribozyme, illustrated in Figure 3-2b, was obtained by comparison with all secondary structural models of these fourteen ribozymes. The other thirteen ribozymes fit this secondary structural model as well. Twenty-three nucleotide positions of the R180 ribozyme within the highly conserved regions were variable in other members of the family. Sixteen phylogenetic variations were located within predicted loop regions. Those seven variant positions that fall within predicted base pairs all preserve Watson-Crick or G-U wobble-matched base pairs. For example, the G1:C50 Watson-Crick base pair that closes P1 in the R180 ribozyme was a G1•U51 wobble base pair in the E16#67 ribozyme. Similarly, the U62•G105 wobble base pair within P4 in the R180 ribozyme was a U62:A105 Watson-Crick base pair in R202, E16#67, and E25#95 ribozymes. The fourteen ribozymes fit this secondary structural model very well until they diverge drastically (pink color box, Figure 3-2b) prior to reconverging for the final twenty-nucleotide fixed primer-binding site. This area of primary sequence diversion generated inconsistent secondary structures in different members of the family, suggesting that this variable region may not be structurally or functionally important.

The structural model predicts nine stem helices (P1-P9), four internal loops (L1/2, L3/4, L4/5, and L6/7), four hairpin loops (L1-L4), and one three-way junction (J7/8/9). The secondary structure of the R180 ribozyme was probed by nuclease digestion experiments with single-strand specific nuclease S1, RNase T1, RNase T2, and double-strand specific RNase V1. The nuclease digestion products were resolved by subjecting them to 20% polyacrylamide gel electrophoresis (Figure 3-2c). The enzymatic probing results are summarized in Figure 3-2d. The guanine nucleotides in the hypothesized internal loops and single-stranded regions (G39, G52, G89, G91, G116, G118, and G134)

and in the hairpin loops (G23, G83, and G144) were cleaved by single-strand specific RNase T1. The strong cutting patterns generated by single-strand specific RNase T2 (A19, A21, A22, A37, C38, A40, U41, U82, G89, U90, C94, A95, A114, U115, U129, A130, A143, G144, and A145) correlated well with the predicted internal loops, hairpin regions, and bulge regions. The predicted single-stranded positions at A19, A21, A22, G23, C38, G39, A40, U82, G83, G89, G116, G118, A143, G144, and A145 were strongly cleaved by Nuclease S1. The cleavage sites of double-strand specific RNase V1 correlated with the helical P1, P2, P3, P4, P5, P6, and P8 regions of the secondary structural model. The RNase V1 cleavage positions located on both sides of the P2, P3, P4, and P8 helices provided support that these regions are double stranded. With the exception of one putative double-stranded region of P4 that was also cleaved by single-strand specific nucleases, the nuclease digestion results agree well with the secondary structural model of the R180 ribozyme.

Reaction and Product Validation of R180 Catalysis

Several control reactions were carried out to validate the ribozyme-mediated formation of a peptide bond. These reactions were monitored by streptavidin gel-shift electrophoresis (Figure 3-3a). The installation of the nucleophilic Phe residue onto the 5'-end of a 5'-GMPS-capped ribozyme was achieved by sulfur-selective attack on a bromoacetyl-activated Phe-containing linker. To verify that the peptidyl transferase reaction was dependent on the presence of the aminoacyl-containing linker, a 5'-GTP-capped RNA was transcribed as the control. Treatment of 5'-GMPS- or 5'-GTP-initiated R180 RNAs with the same Phe-containing linker reagent should yield the successfully

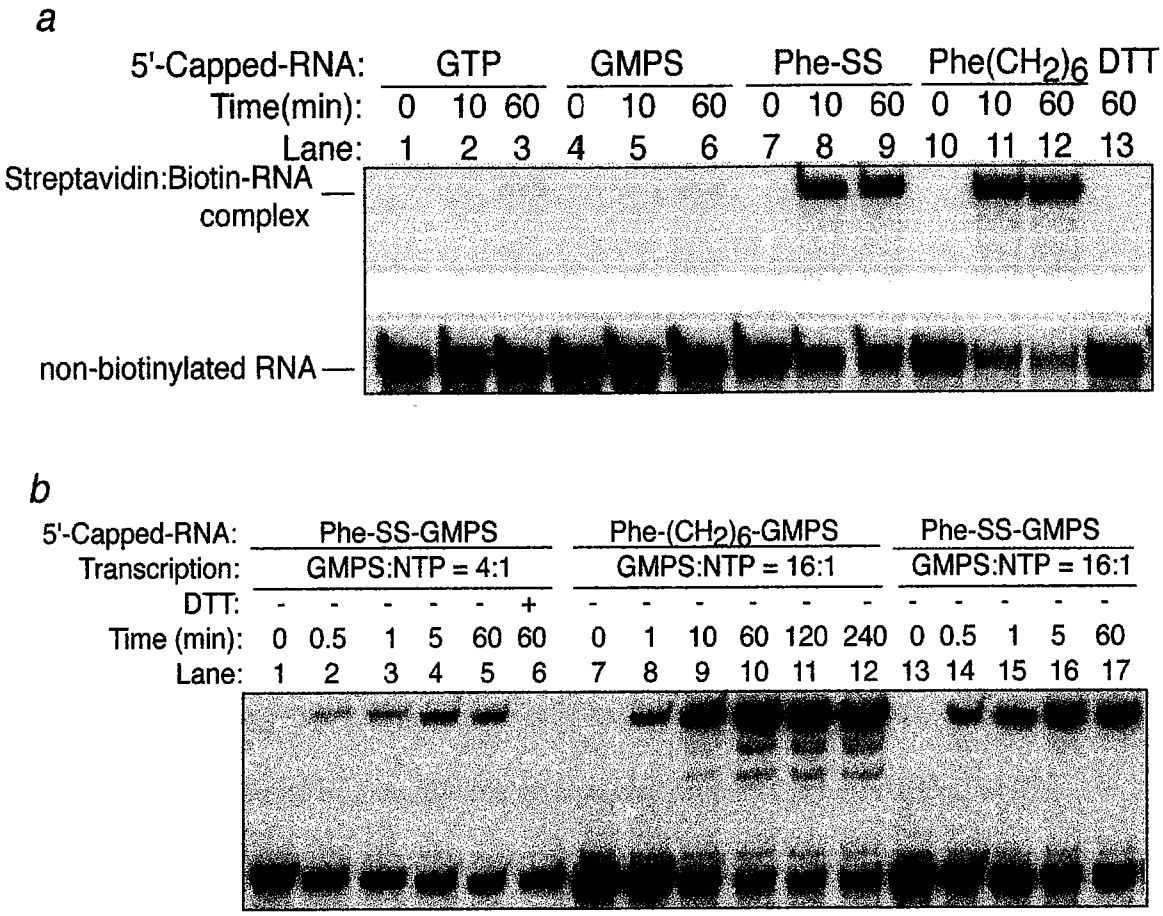

Figure 3-3. The R180 ribozyme requires a 5'-aminoacyl-capped RNA for activity. (a) Autoradiogram of the products of the peptide bond-forming reaction between 5'-capped-RNAs and biotin-Met-5'-AMP anhydride as detected by a streptavidin band-shift assay. RNA was prepared by *in vitro* transcription either with GTP alone (GTP lanes) or with a ratio of GMPS:GTP = 16:1. The GMPS-containing RNAs were used either without further reaction (GMPS lanes) or following the installation of a phenylalanyl residue on a linker containing an internal disulfide bond (Phe-SS lanes) or lacking a disulfide bond [Phe$(CH_2)_6$ lanes]. The reactions were performed with 2 μM 5'-capped-RNA (R180) and 50 μM biotin-Met-AMP in 300 mM KCl, 100 mM $MgCl_2$, and 50 mM HEPES buffer, pH 7.4, 25 °C. Lane 13: same as lane 9 but treated with DTT. The bottom bands are the unreacted RNA and the top bands are the streptavidin:biotinyl-RNA complex. (b) Autoradiogram of the peptide bond-forming reaction of 5'-Phe-SS-GMPS-RNA with biotin-Met-AMP anhydride, RNA prepared with the indicated ratios of GMPS to GTP.

modified 5'-Phe-SS-GMPS-RNA or unmodified 5'-GTP-RNA, respectively. When the linker-exposed 5'-GTP-RNA was incubated with Biotin-Met-5'-AMP anhydride under the same reaction conditions as those of 5'-Phe-SS-GMPS-RNA, no new band was formed (lanes 1-3, Figure 3-3a). When 5'-GMPS-RNA (R180) without phenylalanine linked to its 5'-end was incubated with biotin-Met-AMP anhydride, again no product was observed (lanes 4-6, Figure 3-3a). Together, these two negative controls demonstrate that the ribozyme-catalyzed peptidyl transferase reaction requires a 5'-GMPS-capped RNA that has been matured by covalent modification with the Phe-containing linker.

When 5'-Phe-SS-GMPS-RNA (R180) was incubated with biotin-Met-AMP, a new band was formed at an approximate 50% yield at the reaction's final extent (lanes 7-9, Figure 3-3a; lanes 13-17, Figure 3-3b). A non-cleavable linker in which two sulfur atoms were replaced by two methylene groups was prepared [Phe-$NH(CH_2)_6NH$-$C(O)CH_2Br$]. Incubation of 5'-Phe-$NH(CH_2)_6NHC(O)CH_2$-GMPS-RNA (R180) with biotin-Met-5'-AMP anhydride resulted in formation of the product in about 80% yield at the reaction's final extent (lanes 10-12, Figure 3-3*a*; lanes 7-12, Figure 3-3*b*). This indicates that the majority of RNA molecules can be folded into a uniform active conformation. This result also suggests that the coupling efficiency of Phe-$NH(CH_2)_6NHC(O)CH_2Br$ with 5'-GMPS-RNA is greater than that of Phe-$NHCH_2CH_2SSCH_2CH_2NHC(O)CH_2Br$, because both were prepared from the same 5'-GMPS-RNA transcript. The incomplete reaction extent that was observed could be explained partially by the transcription reaction conditions. The 5'-GMPS-RNA transcript was generated in the presence of both GMPS and GTP (molar ratio = 16:1) resulting in the occasional incorporation of GTP at the 5'-terminus rather than the desired

GMPS as a stochastic event. Since the GTP-capped fraction of the total transcribed RNA cannot be conjugated to the Phe-linker, the anticipated 5'-heterogeneity of the "GMPS-RNA" is expected to prevent complete reaction. Consistent with this prediction, Figure 3-3*b* shows the time course of the peptide bond-forming reactions by three R180 ribozymes with different linkers and RNAs. The yield at the final reaction extent was only 25% for 5'-Phe-SS-GMPS-RNA that was made from a 5'-GMPS-RNA transcript with a GMPS:NTP ratio of 4:1 (lanes 1-6, Figure 3-3*b*) and 50% for a ratio of 16:1 (lanes 13-17, Figure 3-3*b*). The observed rate constant with 50 μM biotin-Met-AMP was 0.18 min^{-1} for 5'-Phe-$NH(CH_2)_6NHC(O)CH_2$-GMPS-RNA (lanes 7-12, Figure 3-3*b*) and 0.82 min^{-1} for 5'-Phe-SS-GMPS-RNA. The reaction rate of 5'-Phe-$NH(CH_2)_6NHC(O)CH_2$-GMPS-RNA is about 5-fold slower than 5'-Phe-SS-GMPS-RNA although, as noted earlier, a larger fraction of this RNA reacts. After treatment with dithiothreitol (DTT), the product band disappeared in the case of 5'-Phe-SS-GMPS-RNA (lane 13, Figure 3-3*a*; lane 6, Figure 3-3*b*), but did not disappear in the case of its 5'-Phe-$NH(CH_2)_6NHCOCH_2$-RNA congener in which the disulfide has been replaced with two methylene groups (data not shown), indicating that the coupled biotin was located at an RNA-distal position (*i. e.* on the phenylalanine side of the disulfide bond) of 5'-Phe-SS-GMPS-RNA. The reaction product, Biotin-Met-Phe-cysteamine, was isolated by reverse-phase high-performance liquid chromatography (RP-HPLC) and confirmed by electrospray-ionization mass spectrometry (ESI-MS) (Sun et al., 2002).

Initial investigation of the R180 ribozyme kinetics was performed with a fixed concentration of the ribozyme and various concentrations of Biotin-Met-5'-AMP anhydride. The reaction condition was 100 mM $MgCl_2$, 300 mM KCl and 50 mM Hepes

at pH 7.4. The R180 ribozyme demonstrated similar behavior to the saturation kinetics of classical protein enzymatic catalysis (Figure 3-4). By fitting the data to the Michaelis-Menten equation, we obtained best-fit values of k_{cat} = 4.05 min^{-1} and K_m = 210 ± 26 μM at pH 7.4 and 25 °C. The apparent second-order rate constant, k_{cat}/K_m, equals 19,300 $M^{-1} \cdot min^{-1}$. Thus, the catalytic efficiency of the R180 ribozyme is modest compared to many protein enzymes. Kinetic studies of the non-cleavable 5'-Phe-$NH(CH_2)_6NHC(O)CH_2$-GMPS-RNA with biotin-Met-5'-AMP anhydride gave k_{cat} = 4.72 min^{-1} and K_m = 1.04 mM. The observed catalytic rates for both linkers were similar but the K_m for the non-cleavable linker was about 5 times higher than that of the native linker ribozyme suggesting that the linker of 5'-Phe-linker-RNA affects the equilibrium binding constant of substrate rather than the rate of the chemical step.

The Aminoacyl-5'-Adenylate as the Substrate for A Previous Isolated Peptide-Synthesizing Ribozyme (the C25 Ribozyme)

Previously, we reported another peptide bond-forming ribozyme, the C25 ribozyme (Zhang & Cech, 1997, 1998). In both R180 and C25-catalyzed reactions, peptide bond was formed between an amino acid tethered to the 5' end of the RNA and the other amino acid substrate free in the solution. However, the R180 ribozyme used pure Bio-Met-5'-AMP anhydride as the free substrate, while for C25, it was a sample mixture (referred to Sample **I** in this chapter) of predominantly Bio-Met-2'(3')-AMP monoester (Zhang & Cech, 1997). Because NMR, HPLC, and mass spectrometer analyses identified that Sample **I** contained approximately 2% other components (Biotin-Met-5'-AMP anhydride, bis(Biotin-Met)-2', 3'-AMP diester, and others) (Sun et al.,

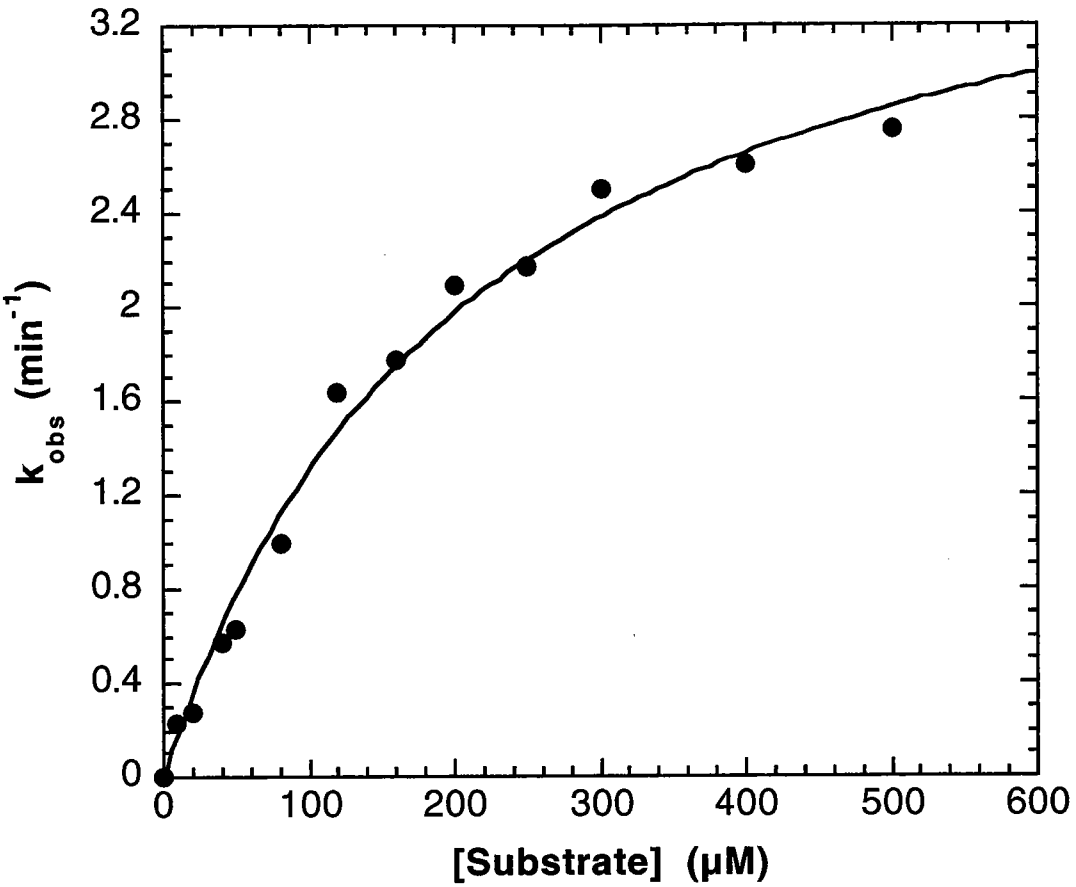

Figure 3-4. Michaelis-Menten plot for the peptide bond-forming reaction of biotin-Met-5'-AMP catalyzed by R180 ribozyme. Reactions were run in 0.5 μM R180 5'-Phe-SS-GMPS-RNA and 0 to 500 μM biotin-Met-AMP anhydride. The continuous line corresponds to the best-fit values of K_m and k_{cat}, obtained with the KaleidaGraph program.

2002), we were interested in examining whether the C25 ribozyme could also use Biotin-Met-5'-AMP anhydride in catalyzing peptide bond formation.

Sample **I** was prepared by Gottikh's method (Gottikh et al., 1970; Zhang & Cech, 1997). We re-purified Sample **I** by C18 reverse phase column to obtain pure Bio-Met-2'(3')-AMP monoester. We also synthesized bis(Biotin-Met)-2', 3'-AMP diester. Sample **I**, monoester, diester, and anhydride were all characterized by NMR, mass, and HPLC spectroscopy (Sun et al., 2002).

All four compounds were tested for peptide bond forming activity with the R180 and C25 ribozymes (Figure 3-5). The R180 ribozyme was most active with anhydride (Figure 3-5a, lanes 7-9). It showed little activity with monoester (Figure 3-5a, lanes 1-3), Sample **I** (Figure 3-5a, lanes 4-6), and diester (Figure 3-5a, lanes 10-12). In contrast, the C25 ribozyme was most active with Sample **I** (Figure 3-5b, lanes 4-6), and also exhibited potential reactivity with anhydride (Figure 3-5b, lanes 7-9). However, the C25 ribozyme was not active with either monoester (Figure 3-5b, lanes 1-3) or diester (Figure 3-5b, 10-12). It was unexpected that C25 was not active with pure monoester since the monoester was the most abundant component in Sample **I**, and we have assumed that it was the substrate for C25 in catalyzing peptide bond formation (Zhang & Cech, 1997). The investigation of the real substrate for C25 will be reported elsewhere (Cui et al., in preparation). Here, we only focused on the comparison between the R180 and C25 ribozymes in using different substrates.

Nonetheless, the above results suggested that the R180 and C25 ribozymes share one common substrate, Biotin-Met-5'-AMP, in catalyzing dipeptide synthesis. It is very

a

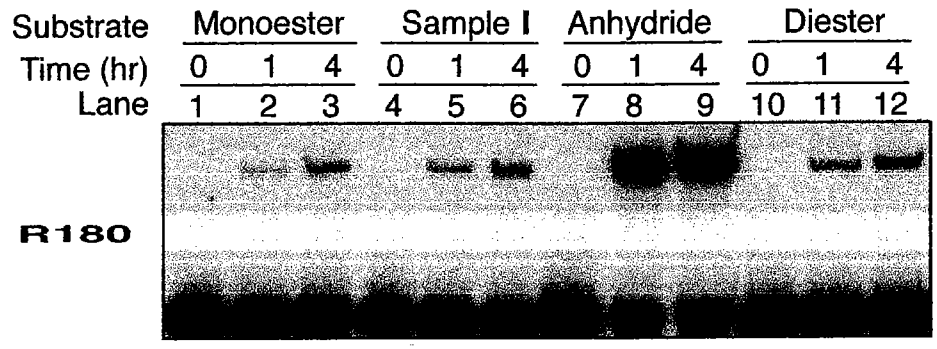

b

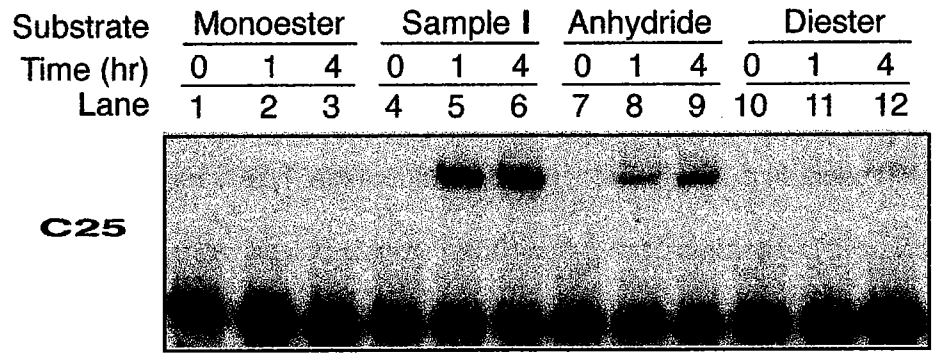

Figure 3-5. The peptide-synthesizing activity of the R180 and C25 ribozymes with different substrates. Reaction were performed with 1.5 μM 5'-Phe-SS-RNA (C25 or R180), 100 μM substrates in the presence of 100 mM $MgCl_2$, 300 mM KCl and 50 mM HEPES (pH 7.4) at 25 °C.

likely that these two ribozymes show distinct specificity upon the substrate binding since they differ in their primary sequences, secondary structures and catalytic activities.

Amino Acid Specificity for The R180 and C25 Ribozymes

Non-ribosomal peptide synthesis and polyketide biosynthesis use an exceedingly diverse group of precursors for assembling peptide and polyketide compounds (Kleinkauf & Von Dohren, 1990). To investigate the amino acid specificity of the R180 and C25-catalyzed peptide bond formation, we employed a series of biotin-aminoacyl-5'-AMP anhydrides with different 5'-aminoacyl'-SS-GMPS-RNAs. In order to examine amino acid specificity at both donor and acceptor sites, we prepared six biotin-aminoacyl-AMP anhydrides [aminoacyl: methionine (Met), leucine (Leu), glutamine (Gln), phenylalanine (Phe), arginine (Arg), and alanine (Ala)] and five 5'-aminoacyl'-SS-GMPS-RNAs [aminoacyl': Phe, Leu, Gln, tryptophan (Trp), and lysine (Lys)]. 5'-Aminoacyl'-SS-GMPS-RNAs were prepared by a two-step chemical linkage from 5'-GMPS-RNA: briefly, the *in vitro* transcribed 5'-GMPS-RNA was reacted with *N,N'*-bis(bromoacetyl)-cystamine and then treated with DTT to yield 5'-cysteamine-GMPS-RNA that was coupled with aminoacyl'-pyridyldithioethyl amide to produce 5'-aminoacyl'-SS-GMPS-RNA (the detailed synthesis will be described elsewhere).

The R180-mediated reactions of six biotin-aminoacyl-AMP anhydrides with five 5'-aminoacyl'-SS-GMPS-RNAs were studied. Surprisingly, all six aminoacyl donors and five aminoacyl acceptors were actively used by the R180 ribozyme, and the activity observed in each case was quite similar. The rate constants for all thirty reactions catalyzed by the R180 ribozyme are listed in Table 3-1. The observed rate constant of

Table 3-1. The observed rate constants of different combinations of five 5'-aminoacyl-SS-GMPS-R180 with six biotin-amidocaproyl-aminoacyl-AMP phosphoanhydrides*.

Entry	Substrate	Ribozyme	$k_{obs.}$ (min^{-1})	Relative rate
1	**Biotin-Met-AMP**	5'-Phe-SS-GMPS-R180	**0.76 ± 0.18**	**1.00**
2	Biotin-Phe-AMP		0.20 ± 0.06	0.26
3	Biotin-Leu-AMP		0.17 ± 0.05	0.22
4	Biotin-Gln-AMP		0.31 ± 0.05	0.41
5	Biotin-Arg-AMP		0.32 ± 0.03	0.42
6	Biotin-Ala-AMP		0.36 ± 0.02	0.47
7	Biotin-Met-AMP	5'-Lys-SS-GMPS-R180	0.19 ± 0.02	0.25
8	Biotin-Phe-AMP		0.027 ± 0.008	0.04
9	Biotin-Leu-AMP		0.034 ± 0.007	0.05
10	Biotin-Gln-AMP		0.16 ± 0.02	0.21
11	Biotin-Arg-AMP		0.12 ± 0.01	0.16
12	Biotin-Ala-AMP		0.17 ± 0.02	0.22
13	Biotin-Met-AMP	5'-Gln-SS-GMPS-R180	0.17 ± 0.01	0.22
14	Biotin-Phe-AMP		0.022 ± 0.007	0.03
15	Biotin-Leu-AMP		0.031 ± 0.005	0.04
16	Biotin-Gln-AMP		0.16 ± 0.02	0.21
17	Biotin-Arg-AMP		0.11 ± 0.02	0.14
18	Biotin-Ala-AMP		0.16 ± 0.03	0.21
19	Biotin-Met-AMP	5'-Leu-SS-GMPS-R180	0.36 ± 0.03	0.47
20	Biotin-Phe-AMP		0.089 ± 0.017	0.12
21	Biotin-Leu-AMP		0.076 ± 0.019	0.10
22	Biotin-Gln-AMP		0.23 ± 0.02	0.30
23	Biotin-Arg-AMP		0.19 ± 0.02	0.25
24	Biotin-Ala-AMP		0.17 ± 0.003	0.22
25	Biotin-Met-AMP	5'-Trp-SS-GMPS-R180	0.27 ± 0.01	0.36
26	Biotin-Phe-AMP		0.037 ± 0.009	0.05
27	Biotin-Leu-AMP		0.040 ± 0.010	0.05
28	Biotin-Gln-AMP		0.17 ± 0.04	0.22
29	Biotin-Arg-AMP		0.14 ± 0.01	0.18
30	Biotin-Ala-AMP		0.17 ± 0.04	0.22

*All reactions were performed with 0.5 μM 5'-aa-SS-GMPS-R180 and 50 μM biotin-aminoacyl-AMP in the presence of 300 KCl, 100 $MgCl_2$ and 50 mM HEPES (pH 7.4) at 25 °C. Rate constants were obtained by averaging three or more kinetic runs. Other conditions are as described in the method section. Entry 1 (bold) is the prototype ribozyme.

the prototype reaction of Biotin-Met-5'-AMP with 5'-Phe-SS-GMPS-R180 was 0.76 min^{-1}, which was 35-fold faster than the slowest reaction of 5'-Gln-SS-GMPS-R180 with Biotin-Phe-5'-AMP (0.022 min^{-1}). The observed rate constants of twenty-one combinations were between 0.11 min^{-1} and 0.37 min^{-1}, a range of less than four folds. The order of the peptide bond-forming activity of the aminoacyl donor was Met > Ala ≈ Gln ≈ Arg > Leu ≈ Phe, but the range of the relative rates was less than eight folds. The Biotin-Gln-5'-AMP and Biotin-Arg-5'-AMP, both having polar chains, were better substrates than Biotin-Phe-5'-AMP and Biotin-Leu-5'-AMP with aromatic and aliphatic side chains, respectively. However, the best substrate was Biotin-Met-5'-AMP with a linear neutral side chain. These results suggest that the steric nature of the side chain may be a more important factor than the hydrophilicity at the aminoacyl donor site. Among the aminoacyl acceptors, Phe was the best and four other acceptors (Lys, Leu, Gln, and Trp) displayed little difference, from polar Gln and Lys to the non-polar Leu and Trp. It is clear that the aminoacyl acceptor site of the R180 ribozyme can accept several different classes of amino acids.

Similar experiments were performed with the C25 ribozyme to examine the amino acid specificity on both donor and acceptor sites. The observed rate constants of the 5'-Phe-SS-C25 with six Biotin-aminoacyl-5'-AMP substrates and five 5'-aminoacyl-SS-GMPS-C25 with Biotin-Met-5'-AMP substrate were summarized in Table 3-2. All six aminoacyl donors were actively used by the C25 ribozyme and the activity difference was less than five folds. The C25 ribozyme also displayed no discrimination for amino acid at the acceptor site. These results suggest that amino acid also contributes little to substrate binding for the C25 ribozyme. The wide range of aminoacyl substrates showing

Table 3-2. The observed rate constants of five 5'-aminoacyl-SS-GMPS-C25 with Bio-Met-5'-AMP and 5'-Phe-SS-GMPS-C25 with six biotin-aminoacyl-5'-AMP.

Entry	Substrate	Ribozyme	$k_{obs.}$ (min^{-1})	Relative rate
1	**Biotin-Met-AMP**		**0.023 ± 0.001**	**1.00**
2	Biotin-Phe-AMP		0.018 ± 0.001	0.78
3	Biotin-Leu-AMP	5'-Phe-SS-GMPS-C25	0.009 ± .0003	0.39
4	Biotin-Gln-AMP		0.027 ± 0.024	1.17
5	Biotin-Arg-AMP		0.039 ± 0.004	1.69
6	Biotin-Ala-AMP		0.024 ± 0.002	1.04
7		5'-Phe-SS-GMPS-C25	0.023 ± 0.001	1.00
8		5'-Lys-SS-GMPS-C25	0.029 ± 0.003	1.26
9	Biotin-Met-AMP	5'-Leu-SS-GMPS-C25	0.025 ± 0.002	1.09
10		5'-Trp-SS-GMPS-C25	0.023 ± 0.004	1.00
11		5'-Gln-SS-GMPS-C25	0.028 ± 0.001	1.22

*All reactions were performed with 0.5 μM 5'-aa-SS-GMPS-C25 and 50 μM biotin-aminoacyl-AMP in the presence of 300 KCl, 100 $MgCl_2$ and 50 mM HEPES (pH 7.4) at 25 °C. Rate constants were obtained by averaging three or more kinetic runs. Other conditions are as described in the method section. Entry 1 (bold) is the prototype ribozyme.

similar activity is a remarkable feature of the R180 and C25 ribozymes, which makes these ribozymes ribosome-like because the ribosome recognizes 20 kinds of amino acids in making peptides. This phenomenon further suggests that catalytic RNAs might have existed in the ancient world to catalyze uncoded peptide synthesis.

Distinguished Recognition of The AMP Moiety on Bio-Met-5'-AMP by the R180 and C25 Ribozymes

The amino-acid-specificity experiments suggest that amino acid is not the substrate binding site for both R180 and C25 ribozymes. The AMP moiety in the substrate serves as the leaving group in both ribozyme-catalyzed reactions. To examine the role of AMP upon substrate binding, we designed eight kinds of substrate derivatives with substitution of the AMP moiety. Four types of nucleotide-leaving-group derivatives (Bio-Met-5'-AMP/GMP/CMP/UMP) and four types of non-nucleotide-leaving-group derivatives (Bio-Met-5'-IMI/PNP/NHS/CME) were chemically synthesized. Both C25 ribozyme and R180 ribozyme were tested for their activity with these substrate derivatives (Figure 3-6). The R180 ribozyme showed similar activity with all four Bio-Met-5'-NMP (Figure 3-6a) with rates of 0.50 min^{-1} for Bio-Met-5'-AMP, 0.30 min^{-1} for Bio-Met-5'-GMP, 0.53 min^{-1} for Bio-Met-5'-CMP, and 0.35 min^{-1} for Bio-Met-5'-UMP. However, the C25 ribozyme was only active with Bio-Met-5'-AMP (0.022 min^{-1}, Figure 3-6b, lanes1-6) while it was barely active with the other three Bio-Met-5'-G/C/UMP (Figure 3-6b, lanes 7-24). Similarly, all four non-nucleotide-leaving-group derivatives (Bio-Met-5'-IMI/PNP/NHS/CME) were active substrates for the R180 ribozyme (Figure 3-6c, lanes 6-25), but not active for the C25 ribozyme (Figure 3-6d, lanes 6-25). The

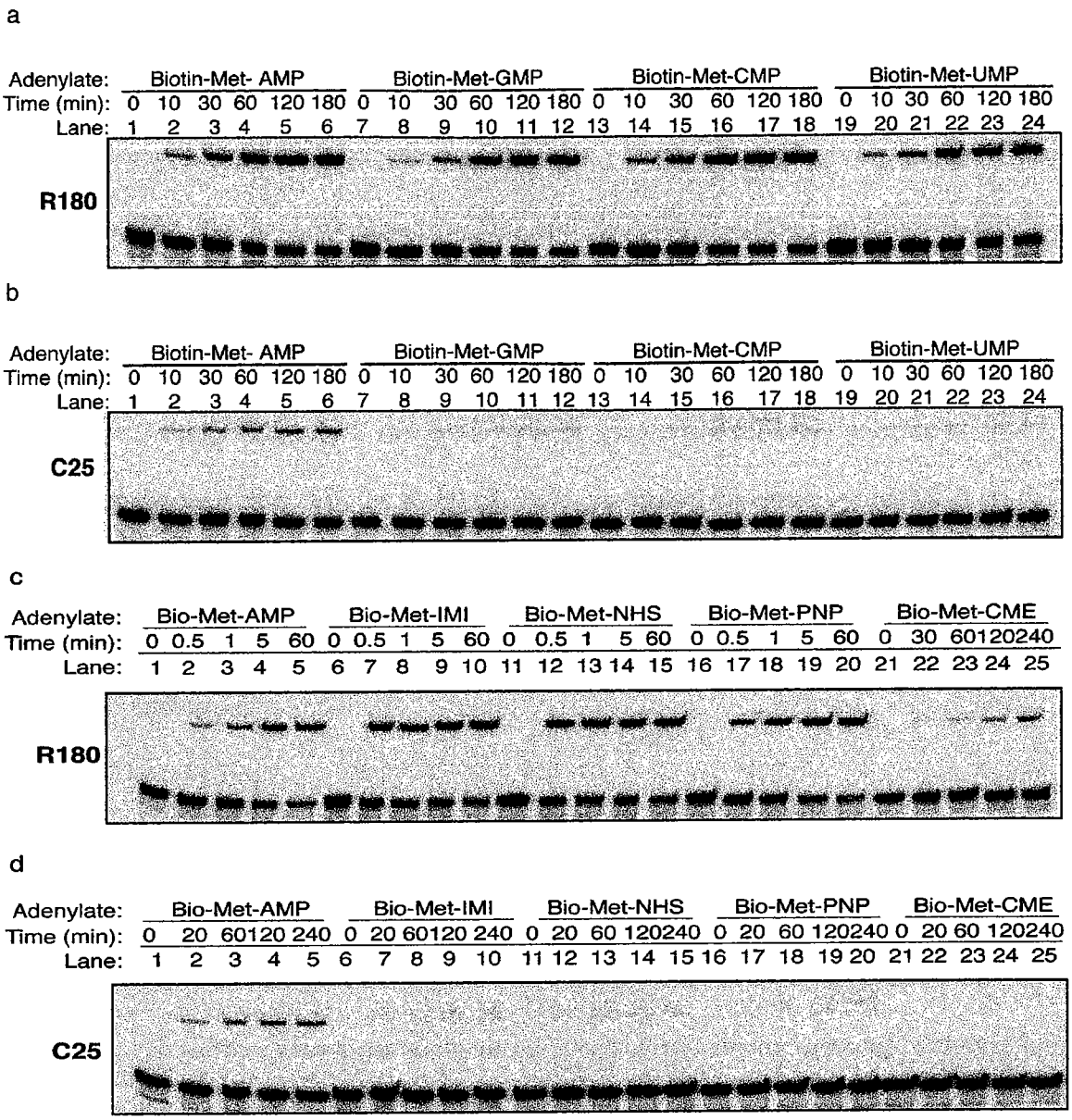

Figure 3-6. Dipeptide-synthesis activity by the R180 ribozyme (a, c) or the C25 ribozyme (b, d) with different substrate derivatives. a & b shows the activity with Bio-Met-5'-NMP (AMP, GMP, CMP, UMP) substrates, c & d shows the activity with Bio-Met-5'-X substrates. IMI: Imidazole, NHS: NH ester, PNP: Pyronitrophenol, CME: cyanolmetholester. Reaction were performed with 0.5 μM 5'-Phe-SS-RNA (C25 or R180), 50 μM Biotin-Met-5'-NMP in the presence of 100 mM $MgCl_2$, 300 mM KCl and 50 mM HEPES (pH 7.4) at 25 °C.

R180 ribozyme was even more active with Bio-Met-5'- IMI/PNP/NHS than with Bio-Met-5'-AMP, indicating that IMI/PNP/NHS are more active leaving groups than AMP; the activity with Bio-Met-5'-CME was lower since CME is a poor leaving group. These results suggest that the AMP moiety of Bio-Met-5'-AMP is strongly and specifically recognized by the C25 ribozyme, but not by the R180 ribozyme.

Altogether, the amino-acid-specificity and the leaving-group-substitution experiments suggest that the R180 and C25 ribozymes show different specificity upon binding to the substrate. For the R180 ribozyme-mediated dipeptide synthesis, it is Biotin but not AMP or amino acid that plays an important role for substrate binding; however, for the C25 ribozyme-mediated dipeptide synthesis, AMP contributes most to substrate binding.

Long Peptide Synthesis by the R180 and C25 Ribozymes

The common characteristics of the R180 and C25 ribozymes is that they show no specificity for amino acids at both donor and acceptor sites in catalyzing dipeptide synthesis. We further investigated whether C25 and R180 ribozymes could catalyze long peptide synthesis by elongating the number of amino acids at both the donor and the acceptor sites. At the peptidyl acceptor site, Phe was replaced by Phe-Cys and 5'-Phe-Cys-S-GMPS-RNA was prepared as described in Experimental Procedures. At the donor site, a tri-aminoacyl adenylate was synthesized as Biotin-$(Gly)_3$-5'-AMP. Different combinations of 5'-Phe-SS-GMPS-RNA or 5'-Phe-Cys-S-GMPS-RNA with Biotin-Met-5'-AMP or Biotin-$(Gly)_3$-5'-AMP substrate were examined for tri-, tetra-, or penta-peptide synthesis (Figure 3-7, Table 3-3). Because the absolute catalytic activity of these

two ribozymes were different, we examined the efficiency of long peptide synthesis by comparing the relative rate of long peptide forming activity to the prototype dipeptide forming activity. R180 was active in catalyzing tripeptide (Figure 3-7a, lanes 11-15) and tetrapeptide (Figure 3-7a, lanes 6-10) synthesis, but it could barely catalyze pentapeptide synthesis (Figure 3-7a, lanes 16-20). The relative rates of R180-catalyzed long peptide synthesis were 0.10 for tripeptide and 0.04 for tetrapeptide synthesis, suggesting that the catalytic activity of R180 is greatly hampered by changing the length of the amino acids at either acceptor or donor site. In contrast, the C25 ribozyme was very active in catalyzing tri-, tetra-, and penta-peptide synthesis (Figure 3-7b, lanes 6-10, 11-15, 16-20) and the relative rates were 0.77 for tripeptide, 1.9 for tetrapeptide and 1.8 for pentapeptide synthesis. Therefore, the C25 ribozyme was more efficient in catalyzing long peptide synthesis than the R180 ribozyme.

The different abilities of these two ribozymes in catalyzing long peptide synthesis might reflect their difference in substrate binding. For the R180 ribozyme, although Biotin was demonstrated to interact strongly with the ribozyme upon substrate binding, the general conformation of Bio-Met-5'-AMP might also contribute to the catalytic activity; while for the C25 ribozyme, only the AMP moiety was responsible for substrate binding and contributed most to the catalytic activity. Thus replacement of one Met residue with three Gly residues greatly hampered the R180 activity (Figure 3-7a, lanes 6-10, 16-20) while it didn't affect the C25 activity (Figure 3-7b, lanes 6-10, 16-20). When the amino acid residue (Phe) tethered to the 5' end of the RNA was prolonged to two amino acids (Phe-Cys), both ribozyme activities were decreased (Figure 3-7a, lanes 11-15; Figure 3-7b, lanes 11-15) suggesting the 5' distal region of the RNA are important for

a

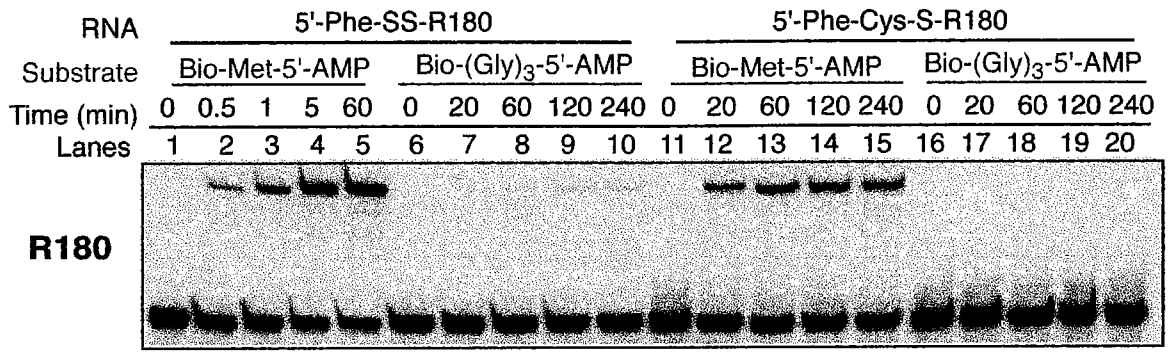

b

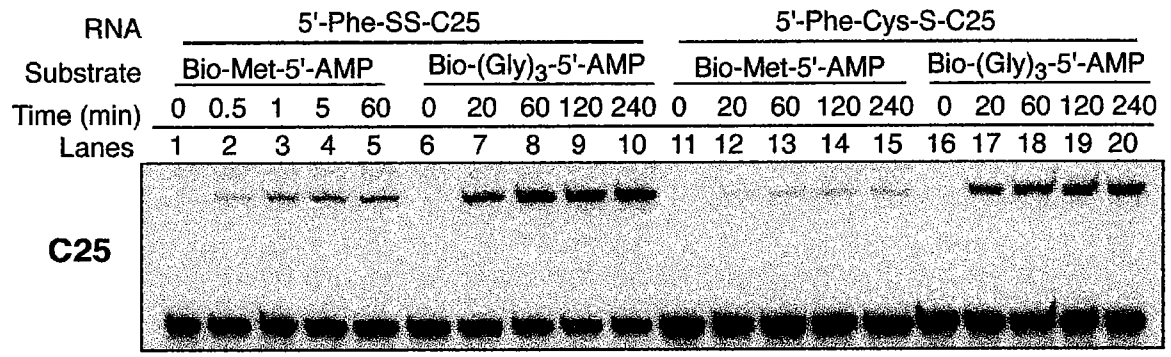

Figure 3-7. Longer peptide synthesis catalyzed by the R180 (a) and C25 (b) ribozymes. Reactions were performed with 1.0 μM 5'-Phe-SS-RNA or 5'-Phe-Cys-S-GMPS-RNA, 100 μM Biotin-Met-5'-AMP or Biotin-$(Gly)_3$-5'-AMP in the presence of 100 mM $MgCl_2$, 300 mM KCl and 50 mM HEPES (pH 7.4) at 25 °C.

Table 3-3. Comparison between the R180 ribozyme and the C25 ribozyme in catalyzing longer peptide synthesis.

	Bio-Met-5'-AMP		Biotin-$(Gly)_3$-5'-AMP	
	k_{obs} (min^{-1})	Relative rate	k_{obs} (min^{-1})	Relative rate
5'-Phe-SS-R180	**0.73 ± 0.03**	**1.0**	0.031 ± 0.005	0.04
5'-Phe-Cys-S-GMPS-R180	0.070 ± 0.002	0.10	---	---
5'-Phe-SS-C25	**0.035 ± 0.001**	**1.0**	0.065 ± 0.005	1.9
5'-Phe-Cys-S-GMPS-C25	0.027 ± 0.004	0.77	0.062 ± 0.004	1.8

Reactions were performed with 1.0 μM 5'-Phe-SS-RNA or 5'-Phe-Cys-S-GMPS-RNA, 100 μM Biotin-Met-5'-AMP or Biotin-$(Gly)_3$-5'-AMP in the presence of 100 mM $MgCl_2$, 300 mM KCl and 50 mM HEPES (pH 7.4) at 25 °C.
Relative rate = k_{obs} (tri, tetra, or pentapeptide synthesis) / k_{obs} (dipeptide synthesis).

catalysis perhaps by folding into an active conformation. We suspect that the catalytic center of R180 might be wrapped inside the ribozyme and leave narrow entrance for longer peptides; however, the C25 catalytic center might be open or big enough to accommodate longer peptides.

Conclusion

In summary, the highly active R180 ribozyme family has been selected in vitro to catalyze peptide bond formation using the aminoacyl-5'-adenylate as the substrate. A previous isolated ribozyme (the C25 ribozyme) could also employ the aminoacyl-5'-adenylate in catalyzing peptide bond formation. The R180 and C25 ribozymes exhibit differential recognition of the Bio-Met-5'-AMP substrate. However, both ribozymes demonstrate no amino acid specificity in catalyzing dipeptide synthesis. The C25 ribozyme is more efficient in catalyzing longer peptide synthesis than the R180 ribozyme.

Chapter IV

Characterization of the R180 Ribozyme Catalysis: Metal Ion Requirement, pH Dependence and Kinetics

In the last chapter, I have described the identification of a highly active peptide-synthesizing ribozyme (the R180 ribozyme) and investigated certain characteristics including secondary structure, amino acid specificity and substrate binding specificity. Another important aspect of ribozyme catalysis is the metal ions. It is well known that most ribozymes require metal ions for activity, particularly divalent metal ions. Divalent metal ions are essential for the structural folding and catalytic function of ribozymes. It was once thought that all ribozymes might be metalloenzymes (Pyle, 1993; Pyle, 1996; Hanna & Doudna, 2000). For instance, extensive studies have categorized the *Tetrahymena thermophila* group I intron as a metalloenzyme (Cech et al., 1981; Golden et al., 1998; Basu et al., 1998; Strobel, 1998) and its catalysis is mediated through a three-metal-ion mechanism (Weinstein et al., 1997; Shan et al., 1999; Strobel & Ortoleva-Donnelly, 1999). However, recent experiments have provided evidence that some ribozymes can act in the absence of divalent metal ions. Three small naturally occurring ribozymes (hammerhead, hairpin, and *Neuropora* VS) are active in the presence of high concentrations of monovalent metal ions alone (Murray et al., 1998), suggesting that a high positive charge density rather than divalent metal ion per se is the fundamental requirement for ribozyme catalysis (Murray et al., 1998). In subsequent studies, nearly all modified hammerhead ribozymes have shown similar deleterious effects in both divalent and monovalent metal ions (O'Rear et al., 2001), and the pH dependence of

hammerhead cleavage is similar between divalent and monovalent metal ions (Curtis & Bartel, 2001), suggesting that these metal ions might promote catalysis by facilitating correct conformational folding and that the direct chemical role of metal ions in hammerhead catalysis could be minor. The basis for the different abilities of divalent and monovalent metal ions to promote ribozyme catalysis is not very clear but could reflect their difference in the positive charge density and the geometry of hydration of the ions (Murray et al., 1999; Curtis & Bartel, 2001; O'Rear et al., 2001; Takagi et al., 2001).

In this chapter, the pH dependence and metal ion requirement of the peptidyltransferase *cis*-ribozyme (R180) and *trans*-ribozyme (TR158) are presented. A hypothesized mechanism of the peptide bond formation catalyzed by the ribozyme is also proposed.

Experimental Procedures

Ribozymes preparation. The R180 and TR158 ribozymes were prepared by run-off transcription using the corresponding cDNA templates. The R180 ribozyme was re-engineered by deleting 22 nucleotides at the 5' end and mutating C24 to G. The resulted *trans* ribozyme (TR158) was 22-nt shorter than the R180 ribozyme. Transcription reactions were carried out in 40 mM Tris•HCl (pH 7.4), 12 mM $MgCl_2$, 40 mM DTT, 4 mM spermidine, and 0.08% Triton X-100 with 5 μg of DNA template per 100 μl reaction at 37 °C. The ^{32}P-labeled R180 ribozymes were synthesized in the presence of 10 μCi/200μl reaction of α-^{32}P-ATP, 2 mM each ATP/GTP/CTP/UTP, and 32 mM guanosine-5'-monophosphorothioate (GMPS). The TR158 ribozymes were synthesized

in the presence of 2 mM each ATP/GTP/CTP/UTP only. Both ^{32}P-labeled R180 ribozymes and non-labeled TR158 ribozymes were purified by 8% polyacrylamide /7.5 M urea denaturing gel electrophoresis (PAGE). Ribozymes were visualized by UV. The gel containing the ribozymes was excised, squeezed through a syringe, and soaked in TE buffer (10 mM Tris and 1 mM EDTA buffer, pH 7.4) at 4 °C overnight. Then the soaking solution was separated from the gel by filtration and centrifugation at 5,000 g for 10 minutes. Both ribozymes were precipitated by 250 mM NaCl and cold ethanol in dry ice for two hours. The TR158 ribozymes were then resuspended in deionized water and stored at -20 °C. The ^{32}P-labeled 5'-GMPS-R180 RNAs were further reacted with 100 mM either Phe-NH$(CH_2)_2$-S-S-$(CH_2)_2$NH-C(O)CH_2Br (disulfide linker) or Phe-NH$(CH_2)_6$NH-C(O)CH_2Br (non-cleavable linker) in the presence of 40 mM HEPES (pH 7.8), 150 mM NaCl, and 10 mM EDTA. The coupling reactions were carried out by continuously rotating at room temperature for 3 hours. Then, the reaction mixtures were extracted by phenol/chloroform to remove excess linker. Finally, the 5'-Phe-R180 ribozymes were precipitated in cold ethanol, resuspended in deionized water and stored at -20 °C for kinetic studies.

Preparation of 5'-Phe-linker-20-mer substrates for the *trans* reaction. The 20-mer RNA oligonucleotide (GGGAGAGACCUGCCAUUCAC, the first 20-nt sequence at the 5' end of the R180 ribozyme) were chemically synthesized and labeled with γ-^{35}S-ATP by T4 polynucleotide kinase (PNK). The labeling reaction was performed with 10 nmol of 20-mer RNA oligonucleotides, 200 units of PNK, and 200 pmol (250 μCi) of γ-^{35}S-ATP in the presence of 70 mM Tris-HCl (pH 7.6), 10 mM $MgCl_2$ and 5 mM DTT at 37 °C for 2 hours. Then an excess of γ-thiophosphate-ATP (4.5

mM) was added in order to convert all 20-mer RNA oligonucleotides into 5'-thiophospate-20-mer RNAs. The ^{35}S-labeled 20-mer RNA oligonucleotides were purified by 20% polyacrylamide/7.5 M urea denaturing gel and linked to either disulfide linker or non-cleavable linker as described above. The resulted 5'-Phe-linker-20-mer substrates were stored at –20 °C for the *trans* reactions.

Metal cation dependence. Kinetic analyses were performed with different species and various concentrations of metal cations. The metal cation requirement for the ribozyme-catalyzed reaction was examined by both *cis*- and *trans*-reaction systems. Reactions were performed with 0.5 μM 5'-Phe-R180 ribozyme for *cis*-reactions or 10 μM TR158 ribozyme and 0.1 μM 5'-Phe-linker-20 mer for *trans*-reaction, and 500 μM Bio-Met-AMP substrate in the presence of 50 mM Bis•Tris propane buffer (pH 7.4) and 10 mM Mg^{2+}, Ca^{2+}, Zn^{2+}, Cu^{2+}, Mn^{2+}, Co^{2+}, $Co(NH_3)_6^{3+}$, or 1.0 M Li^+, Na^+, K^+, NH_4^+. The metal-cation concentration dependence were assayed in the presence of 1~800 mM Mg^{2+}, 300~2000 mM Li^+, or 600~1875 mM K^+. For monovalent cations, 25 mM EDTA was included in the reactions. The observed rate constants (k_{obs}) were obtained for each specific concentration with a single kind of metal ion. The data were analyzed by KaleidaGraph software.

pH dependence and isotope effects. Kinetic analyses were performed as described above at different pHs with both *cis*- and *trans*-reaction systems. The pH buffers used in the reactions were 50 mM MES for pH 5.5~6.5 and 50 mM Bis•Tris propane for pH 6.5~9.0. For *cis* reactions, pH dependence assays were performed with 0.5 μM R180 ribozyme, 100 μM Bio-Met-AMP, and 50 mM buffer in the presence of either 100 mM Mg^{2+} or 1.0 M Li^+. The observed rate constants were log plotted against

pH [log (k_{obs}) vs. pH]. For *trans* reactions, pH dependence was examined with 10 μM TR158 ribozyme, 0.1 μM 5'-Phe-20-mer substrate, 100 μM Bio-Met-AMP, and 50 mM pH buffer in the presence of either 10 mM Mg^{2+} or 1.0 M Li^{+}. At each specific pH value, the reactions were carried out at different concentrations of Bio-Met-AMP substrate (10~700 μM for Mg^{2+}, 50~2000 for Li^{+}) to generate Michaelis-Menten curves. k_{cat} and K_m values were obtained from the Michaelis-Menten plots at each pH. The relationship between k_{cat} and pH was displayed by plotting log (k_{cat}) vs. pH.

For the solvent isotope experiments, all buffers were made in 99.9% D_2O, lyophilized, and re-dissolved in 99.9% D_2O (repeat twice) to exhaust any exchangeable proton. pD was calculated by adding 0.4 to a pH meter reading (titrated with KOD). Salts, ribozyme, and substrate were lyophilized, dissolved in 99.9% D_2O, and this process was repeated twice. pD dependence experiments of the *trans* TR158-catalyzed dipeptide-forming reaction were performed as described above. The observed rate constants were log plotted against pD [log (k_{obs}) vs. pD].

Kinetics studies. For *cis* reactions, 0.5 μM R180 ribozyme was preincubated with 1~1000 mM metal cations in the presence of 50 mM Bis•Tris propane buffer (pH 7.5) at 50 °C for 10 min, and then the mixture was slowly cooled down to room temperature. The reaction was initiated by addition of Bio-Met-AMP anhydride substrate at 25 °C. 1 μl aliquot of the reaction mixture was removed from the reaction tube at the specific time points, quenched with 2 μl of quench buffer (50 mM HEPES, pH 7.5, 25 mM EDTA, 90% formamide dye with 0.09% bromphenol blue and 0.09% xylene cyanol FF), and stored in dry ice. Each sample was incubated with 10 μg of streptavidin at room temperature for 15~20 minutes prior to being loaded on 8% polyacrylamide /7.5 M urea

denaturing gel. Reaction products were quantitated by Molecular Dynamics Phosphorimager and the fraction of the product relative to the total reactant was plotted against different time points. The observed rate constants (k_{obs}) were obtained by curve fitting in KaleidaGraph.

For *trans* reactions, 10 μM TR158 ribozyme was mixed with 0.1 μM 5'-Phe-linker-20 mer substrate in the presence of 1~1000 mM metal cations and 50 mM Bis•Tris propane buffer (pH 7.5). Other conditions were same as described above except that all samples were directly loaded onto 20% polyacrylamide /7.5 M urea denaturing gel without streptavidin incubation.

Results

Trimolecular Reaction of Dipeptide Synthesis

The R180 ribozyme-catalyzed reaction was bimolecular in dimension with one amino acid (phenylalanine) covalently linked to the 5' end of the ribozyme as a peptidyl acceptor and the other substrate (Bio-Met-5'-AMP anhydride) as a peptidyl donor free in the solution (Figure 4-1a). In order to mimic most enzymatic reactions in which the enzyme is physically separated from its substrate prior to the binding and chemical steps, a trimolecular reaction was designed in which the ribozyme itself was separated from two amino acid substrates. Hence, we call the prototype bimolecular reaction the '*cis*-reaction', and the newly designed trimolecular reaction the '*trans*-reaction'.

Based on the secondary structure, a new substrate (5'-Phe-linker-20-mer) was designed as a 20-mer RNA oligonucleotide (5'-GGGAGAGACCUGCCAUUCAC-3')

a. R180-catalyzed biomolecular reaction (cis reaction)

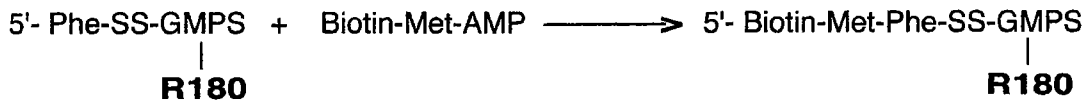

b.

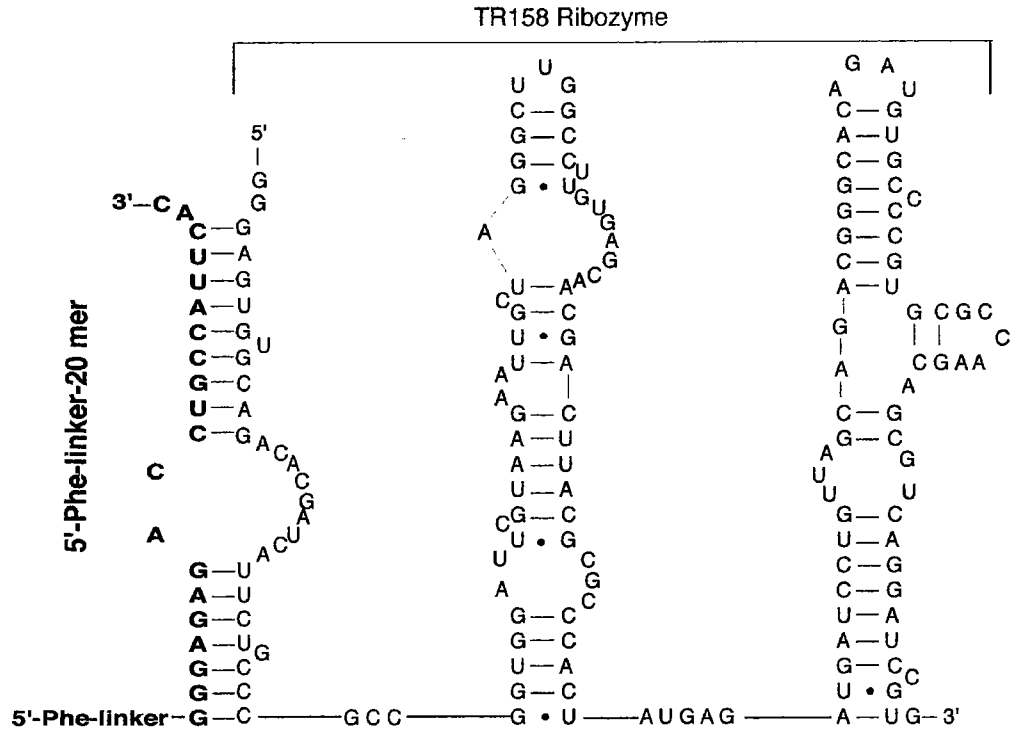

c. TR158-catalyzed trimolecular reaction (trans reaction)

Figure 4-1. (a) The peptide bond-forming reaction catalyzed by the R180 ribozyme (*cis*-reaction). Phenylalanine is covalently linked to the 5' end of the R180 ribozyme through a disulfide bond. Another substrate is the Bio-Met-AMP anhydride. Peptide bond is formed between the two amino acids (Phe and Met). (b) Design of the *trans* substrate based on the secondary structure of the R180 ribozyme. The new substrate was designed as a 20-mer RNA oligonucleotide (5'-GGGAGAGACCUGCCAUUCAC-3') linked with phenylalanine at the 5' end (bold). The 5'-end truncated *trans* ribozyme (TR158) is 22-nt shorter than the R180 ribozyme and C24 is mutated to G to create three Gs at the 5'-end of the RNA. (c) The peptide bond-forming reaction catalyzed by the TR158 ribozyme (*trams*-reaction).

linked with a phenylalanine at its 5' end (Figure 4-1b). Correspondingly, the R180 ribozyme was shortened by 22 nucleotides and the cytosine at position 24 was mutated to guanine to create three consecutive Gs at the 5' end of the *trans* ribozyme (TR158, Figure 4-1b). Therefore, the *trans*-reaction system contains three components: the TR158 ribozyme (158 nt), 5'-Phe-linker-20-mer, and Bio-Met-5'-AMP anhydride (Figure 4-1c).

Ribozyme activity was studied by comparison between the *cis*-reaction system and the *trans*-reaction system. Reactions were carried out with 0.5 μM 5'-Phe-R180 ribozymes for *cis*-reactions or 10 μM TR158 ribozymes and 0.1 μM of the 5'-Phe-linker-20-mer for *trans*-reactions in the presence of 100 mM Mg^{2+}, 300 mM K^{+}, and 500 μM Bio-Met-5'-AMP. In the *cis*-reaction system, phenylalanine was linked to the 5' end of the R180 ribozyme via either a disulfide linker (-$NH(CH_2)_2$-SS-$(CH_2)_2NHC(O)CH_2$-) or a noncleavable linker (-$NH(CH_2)_6NHC(O)CH_2$-). Similarly, in the *trans*-reaction system, phenylalanine was linked to the 5' end of 20-mer oligonucleotide with either the disulfide linker or noncleavable linker. Figure 4-2 showed the typical gel-shift assays for analyzing the ribozyme-catalyzed reactions. In the *cis*-reactions (Figure 4-2a), the top band corresponds to the complex of the biotinylated dipeptide attached to the 5' end of the R180 RNA (5'-Bio-Met-Phe-R180) with streptavidin, and the low band corresponds to 5'-Phe-linker-R180 RNA. In the *trans*-reactions (Figure 4-2b), the top band is the formed dipeptide linking to the 5' end of the 20 mer substrates (5'-Bio-Met-Phe-linker-20-mer), and the low band is the 5'-Phe-linker-20-mer RNA substrates. The R180 and TR158 ribozymes were fully active for dipeptide synthesis with over 80% yield at the reaction's final extent in both *cis* and *trans* systems. The observed rate constants of the peptide bond formation were 0.51 min^{-1} for the *cis*-reaction with a disulfide linker (lanes

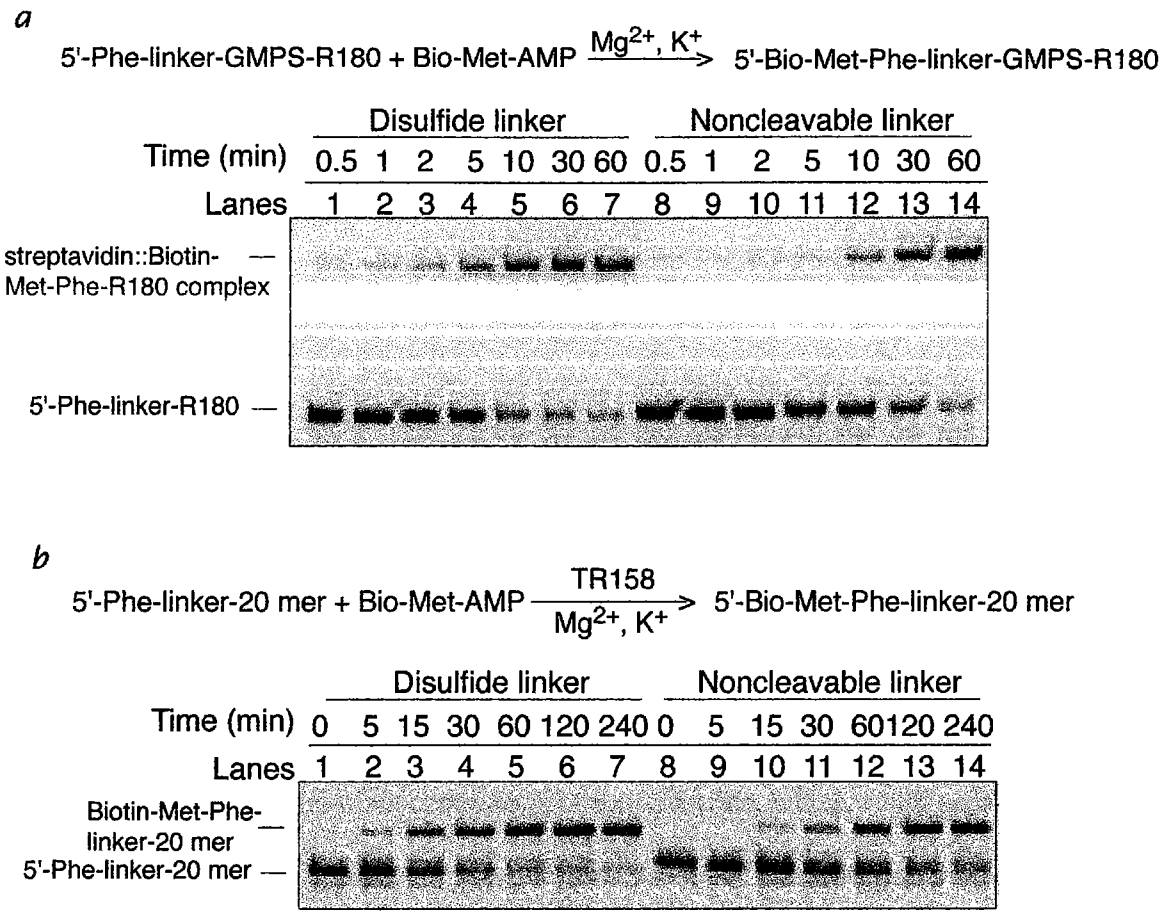

Figure 4-2. Autoradiograms of *cis*- and *trans*-reaction systems catalyzed by R180 and TR158 ribozymes. (a) *Cis*-reaction. The reactions were performed with 0.5 μM 5'-Phe-linker-R180 ribozymes, 500 μM Bio-Met-AMP in the presence of 100 mM $MgCl_2$, 300 mM KCl and 50 mM Bis•Tris propane buffer (pH 7.5). The phenylalanine substrate was linked to the 5' end of R180 via either a disulfide linker or a noncleavable linker. The top band corresponds to the product 5'-Bio-Met-Phe-R180 complexed with streptavidin, and the low band corresponds to the inactive R180 ribozymes (5'-Phe-R180). (b) *Trans*-reaction. The reactions were performed with 10 μM TR158 ribozyme, 0.1 μM 5'-Phe-linker-20-mer substrate, and 500 μM Bio-Met-AMP in the presence of 100 mM $MgCl_2$, 300 mM KCl and 50 mM Bis•Tris propane buffer (pH 7.5). The phenylalanine substrate was linked to the 5' end of the 20mer substrate via either a disulfide linker or a noncleavable linker. The top band corresponds to the formed dipeptide linked to the 5' end of the 20mer substrates (5'-Bio-Met-Phe-20-mer), and the lower band corresponds to the 5'-Phe-20-mer substrate.

1-7, Figure 4-2a), 0.14 min^{-1} for the *cis*-reaction with a noncleavable linker (lanes 8-14, Figure 4-2a), 0.21 min^{-1} for the *trans*-reaction with a disulfide linker (lanes 1-7, Figure 4-2b), and 0.081 min^{-1} for the *trans*-reaction with a noncleavable linker (lanes 8-14, Figure 4-2b). The ribozyme activities in the *cis*-reactions were higher than those in the *trans*-reactions, and the activities with the disulfide linker were higher than those with the noncleavable linker.

The advantage of the *trans*-reaction system is that the dipeptide product can be directly observed by loading onto a high-percentage polyacrylamide gel in the absence of streptavidin. The disadvantage of the *cis*-system in kinetic studies is that Bio-Met-5'-AMP at high concentrations will compete with the product (Bio-Met-Phe-R180) in binding with streptavidin; thus, the product formation observed in the gel-shift assay might be inaccurate at high concentrations of the substrate, which could lead to the imprecise estimation of the observed rate constants. The *trans*-reaction system overcomes this problem, and since the noncleavable linker is more stable than the disulfide linker, we have chosen the *trans*-reaction system with the noncleavable linker for the subsequent studies of the ribozyme-catalyzed dipeptide reactions. As a comparison, experiments have also been done using *cis*-reaction system with the disulfide linker.

Metal Ion Requirement

Meta Ion Specificity

We investigated the metal ion specificity of the dipeptide-forming reaction catalyzed by the R180 or TR158 ribozymes. The experiments on metal ion requirement

were performed with the *cis*-disulfide and *trans*-noncleavable systems in the presence of a single kind of metal ion only. Figure 4-3 shows the ribozyme activities with the different metal ions: Figures 4-3a and 4-3b are the *cis*-disulfide reactions and Figures 4-3c and 4-3d are the *trans*-noncleavable reactions. In the absence of any metal ion at all, no product was formed (lanes 1-3, Figure 4-3a; lanes 1-4, Figure 4-3c) in either system. Both ribozymes were active in Mg^{2+} or Ca^{2+} alone, and Ca^{2+} was even better than Mg^{2+} (lanes 4-9, Figure 4-3a; lanes 5-14, Figure 4-3c). However, the ribozymes were not active with Zn^{2+}, Cu^{2+}, Mn^{2+}, or Co^{2+} alone (lanes 10-21, Figure 4-3a; lanes 15-30, Figure 4-3c). To examine whether Mg^{2+} could promote catalysis through the outer-sphere-mediated effect, the reactions were also performed in the presence of 10 mM $Co(NH_3)_6^{3+}$ (lanes 22-24, Figure 4-3a; lanes 31-34, Figure 4-3c) since $Co(NH_3)_6^{3+}$ has a similar atomic geometry to $Mg(H_2O)_6^{2+}$ (Jou & Cowan, 1991; Hampel & Cowan., 1997; Young et al., 1997; Suga et al., 1998). Both ribozymes were not active with $Co(NH_3)_6^{3+}$, suggesting that $Co(NH_3)_6^{3+}$ cannot replace $Mg(H_2O)_6^{2+}$ in catalyzing the dipeptide formation through an outer-sphere-mediated effect (Misra & Draper, 1998).

The above results indicate that divalent metal ions are important for the R180 and TR158 ribozymal activities. However, the recent studies reveal that the naturally occurring hammerhead, hairpin, and *Neuropora* VS ribozymes are active in the presence of monovalent metal ions alone (Murray et al., 1998; Curtis & Bartel, 2001; O'Rear et al., 2001), suggesting that not all naturally occurring ribozymes require divalent metal ions for catalysis. We examined the activities of the R180 and TR158 ribozymes in the presence of monovalent cations alone. Four kinds of monovalent ions (Li^+, Na^+, K^+, and NH_4^+) were tested (Figure 4-3b for R180 and Figure 4-3d for TR158). In these reaction

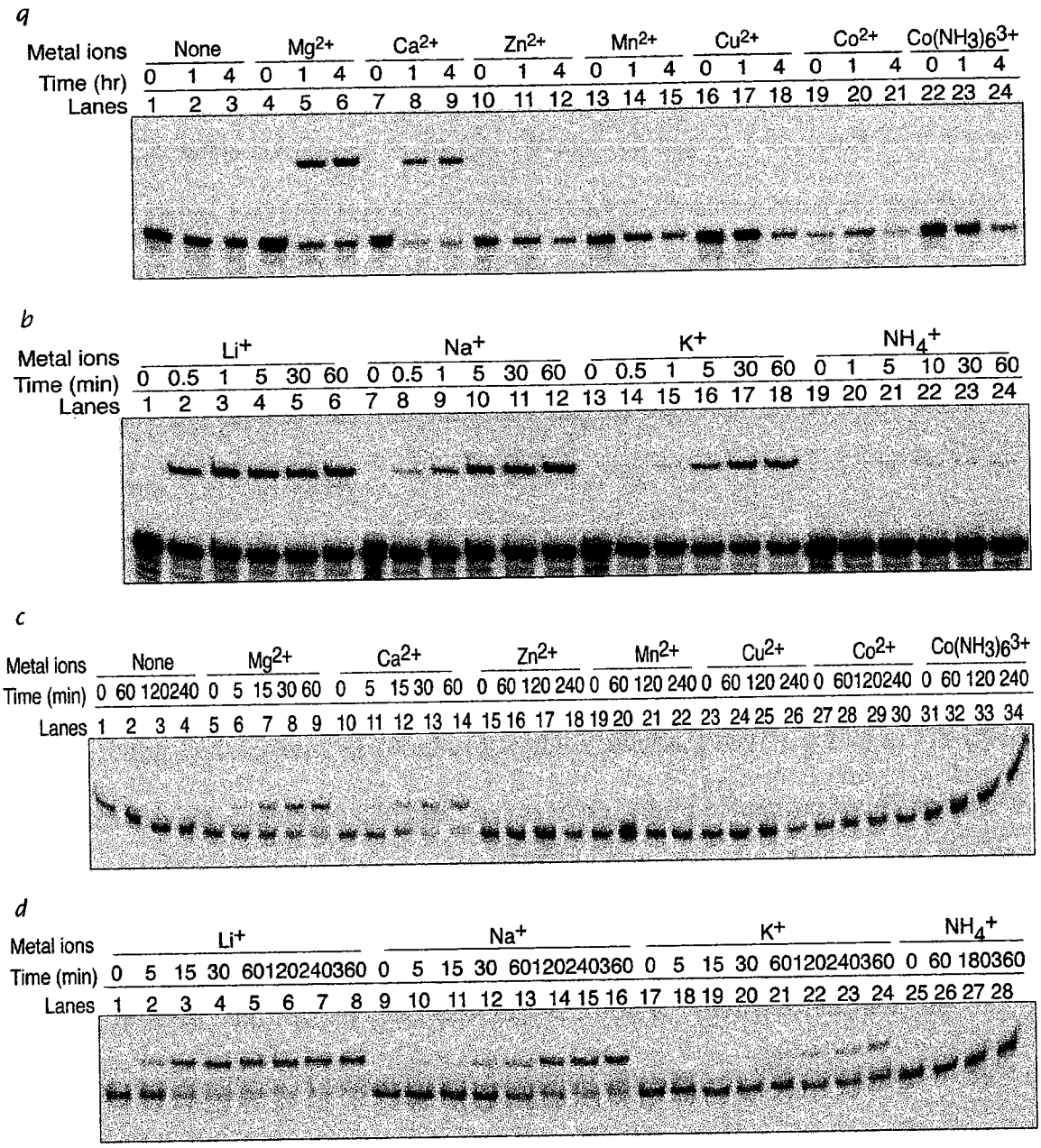

Figure 4-3. Autoradiograms of metal ion specificity of the dipeptide synthesis by *cis*- and *trans*-ribozymes. *Cis*-reactions were performed with 0.5 μM 5'-Phe-R180 ribozymes, 500μM Bio-Met-AMP substrate and 50 mM Bis•Tris propane buffer (pH 7.4) in the presence of 10 mM Mg^{2+}, Ca^{2+}, Zn^{2+}, Cu^{2+}, Mn^{2+}, Co^{2+}, $Co(NH_3)_6^{3+}$ (a) or 1.0 M Li^+, Na^+, K^+, $NH4^+$ (b). *Trans*-reactions were performed with 10 μM TR158 ribozymes, 0.1 μM of the 5'-Phe-linker-20-mer substrate, 500μM Bio-Met-AMP substrate in the presence of 50 mM Bis•Tris propane buffer (pH 7.4) and 10 mM Mg^{2+}, Ca^{2+}, Zn^{2+}, Cu^{2+}, Mn^{2+}, Co^{2+}, $Co(NH_3)_6^{3+}$ (c) or 1.0 M Li^+, Na^+, K^+, $NH4^+$ (d).

conditions, 25 mM EDTA were included in order to remove any trace amount of divalent metal ions. Excitingly, both ribozymes were highly active in the presence of Li^+ (lanes 1-6, Figure 4-3b; lanes 1-8, Figure 4-3d), Na^+ (lanes 7-12, Figure 4-3b; lanes 9-16, Figure 4-3d), or K^+ (lanes 13-18, Figure 4-3b; 17-24, Figure 4-3d) alone; but there was no or very low activity with NH_4^+ alone (lanes 19-24, Figure 4-3b; lanes 25-28, Figure 4-3d). These results suggest that both R180 and TR158 ribozymes do not require divalent metal ions in catalyzing peptide bond formation and they are very active with monovalent cations alone.

The observed rate constants of peptide bond formation by the R180 or TR158 ribozymes in 10 mM divalent or 1.0 M monovalent metal ions are summarized in Table 4-1. In *cis*-reaction, the observed rate constants were 0.12 min^{-1} in 10 mM Mg^{2+} (third column, entry 1), 0.15 min^{-1} in 10 mM Ca^{2+} (third column, entry 2), 0.24 min^{-1} in 1.0 M Li^+ (third column, entry 3), 0.026 min^{-1} in 1.0 M Na^+ (third column, entry 4), and 0.015 min^{-1} in 1.0 M K^+ (third column, entry 5). Both divalent metal ions showed similar activity for the R180 ribozyme but the activity in 1.0 M Li^+ was about 10-fold faster than that in 1.0 M Na^+ and 16-fold faster than that in 1.0 M K^+. In *trans*-reaction, the observed rate constants of peptide bond formation catalyzed by TR158 ribozyme were 0.067 min^{-1} in 10 mM Mg^{2+} (last column, entry 1), 0.099 min^{-1} in 10 mM Ca^{2+} (last column, entry 2), 0.18 min^{-1} in 1.0 M Li^+ (last column, entry 3), 0.029 min^{-1} in 1.0 M Na^+ (last column, entry 4), and 0.022 min^{-1} in 1.0 M K^+ (last column, entry 5). The observed rate constant of the *trans*-reaction in 1.0 M Li^+ was 6-9 times larger than that in 1.0 M Na^+ and K^+. Interestingly, the peptide bond forming reaction in 1.0 M Li^+ was 2-fold faster than that in 10 mM Mg^{2+} or Ca^{2+} in both *cis*- and *trans*-reactions. The order of the

Table 4-1. Ribozyme activity in the presence of divalent and monovalent metal ions measured by *cis*- and *trans*-reaction systems.[a]

No.	Metal ions	Observed rate constants (k_{obs}) (min^{-1})	
		***Cis*-reaction**	***Trans*-reaction**
1	10 mM Mg^{2+}	0.12 ± 0.01	0.067 ± 0.009
2	10 mM Ca^{2+}	0.15 ± 0.03	0.099 ± 0.027
3	1.0 M Li^{+}	0.24 ± 0.08	0.18 ± 0.03
4	1.0 M Na^{+}	0.026 ± 0.002	0.029 ± 0.002
5	1.0 M K^{+}	0.015 ± 0.0001	0.020 ± 0.001

a) The observed rate constants were measured with both cis and *trans* systems in the presence of different metal ions. The dipeptide-forming reactions were carried out with 0.5 μM R180 ribozyme and 100 μM Bio-Met-AMP for the *cis*-system and 10 μM TR158 ribozyme, 100 μM Bio-Met-AMP, 0.1 μM 5'-Phe-linker-20-mer for the *trans*-system in the presence of 10 mM Mg^{2+} or Ca^{2+}, or 1.0 M Li^{+}, Na^{+}, K^{+} alone at 25 °C.

ribozyme activity in monovalent ions is $Li^+ > Na^+ > K^+ >> NH_4^+$. As we know, the order of the of the charge density is $Li^+ > Na^+ > K^+ > NH_4^+$ and the classical ion radius of four monovalent ions is of course $Li^+ < Na^+ < K^+ < NH_4^+$. Also, the hard metal ions (Martin, 1986), like Li^+, Na^+, K^+, Mg^{2+}, Mn^{2+}, or Fe^{3+}, preferentially interact with hard oxygen sites of the phosphate groups of nucleic acids. Li^+ can form stronger complexes with phosphate than Na^+ (Pregel et al., 1995). Our results are in good agreement with the observation that the order of the binding affinity of alkali-metal ions with phosphate diester was $Li^+ > Na^+ > K^+ > Cs^+$ by the study of alkali-metal ion catalysis in nucleophilic displacement reactions of phosphate diester (Pregel et al., 1995). The ribozymes reached full activity in 1.0 M Li^+, and this concentration is much lower than the reported value (4.0 M) in which the small natural ribozymes still couldn't reach their full activity as in the presence of divalent metal ions (Murray et al., 1998). Therefore, the R180 and TR158 ribozymes are the first example of *in vitro* selected ribozymes that is fully active in the presence of monovalent metal ions alone. It would be interesting to understand the roles played by monovalent metal ions in this ribozyme's folding and functions.

Metal Ion Concentration Dependence

The concentration dependence of the ribozyme activity was studied at different concentrations of Mg^{2+}, Li^+, or K^+ in both *cis*-disulfide and *trans*-noncleavable systems. Figure 4-4a shows the concentration-dependence results for the R180 ribozyme and Figure 4-4b shows the results of the TR158 ribozyme. In the Mg^{2+}-catalyzed reactions, the plot of $\log(k_{obs})$ `vs.` $[Mg^{2+}]$ displayed a linear relationship between 1.0 mM and 10 mM Mg^{2+} for the TR158 ribozyme, then the ribozyme activity increased slowly when

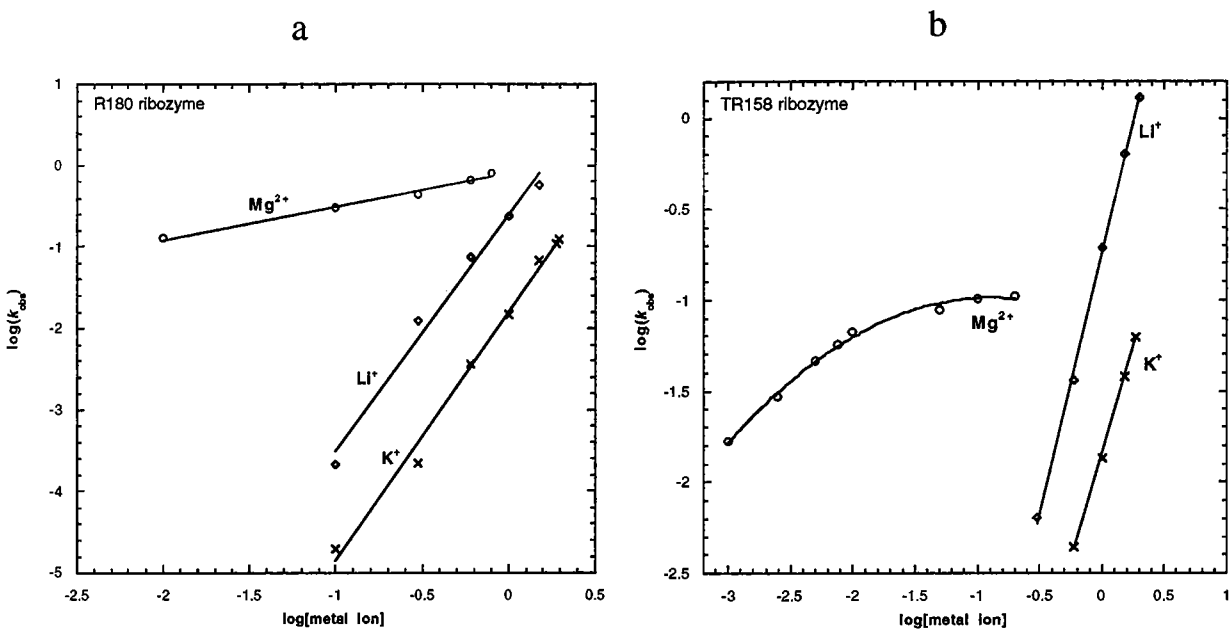

Figure 4-4. Metal ion concentration dependence of the ribozyme catalysis in the presence of Mg^{2+} (O), Li^{+} (●), or K^{+} (X) by R180 and TR158 ribozymes. (a) *Cis*-reactions were performed with 0.5 μM R180 ribozyme, 500μM Bio-Met-AMP substrate, and 50 mM Bis•Tris propane buffer (pH 7.4) in 10~800 mM Mg^{2+}, 100~1500 mM Li^{+}, or 100~1925 mM K^{+}. The lines were drawn as linear with best-fit slopes of 0.41 for Mg^{2+}, 2.91 for Li^{+}, and 3.04 for K^{+}. (b) *Trans*-reactions were performed with 10 μM TR158 ribozyme, 0.1 μM 5'-Phe-linker-20mer substrate, 500μM Bio-Met-AMP substrate, and 50 mM Bis•Tris propane buffer (pH 7.4) in 1~200 mM Mg^{2+}, 300~2000 mM Li^{+}, or 600~1875 mM K^{+}. The lines were drawn as linear with best-fit slopes of 0.6 for Mg^{2+}, 2.85 for Li^{+}, and 2.35 for K^{+}.

$[Mg^{2+}] > 10$ mM and finally reached saturation at $[Mg^{2+}] \geq 100$ mM (Figure 4-4b). This result is consistent with the described properties of most ribozymes whose activity is saturated at a certain concentration of magnesium and only a certain amount of magnesium is required for structural folding and functions of the ribozymes. However, the plot of $\log(k_{obs})$ vs. $[Mg^{2+}]$ for the R180 ribozyme gave a linear relationship (Figure 4-4a). No saturation of the R180 activity was observed up to 800 mM Mg^{2+}. This is a unique property for the R180 ribozyme compared to other ribozymes. The difference of Mg^{2+} concentration dependence between *trans*- and *cis*-systems might reflect the different microenvironment created by the two systems. Obviously, the secondary structures of the R180 and TR158 ribozymes are different (Figure 3-2b, 4-1b). The L1 hairpin loop in R180 ribozyme does not exist in the *trans* TR158 ribozyme. This change might cause the difference in the tertiary structural folding of the TR158 ribozyme, which might result in the observed difference in divalent metal ion dependence. Although these two systems gave different magnesium concentration dependencies, the best-fit slopes were 0.60 in the linear part of the *trans* reaction and 0.41 in the *cis* reaction, suggesting that both systems are about half-order dependence on the magnesium concentration. We speculate that the ribozyme's requirement in divalent metal ions is most likely for structural folding by neutralizing with phosphate negative charges of the RNA backbone. It is also possible that the divalent metal ions stabilize the transition state intermediate in the peptide bond forming reaction.

For monovalent metal ions, we observed a linear plot of $\log(k_{obs})$ vs. $[Li^+]$ or $[K^+]$ in both *cis*- and *trans*-reactions. No saturation was observed for the R180 and TR158 ribozyme-catalyzed reactions up to 2000 mM Li^+ and 1875 mM K^+. The slopes

of the plots were close to 3 with 2.91 for Li^+-*cis*, 2.85 for Li^+-*trans*, and 3.04 for K^+-*cis*, but the slope of the log(k_{obs}) vs. [K^+] was 2.35 for the K^+-*trans*-reaction. These results indicate that the reactions are about third-order dependent on Li^+ or K^+ concentration. Although both ribozymes required much high concentration of monovalent cations than divalent metal ions because the charge density of the divalent metal ions (Mg^{2+}, Ca^{2+}) is much higher than that of monovalent cations (Li, Na^+, and K^+), they are fully active in 1.0 M Li^+. In contrast, the activity of hammerhead ribozyme in 4.0 M Li^+ is 20-fold less than that in 10 mM Mg^{2+} and the presence of Mg^{2+} is required to achieve full activity (Murray et al., 1998; O'Rear et al., 2001). The concentration-dependence behavior of the R180 and TR158 ribozymes are different in divalent metal ions (half order) and monovalent metal ions (third order), which is similar with what has been observed in the hammerhead ribozyme (first-order dependent on Mg^{2+} and second-order dependent on Li^+, O'Rear et al., 2001). It was proposed that the presence of a high-density positive charge is fundamental for hammerhead ribozyme catalysis (Murray et al., 1998). Our results suggest that Mg^{2+} and Li^+ might function similarly in catalyzing the peptide bond formation and both metal ions might stimulate the catalysis by providing the positive charge for allowing the ribozyme to fold a correct conformation and stabilizing the transition state step in peptide bond formation. The slope differences in concentration dependence of the hammerhead and the R180/TR158 catalysis could imply an inherently different nature of the two ribozymes and/or a fundamental difference in the two catalyzed reactions.

pH Dependence and Isotope Effects

The peptidyltransfer ribozymes exhibited interesting metal ion requirement for catalysis. Investigation of pH dependence will provide more information about the ribozyme-catalyzed peptide bond formation. pH dependence experiments were performed with 0.5 μM R180 ribozyme for the *cis* reactions, or 10 μM TR158 ribozyme, 0.1 μM 5'-Phe-linker-20-mer for the *trans* reactions, 100 μM Bio-Met-AMP and 50 mM pH buffer (MES for pH 5.5-6.5, Bis•Tris propane for pH 6.5-9.5) in the presence of 100 mM Mg^{2+} (only *cis* reactions) or 10 mM Mg^{2+} (only *trans* reactions) or 1.0 M Li^{+} at 25 °C. The observed rate constants (k_{obs}) were plotted against pH (Figure 4-5a. for R180 and Figure 4-5b for TR158). Both *cis*- and *trans*-systems gave similar pH profiles in Mg^{2+} or Li^{+} regardless of the activity difference, suggesting that the divalent and monovalent metal ions might play a similar function in promoting ribozyme catalysis. All pH profiles consist of a linear pH-dependent region (pH 5.5 –7.0, Figure 4-5a; pH 6.0 – 7.5, Figure 4-5b) and a pH-independent plateau (pH 8.0 - 9.0, Figure 4-5a; pH 8.5 – 9.0, Figure 4-5b). The slopes of the linear part of all pH profiles were close to 1 (0.90 for Mg^{2+}-cis, 1.00 for Li^{+}-cis, 0.87 for Mg^{2+}-trans, 0.90 for Li^{+}-trans), suggesting that one proton transfer might be involved in the rate-limiting step of the ribozyme-catalyzed reaction at this pH range. However, these curves also indicate different pK_a values of the functional groups in each system. The best-fit pK_a were 7.5 for Mg^{2+}-*cis*, 7.8 for Li^{+}-*cis*, 8.9 for Mg^{2+}-*trans,* and 8.2 for Li^{+}-*trans*. The pK_a in *trans*-systems was ≥ 0.4 unit larger than that in the *cis*-system, suggesting that the microenvironment of the active site of the ribozyme is somewhat variable with different metal ions or systems although one proton transfer might be involved in the chemical step for both ribozymes. The role of metal ions played

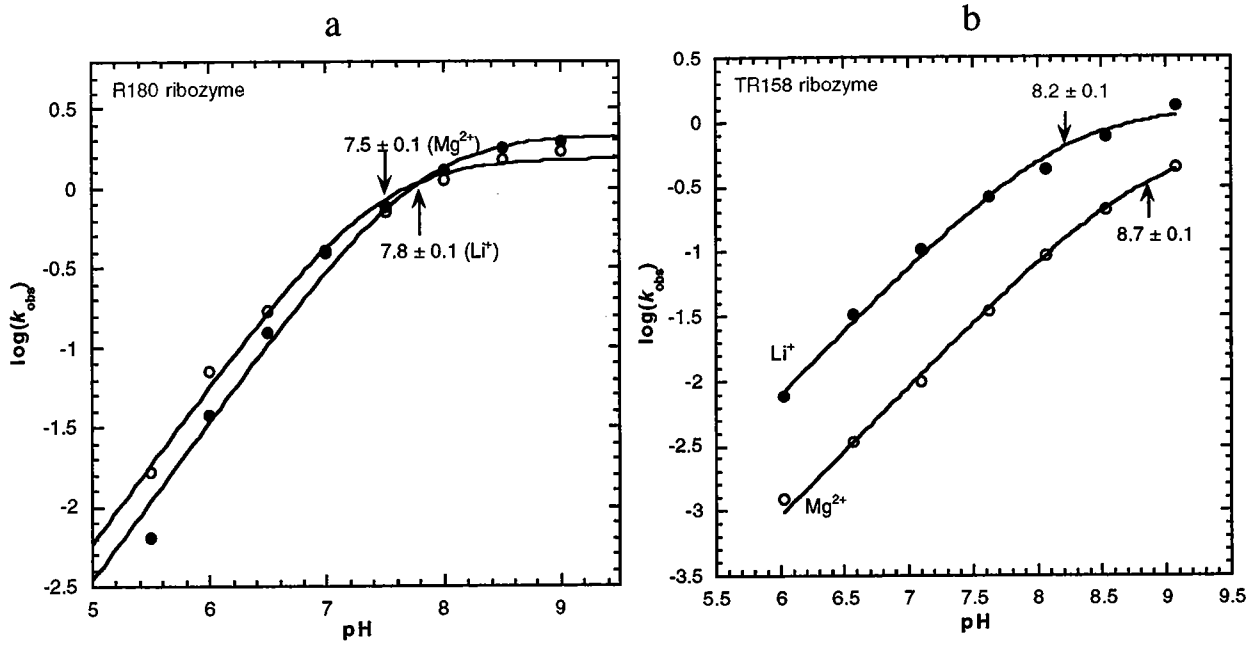

Figure 4-5. The pH profiles (log (k_{cat}) vs. pH) of the peptide bond formation catalyzed by R180 and TR158 ribozymes. The reactions were performed with 10 mM Mg^{2+} (O) and 1.0 M Li^+ (●) in 50 mM MES buffer (pH 5.5-6.0) and 50 mM Bis•Tris propane (pH 6.5-9.0) at 25 °C. (a) *Cis* system: 0.5 μM R180 ribozyme and 100 μM Bio-Met-AMP. The slopes of the linear region between pH 5.5~7.0 were 1.0 in 1.0 M Li^+ and 0.9 in 10 mM Mg^{2+}. (b) *Trans* system: 10 μM TR158 ribozyme, 0.1 μM 5'-Phe-linker-20-mer and 100 μM Bio-Met-AMP. The slopes of the linear part between pH 6.0-7.5 were 0.90 in 1.0 M Li^+ and 0.87 in 10 mM Mg^{2+}.

in these reactions might be assisting the folding of an active conformation and/or stabilizing the reaction intermediate.

To further confirm that proton transfer is involved in the ribozyme catalysis, we examined the isotope effects by replacing all the hydrogen atoms in the reaction with deuterium. Isotope effects, both kinetic and at equilibrium, have proven to be powerful and sensitive probes for dissecting the mechanistic chemistry and the transition state structures of enzyme-catalyzed reactions (Cleland, 1977; Cook, 1991). The introduction of deuterium in place of hydrogen in the hydrogenic sites of water, and its consequent exchange into functional groups of ribozyme and substrates, produces solvent isotope effects that impact enzymatic reactions. pD dependence experiments were performed in the *trans*-reaction system. Similar pD-dependent behavior was observed for Mg^{2+} (Figure 4-6a) and Li^{+} (Figure 4-6b) with a substantial D_2O solvent isotope effect. The observed rate constants over entire pH range were 10-fold lower in D_2O than that in H_2O. The measured pK_a in D_2O was 8.9 for both Mg^{2+} and Li^{+}. These results confirm that proton transfer is involved in the reaction and suggest that the ribozyme-catalyzed peptide bond formation might be a general base catalysis. Bevilacqua and colleagues (Nakano et al., 2000; Nakano & Bevilacqua, 2001) employed similar pH dependence and solvent isotopic effect experiments to characterize the HDV ribozyme-catalyzed reaction. They observed a significant D_2O isotope effect, indicating that transfer of a proton occurs in the chemical step. Together, our pH-metal ion profiles and isotope replacement experiments suggest that one proton transfer is involved in the rate-limiting step of ribozyme-catalyzed peptide bond formation and the reaction is promoted via a general base catalysis mechanism.

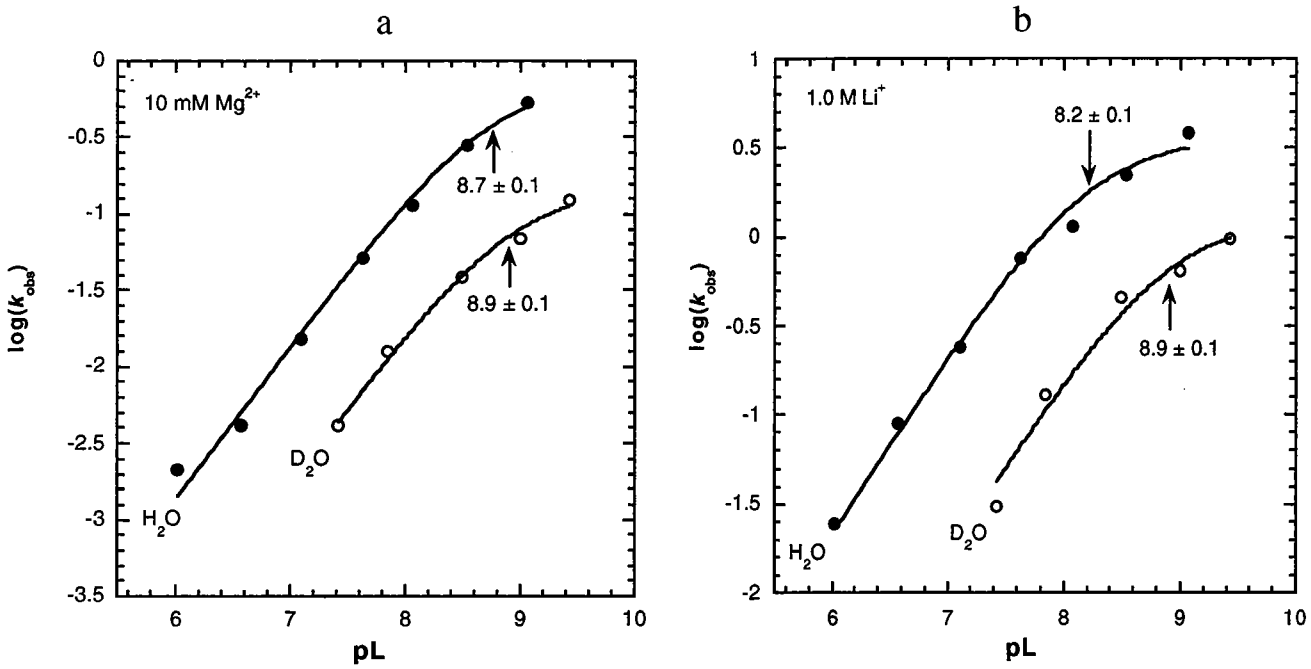

Figure 4-6. The pL profiles of the peptide bond formation catalyzed by TR158 ribozyme in 10 mM Mg^{2+} (a) and 1.0 M Li^{+} (b). All others were same as described in Figure 4-5.

Kinetics Studies

Although the above pH-dependence profiles suggest that one proton transfer is involved in the chemical step of peptide bond formation, it is also possible that the observed pH effect is caused by the change of substrate binding affinity and the change of substrate stability with pH. To rule out the first possibility, I performed kinetic studies at each test pH value to examine the substrate binding affinity. The system used in this study was the *trans*-noncleavable system, since it precisely reflects the product formation at high substrate concentrations. Kinetic studies were carried out at pH range 6.0-9.0 in the presence of either 10 mM Mg^{2+} or 1.0 M Li^{+} at different concentrations of Bio-Met-5'-AMP. The Bio-Met-5'-AMP concentrations were 50-2000 μM for Li^{+} and 10-700 μM for Mg^{2+}. Figure 4-7a and 7b show the Machaelis-Menten plots at various pHs. The obtained K_m and k_{cat} values were summarized in Table 4-2. In 10 mM Mg^{2+} (Figure 4-7a), K_m reached a maximum of 88.8 μM at pH 6.0 and a minimum of 17.2 μM at pH 9.0 (5-fold difference), while k_{cat} displayed a 200-fold difference from pH 6.0 to 9.0. Similar results were observed in 1.0 M Li^{+} (Figure 4-7b). K_m didn't change a lot over the entire pH range (3-fold difference), while k_{cat} increased about 200-fold from 0.031 min^{-1} at pH 6.0 to 6.18 min^{-1} at pH 9.0. Therefore, compared to the great change of k_{cat}, K_m did not change significantly over the entire pH range, suggesting that Bio-Met-5'-AMP stably binds to the ribozyme at different pHs and the substrate binding affinity has little effect on the reaction activity at different pHs.

To examine the substrate stability over the entire pH range, I monitored the time-course curves of Bio-Met-5'-AMP hydrolysis at different pHs by capillary

Table 4-2. Kinetic parameters (k_{cat} and K_m) of the peptide bond formation catalyzed by the TR158 ribozyme at various pHs in the presence of 10 mM Mg^{2+} or 1.0 M Li^+.[a]

No.	pH	Reaction in 10 mM Mg^{2+}			Reaction in 1.0 M Li^+		
		k_{cat} (min^{-1})	K_m (μM)	K_m/k_{cat} (μM·min)	k_{cat} (min^{-1})	K_m (μM)	K_m/k_{cat} (μM·min)
1	6.03	0.0026	88.8	28.7	0.031	378.8	82.6
2	6.57	0.0046	33.8	134.6	0.107	289.1	370.1
3	7.10	0.0166	53.1	312.6	0.290	196.6	1475.1
4	7.63	0.0584	57.8	1010.4	0.896	260.2	3443.5
5	8.07	0.121	32.4	3734.6	1.39	292.4	4753.8
6	8.54	0.275	21.4	12850	2.96	343.6	8614.7
7	9.07	0.520	17.2	30233	6.18	598.8	10321

a) Kinetic studies were performed under different reaction conditions by *trans*-reaction system. Reactions were carried out with 10 μM TR158 ribozyme, 0.1 μM 5'-Phe-linker-20-mer substrate, and 50 mM pH buffer (MES for pH 6.0-6.5 and for pH 6.5-9.0) in the presence of either 10 mM Mg^{2+} or 1.0 M Li^+. At each specific pH value, reactions were carried out at different concentrations of the Bio-Met-AMP substrate (10~700 μM for Mg^{2+}, 50~2000 for Li^+) to obtain k_{cat} and K_m values.

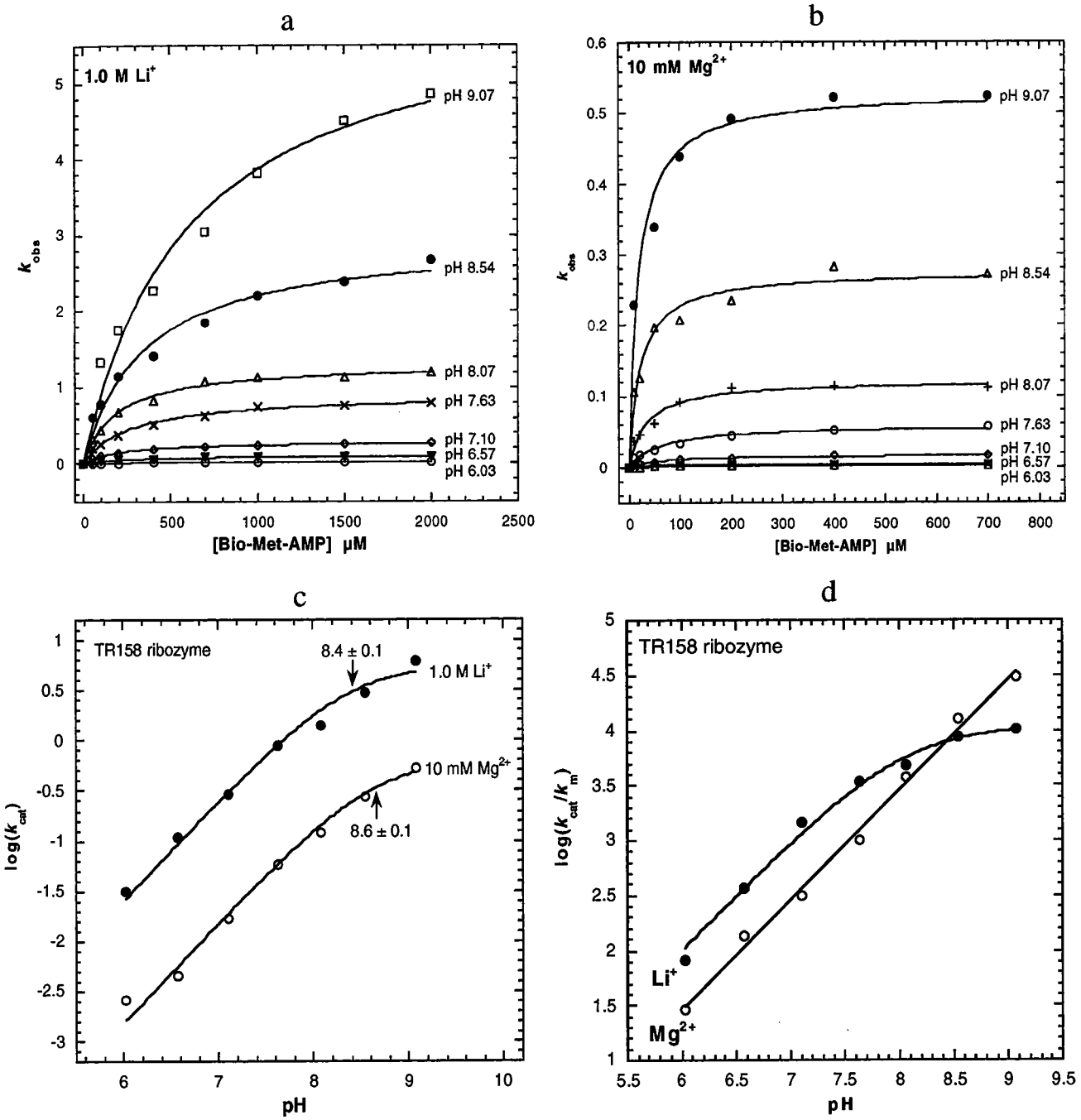

Figure 4-7. Kinetic study of the peptide bond formation catalyzed by TR158 ribozyme. Michaelis-Menten Plots of the TR158 ribozyme-catalyzed reactions at a various pHs in 1.0 M Li^+ (a) and 10 mM Mg^{2+} (b). The reactions were performed with 10 μM TR158 ribozyme, 0.1 μM 5'-Phe-linker-20-mer substrate, and 10-700 μM Bio-Met-AMP anhydride for Mg^{2+} and 50-2000 μM Bio-Met-APM anhydride for Li^+ in 50 mM buffer (pH 5.5-9.5). k_{cat} and K_m values were obtained by the best-fit of the data to Michaelis-Menten equation at the different pHs. (c) The pH profiles of k_{cat} *vs.* pH in 10 mM Mg^{2+} (O) or 1.0 M Li^+ (●). (d) The plots of log (k_{cat} / K_m) versus pH in 10 mM Mg^{2+} (O) or 1.0 M Li^+ (●).

electrophoresis (CE). Under all tested pH conditions (6.0 - 9.0), the half-life of Bio-Met-AMP was longer than the time required for the reaction to reach over 80% completion (Table 4-3), suggesting that there is always enough substrate available for the reaction at different pHs. Considering that Bio-Met-AMP at the minimum concentration (10 μM) is still in large excess (≥ 100-fold) to 5'-Phe-linker-20-mer (0.1 μM), the hydrolysis of Bio-Met-AMP would not affect the activity at various pHs, suggesting that the observed pH effect does not come from the instability of the substrate. Therefore, the observed pH profile corresponds to the proton-mediated chemistry of the catalytic mechanism of ribozyme-catalyzed peptide bond formation.

The pH profiles of $\log(k_{cat})$ *vs.* pH in 10 mM Mg^{2+} and 1.0 M Li^{+} were plotted in Figure 4-7c. These profiles were similar to the pH profiles of $\log(k_{obs})$ *vs.* pH, with $pK_a \geq 8.6$ in 10 mM Mg^{2+} and ≥ 8.4 in 1.0 M Li^{+}, confirming that the pH-profile most likely reflects the chemical step but is not caused by other factors. At low pHs (6.0-7.5), the pH profile was linear with a slope of 1.0, indicating again that a single proton is involved in the rate-limiting step of peptide bond formation. At high pHs (7.5-9.0), the profiles tended to reach a plateau. The reaction rate is independent of pH at high pHs, suggesting that either the concentrations of the functional species do not change with pH, or the concentration of one species increases while the other decreases by the same degree.

Although similar $\log(k_{cat})$ *vs.* pH profiles were observed in Mg^{2+} and Li^{+}, different profiles were displayed by Mg^{2+} and Li^{+} when $\log(k_{cat}/K_m)$ was plotted against pH (Figure 4-7d). For the Mg^{2+}-mediated reactions, the $\log(k_{cat}/K_m)$ vs. pH profile gave a linear relationship over the entire pH range. However, for the Li^{+}-mediated reactions, the $\log(k_{cat}/K_m)$ vs. pH curve was linear and parallel to the Mg^{2+} curve at low pHs (6.0 to

Table 4-3. Comparison of the reaction completion time and the substrate stability at different pHs.

No.	pH	Half-life	Reaction Completion Time
1	6.02	12 hours	6 hours
2	6.57	12 hours	6 hours
3	7.10	6 hours	2 hours
4	7.63	3 hours	2 hours
5	8.07	2 hours	10 minutes
6	8.54	1 hours	5 minutes
7	9.07	15 minutes	1 minute

The stability of Bio-Met-5'-AMP at different pHs was determined by capillary electrophoresis (CE). 500 μM Bio-Met-AMP substrate was incubated with 50 mM different pH buffers at 25 ^{0}C and samples were taken out at different time points for CE analysis. Half-life is the time when half of Bio-Met-5'-AMP is hydrolyzed compared to the amount at time zero at each pH. Reaction completion time refers to the time when the reaction product reaches over 80% of the final yield.

7.5), yet it tended to reach a plateau at high pHs (8.0-9.0). Kinetic studies also indicate that the substrate is more loosely bound to the ribozyme in Li^+ than in Mg^{2+} because K_m values in Li^+ were uniformly higher than those measured in Mg^{2+} (Table 4-2). These results further imply that Mg^{2+} and Li^+ might function similarly in the ribozyme catalysis but the microenvironment of the active center is variable with different metal ions.

Conclusion

Our findings provide comprehensive evidence that divalent metal ions are not necessary for all ribozymes. Monovalent cations, such as Li^+, Na^+, and K^+, could substitute for divalent ions in ribozyme catalysis. The pH profiles of peptide bond formation catalyzed by the R180 or TR158 ribozyme support the idea of a proton transfer in the rate-limiting step. A significant D_2O solvent isotope effect over entire range of tested pH values was observed for peptide bond formation by the TR158 ribozyme, suggesting that the peptide bond formation might take place via a general base catalysis mechanism, perhaps involving a nucleotide base, a buried water, or metal ion-bound hydroxyl. I propose that in the TR158-catalzyed reactions, the amino group of phenylalanine of 5'-Phe-linker-RNA acts as a nucleophile attacking the carbonyl carbon of the methionine of biotin-Met-AMP anhydride to form a tetrahedral intermediate. Deprotonation of the intermediate by a general base (base, phosphate backbone, buried water, or other groups) forms a negatively charged intermediate, resulting in the cleavage of the C-O bond to give the dipeptide product (Figure 4-8). The rate-limiting step could be the deprotonation of the forming intermediate at pH $\leq$ 8.0 with one proton transfer

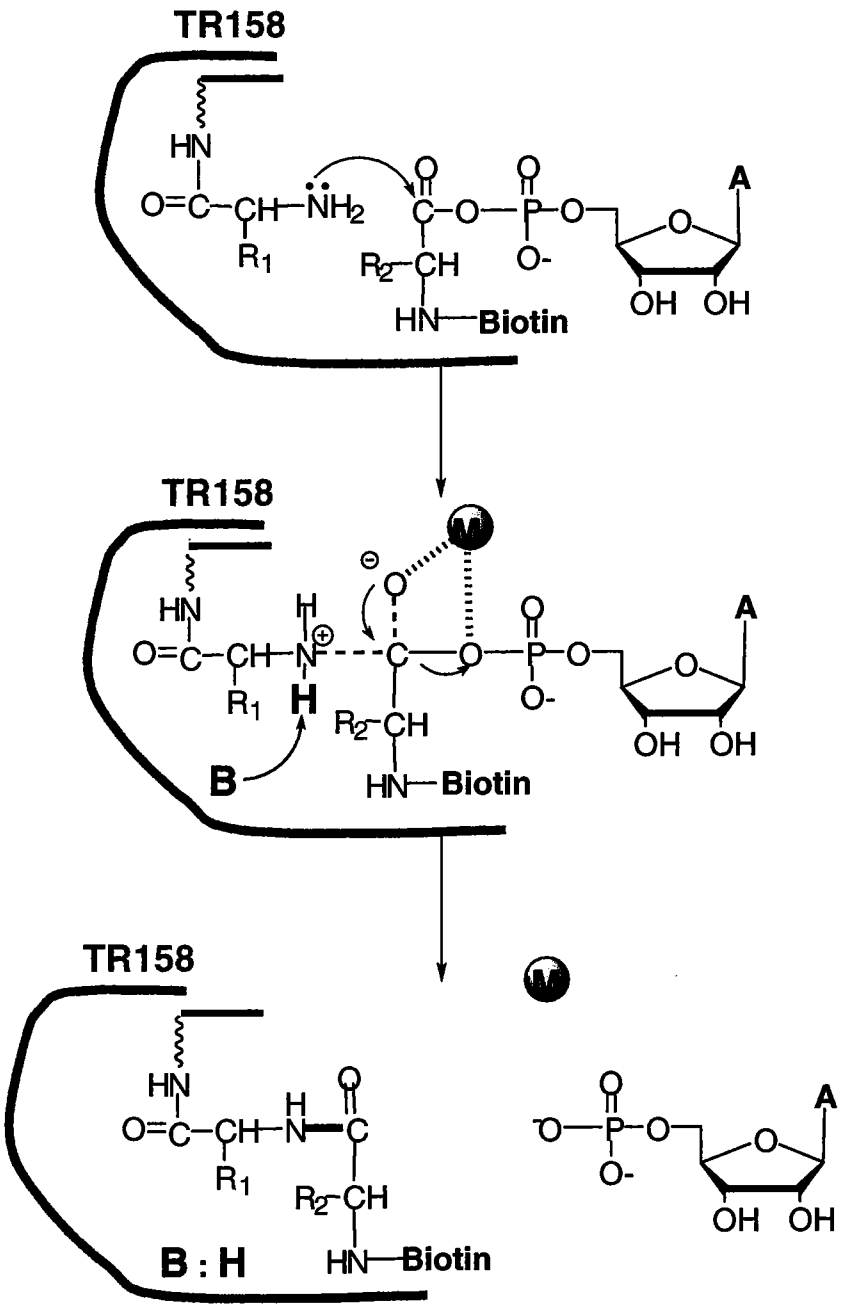

Figure 4-8. Proposed mechanism of TR158-catalyzed peptidyltransfer reaction. The amino group of phenylalanine of 5'-Phe-linker-RNA acts as a nucleophile attacking the carbonyl carbon of the methionine of biotin-Met-AMP anhydride to form a tetrahedral intermediate. Deprotonation of the intermediate by a general base (base, phosphate backbone, buried water, or other groups) forms a negatively charged intermediate, resulting in the cleavage of the C-O bond to give the dipeptide product

involved in this step. The divalent or monovalent ions may confer similar functions to assist folding an active ribozyme conformation and/or stabilize the developing intermediate. Similar catalytic mechanism could be employed by the R180 ribozyme since the TR158 ribozyme is a re-engineered form of R180.

Chapter V

A Novel Assay for Ribosomal Peptidyltransferase Activity

The ribosome is a large ribonucleoprotein complex composed of two subunits, the small subunit and the large subunit. The large subunit is mainly involved in mediating biochemical tasks such as catalyzing the reactions of polypeptide elongation, whereas the small subunit is the major actor in ribosomal recognition processes such as messenger RNA and transfer RNA binding (although the large subunit is also implicated in tRNA binding). Among all these ribosomal activities, peptide bond formation (the peptidyltransfer reaction) is a fundamental and very important step in protein synthesis.

Over decades, researchers have been investigating the active ribosomal component that is responsible for the peptidyltransferase activity. Although a large portion of the ribosome components is protein, it is the ribosomal RNA that is directly involved in catalyzing the peptidyltransfer reaction as suggested by accumulating biochemical, genetic, and crystal structural evidence. A very important piece of evidence is that depletion of most of the proteins in the 50S subunit didn't eliminate the peptidyltransferase activity (Noller et al., 1992), suggesting that the peptidyltransferase activity might reside in the ribosomal RNA. Moreover, mutations at conserved nucleotides in the central part region of domain V within 23S rRNA conferred antibiotic resistance to peptidyltransferase inhibitors (Rodriguez-Fonseca et al., 1995; Triman, 1999). Cross-linking and chemical footprinting experiments also indicated that 23S rRNA is the peptidyltransferase center where tRNA substrates bind and peptide bond formation occurs (Steiner et al., 1988; Moazed & Noller, 1989; Moazed & Noller, 1989).

It becomes more and more clear that the ribosome is a ribozyme with the contribution of lots of wonderful ribosome crystal structures. Ribosome structures from different species have been solved at different resolutions by either NMR or X-ray crystallography (Yusupov et al., 2001; Ban et al., 2000; Cate et al., 1999; Ban et al., 1998; Blanchard & Puglisi, 2001; Harms et al., 2001). For example, in one of the 50S crystal structures, the peptidyltransferase center was solely surrounded by the ribosomal RNAs and no protein molecules were in the vicinity of the synthesized peptide bond (Ban et al., 2000). These structures provide views of what the peptidyltransferase center looks like and confirm the idea that the ribosome is a ribozyme. To access the mechanistic aspects of the ribosome-catalyzed peptide bond formation, adenine 2486 (A2486) on the 23S rRNA was proposed to be the general base in catalyzing the peptidyltransfer reaction because it was observed to be the closest nucleotide to the synthesized peptide bond (Muth et al., 2000; Nissen et al., 2000).

However, the hypothesis that A2486 is the sole key in catalyzing peptide bond formation has been challenged by further studies. Replacement of A2486 with other nucleotides (G, C, U) didn't greatly change the peptidyltransferase activity (Polacek et al., 2001; Thompson et al., 2001; Xiong et al., 2001). Ribosomal peptidyltransferase also withstood mutation at G2482, which was the key nucleotide in providing the unusual pK_a of A2486 (Polacek et al., 2001; Thompson et al., 2001; Xiong et al., 2001). Chemical probing with dimethyl sulfate further demonstrated that conformational changes might occur in the peptidyltransferase center when the reaction conditions were changed (Bayfield et al., 2001; Muth et al., 2001). Therefore, it is still unclear what is the exact mechanism of the ribosomal peptidyltransfer reaction.

From a chemical point of view, peptide bond formation is an easy step that proceeds spontaneously once the reactants are brought into close proximity (Weber & Orgel, 1980). Peptidyltransfer reaction takes place when the α-amine of the aminoacyl-tRNA attacks the carbonyl carbon of the peptidyl-tRNA. The ribosome provides precise orientation of the aminoacyl- and peptidyl-tRNAs, and may use additional catalytic strategies in promoting peptide bond formation (Barta, 2001; Joyce, 2002). Until now, it is still controversial that whether the ribosome only serves as the template in placing the tRNAs together thus peptide bond formation occurs spontaneously, or additional catalytic groups (nucleotides or divalent metal ions) are required to help catalyzing peptide bond formation (Barta et al., 2001; Polacek et al., 2001).

Investigation of the ribosomal peptidyltransfer reaction has been hampered by technical problems associated with the complexity of the ribosome and its substrates. Most studies in peptidyltransferase have employed two assays, the fragment reaction (Monro & Marcker, 1967) and the polyphenylalanine synthesis (Fahnestock et al., 1974). In the fragment reaction, the peptidyltransferase activity is measured by the formation of *N*-formyl-[^{35}S]Met-puromycin from a fragment of *N*-formyl-Met-tRNA^{fMet} (as the peptidyl donor) and puromycin (as the peptidyl acceptor). In the ploy phenylalanine synthesis, the peptidyltransferase activity is determined by monitoring the release of charged poly(Phe) from the ribosome upon addition of puromycin. There are many disadvantages in these assays. First, nonphysiological conditions were applied in this assay with the addition of large amount of methanol or ethanol (30%) in order to increase the affinity of the P-site substrates for the ribosome (Monro & Marcker, 1967; Traut & Monro, 1964). Second, puromycin, which is an analog of aminoacyl-adenosine, does not

closely mimic the natural A-site substrate and loosely binds to the A site (Quiggle & Chladek, 1980). Recent studies even revealed multiple ways of puromycin function in the ribosome (Starck & Roberts, 2002; Miyamoto-Sato et al., 2000) and challenged the conventional functions of puromycin by competitive binding to the A site (Nathans & Niedle, 1963; Steiner et al., 1988; Kirillov et al., 1997) and premature linkage to the C terminus of the peptide (Allen et al., 1962; Nathans, 1964; Traut & Monro, 1964; Zamir et al., 1966; Smith et al., 1965). Another obvious limitation of these assays is the tedious analysis of the peptidyltransferase activity (Monro & Marcker, 1967).

To overcome these technical problems and to gain a better understanding of the mechanistic aspects of ribosomal peptidyltransferase reaction, we developed a novel system to characterize ribosomal peptidyltransferase activity. The new assay simplifies the operation for measuring the activity and most importantly, it specifically and accurately monitors the peptidyltransfer reaction. The improvements include no requirement for alcohol, substrate analogs closely mimicking the authentic ribosomal substrates, and easy analysis of the products. Firstly, two new substrates, OH-CpCpA-3'-*NH*-Phenylalanine (CCA-*NH*-Phe) and OH-CpCpA-Methionine-Biotin (CCA-Met-Biotin) were employed in the new assay (Zhang et al., 2002; Cui et al., in preparation). These two substrates could be easily dissolved in water thus avoiding the addition of any nonphysiological alcohol into the ribosome reaction. Secondly, these two substrates closely mimic the natural ribosomal substrates for protein synthesis. The 3'-terminal CCA sequence is an invariant feature of all natural tRNAs. Both CCA moiety on the P-site and A-site tRNA play important roles in contributing to the peptidyltransferase activity by providing structural binding with 23S rRNA (Quiggle & Chaldek, 1980;

Wower et al., 1994; Wower et al., 1995; Steiner et al., 1988; Gregory & Dahlberg, 1999). CCA-*NH*-Phe is the first designed A-site substrate in replace of either puromycin, C-puromycin (Schmeing et al., 2002; Muth et al., 2001), or CC-puromycin (Polacek et al., 2001), and it more mimics the natural ribosomal substrate than these A-site substrates that have ever been used. On the P site, previous studies have employed fragment of *N*-formyl-Met-tRNA (Monro & Marcker, 1967) and CCA-Phe-Biotin (Schmeing et al., 2002; Muth et al., 2001) as the P-site substrate in assaying ribosomal peptidyltransferase activity. Our assay showed that CCA-Met-Biotin was also active as the P-site substrate. Finally, reaction product could be easily examined by loading on a 24 % polyacrylamide/ 7.5 M urea gel and quantitated by phosphoimager.

After establishing the new assay, several aspects of the 50S-catalyzed peptidyltransfer reaction were investigated, including divalent metal ion requirement, pH dependence, P-site substrate specificity and antibiotic inhibition. Importantly, we examined the 50S peptidyltransferase activity with CCA-*NH*-Phe (A-site substrate) and eight different P-site substrates (tRNA-Met-Biotin, CCA-Met-Biotin, CA-Met-Biotin, AMP-L-Met-Biotin, AMP-D-Met-Biotin, 2' deoxy-AMP-Met-Biotin, 3'deoxy-AMP-Met-Biotin, and 2'-methoxy-AMP-Met-Biotin). Remarkably, 50S was active with all these P-site substrate derivatives except 2'-methoxy-AMP-Met-Biotin, suggesting an important role of the 2'-OH group of the terminal adenosine in the peptidyltransfer reaction.

Experimental Procedures

Preparation of P-site Substrates. The P-site substrates, pCpCpA-Met-Biotin, pCpA-Met-Biotin, AMP-L-Met-Biotin, AMP-D-Met-Biotin, 2' deoxy-AMP-Met-Biotin, 3'deoxy-AMP-Met-Biotin, and 2'-methoxyl-AMP-Met-Biotin, were synthesized by Dr. Zhiyong Cui in our lab. tRNA-Met-Biotin was obtained by ligating the 74 nt tRNA (without CA at the 3' end) with pCpA-Met-Biotin. Ligation was performed with 80 μg pCpA-Met-Biotin, 20 μg tRNA(-CA) in the presence of 55 mM Hepes (pH 7.5), 250 μM ATP, 15 mM $MgCl_2$, 10% DMSO and 200 units of T4 RNA ligase at 37 °C for 30 min. Reaction was quenched by addition of 10% volume of 2.5 M NaOAc and precipitated by 3 volumes of cold ethanol in dry ice. The precipitated tRNA-Met-Biotin was stored at – 20 °C in powder form.

Preparation of A-site Substrate. Chemical synthesis of CCA-*NH*-Phe was described in Zhang et al., 2002. The synthesized 5'-OH-CCA-*NH*-Phe was labeled by ^{32}P. Kinase reaction was carried out with 1 nmol 5'-OH-CCA-*NH*-Phe, 50 μCi γ-^{32}P-ATP, and 20 units of T4-polynucleokinase in the presence of 1 × PNK buffer at 37 ^{0}C for one hour. Excess ATP (100 nmol) was added into the radioactive mix and the labeling reaction was continued for another one hour to convert all 5'-OH-CCA-*NH*-Phe into 5'-^{32}P -CCA-*NH*-Phe. The reaction mixture was then loaded onto 24% non-denaturing polyacrylamide gel for purification. ^{32}P -CCA-*NH*-Phe was detected by film and the gel containing ^{32}P -CCA-*NH*-Phe was cut out, squeezed by syringe and soaked in pure water at 4 ^{0}C overnight. Soaking solution was separated from the gel by centrifugation and loaded on reverse phase C_{18} cartridge. The C_{18} cartridge was pre-conditioned by 5 ml CH_3CN, 5 ml CH_3CN : H_2O and 5 ml H_2O. Soaking solution was allowed to flow through the column by gravity. Then the bound ^{32}P -CCA-*NH*-Phe was eluted by 1 ml

CH_3CN : CH_3OH : H_2O (35 : 35 : 30). After dried by lyophilization, ^{32}P -CCA-*NH*-Phe was dissolved in 100 µl distilled water and stored at –20 ^0C.

Preparation of the Ribosome. Ribosomes and ribosomal subunits were prepared as described (Noll et al., 1973). Bacterial strain *E. Coli* MRE 600 was harvested at a density of A_{650} = 0.5. Cell pellets were resuspended in buffer B (20 mM HEPES, pH 7.6, 5 mM $MgCl_2$, 30 mM NH_4Cl, 2 mM spermidine, and 5 mM 2-mercaptoethanol). Cells were broken by grinding with autoclaved alumni (1 g cell paste/2 gram alumni) in a precooled mortar until a smooth, thick and sticky paste is obtained and 'popping' sounds are heard. The cell paste was extracted by slowly adding buffer B (2 ml per gram of cell paste) and continued grinding. After a few minutes, RNase-free DNase (4 µg/ml) was added and grinding was continued for a few more minutes until a reduction in viscosity is observed. Cell debris and alumina were cleared by centrifugation twice at 30,000 g for 30 minutes. The S30 supernatant was layered on 1.1 M sucrose cushion made in buffer B and centrifuged at 50,000 g in a Beckman 50.2 Ti rotor at 4 ^0C. After 19 hours centrifugation, crude ribosomes were obtained as a transparent pellet. To get 70S ribosomes, the ribosome pellet was washed and resuspended in buffer D (same as buffer B except that the $MgCl_2$ concentration is 10 mM) and stored at –80 ^0C. For continuous preparation of the ribosomal subunits, the pellet was dissolved in buffer C (20 mM HEPES, pH 7.6, 1 mM $MgCl_2$, 300 mM NH_4Cl, 2 mM spermidine, and 5 mM 2-mercaptoethanol) with gentle stirring at 4 ^0C for 2 hours. The solution was clarified by low-speed centrifugation. 60 A_{260} units of the ribosomes were loaded on 34 ml 10-30% sucrose gradient made in buffer C. Centrifugation was performed at 43,000 g in a SW28 rotor at 4 ^0C for 17 hours. Fractions of the sucrose gradient were monitored by UV

absorbance at A_{260} and the corresponding 50S and 30S peaks were collected. Ribosome subunits were precipitated by ethanol and stored in buffer B at –80 ^{0}C.

Peptidyltransferase activity assay. The standard peptidyltransferase activity was performed with 22 μM 50S subunit, 50 μM CCA-Met-Biotin, trace amount of ^{32}P-CCA-*NH*-Phe (~ 5×10^{-4} μM) in the presence of 50 mM Tris•HCl (pH 7.5), 35 mM $MgCl_2$, 100 mM NH_4Cl and 1000 mM KCl at 37 ^{0}C. 1 μl aliquot of the reaction was taken out at specific time points, quenched with 2 μl quench buffer (formamide + 0.05% xylene cyanol) and loaded on 24% polyacrylamide /7.5 M urea denaturing gel. For reaction validation, samples were incubated with 10 μg streptavidin at room temperature for 15 minutes prior to being loaded on the gel. Reaction product was quantitated by Molecular Dynamics Phosphorimager and the fraction of the product relative to the total reactant was plotted against different time points. The observed rate constants were obtained by curve fit using KaleidaGraph.

Divalent metal ion specificity. 5 mM Mg^{2+}, Ca^{2+}, Mn^{2+}, Zn^{2+}, Co^{2+}, or Cu^{2+} was included in the standard reaction condition to examine 50S peptidyltransferase activity.

pH-dependence. pH dependence was investigated under standard reaction condition at different pHs (Bis•Tris propane, pH 6.4 – 9.5; MES, pH 5.5 - 6.3). To examine pH dependence with different divalent metal ions, standard reactions were performed with 20 mM Mg^{2+}, Ca^{2+}, or Mn^{2+} at different pHs. The observed rate constants were plotted against pH and data were fit by KaleidaGraph.

P-site substrate specificity. To examine the 50S activity with different P-site substrates, experiments were performed with standard reaction condition except different

concentrations of P-site substrates were included (200 μM tRNA-Met-Biotin, 200 μM CCA-Met-Biotin, 200 μM CA-Met-Biotin, 200 μM or 1 mM AMP-L-Met-Biotin, 1 mM AMP-D-Met-Biotin, 1 mM 2' deoxy-AMP-Met-Biotin, 1 mM 3'deoxy-AMP-Met-Biotin and 1 mM 2' methoxy-AMP-Met-Biotin).

Antibiotics inhibition study. Reactions were carried out with 50S or 70S, 50 μM CCA-Met-Biotin or tRNA-Met-Biotin, trace amount of ^{32}P-CCA-*NH*-Phe (~ 5×10^{-4} μM), 100 μM antibiotics in the presence of 50 mM Tris•HCl (pH 7.5), 35 mM $MgCl_2$, 100 mM NH_4Cl and 1000 mM KCl at 37 ^{0}C. For each reaction, same amount of 50S or 70S (10 pmol) was included.

Results

A Novel Assay of Ribosomal Peptidyltransferase Activity

Two novel substrates were synthesized for assaying the ribosomal peptidyltransferase activity, OH-CpCpA-3'-*NH*-Phenylalanine (CCA-*NH*-Phe) and OH-CpCpA-Methionine-Biotin (CCA-Met-Biotin) (Zhang et al., 2002; Cui et al., in preparation). The 5' end of CCA-*NH*-Phe was labeled by ^{32}P in order to monitor the peptide bond formation. If these two analogs are active substrates for the ribosome, the free amine on the phenylalanine of ^{32}P-CCA-*NH*-Phe will attack the carbonyl carbon on the methionine of CCA-Met-Biotin and peptide bond will be formed between Phe and Met (Figure 5-1). Therefore, the reaction product (^{32}P-CCA-*NH*-Phe-Met-Biotin) can be separated from the reactant (^{32}P-CCA-*NH*-Phe) on a 24% polyacrylamide/7.5 M urea gel. Figure 5-2a is a typical gel-shift analysis showing the established assay. The lower band

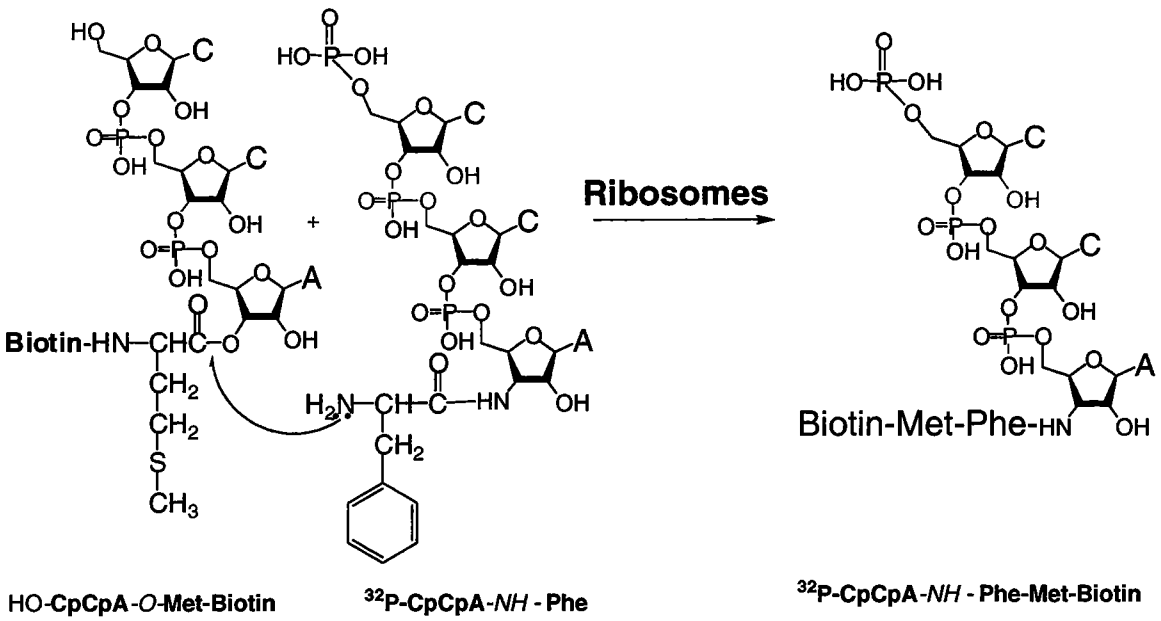

Figure 5-1. Ribosome-catalyzed peptidyltransfer reaction between OH-CpCpA-3'-*NH*-Phenylalanine (CCA-*NH*-Phe) and pCpCpA-Methionine-Biotin (CCA-Met-Biotin). The 5' end of CCA-*NH*-Phe was labeled by ^{32}P in order to monitor the peptide bond formation by running on an acrylamide gel. The free amine on phenylalanine attacks the carbonyl carbon on methionine and peptide bond is formed between the two amino acids.

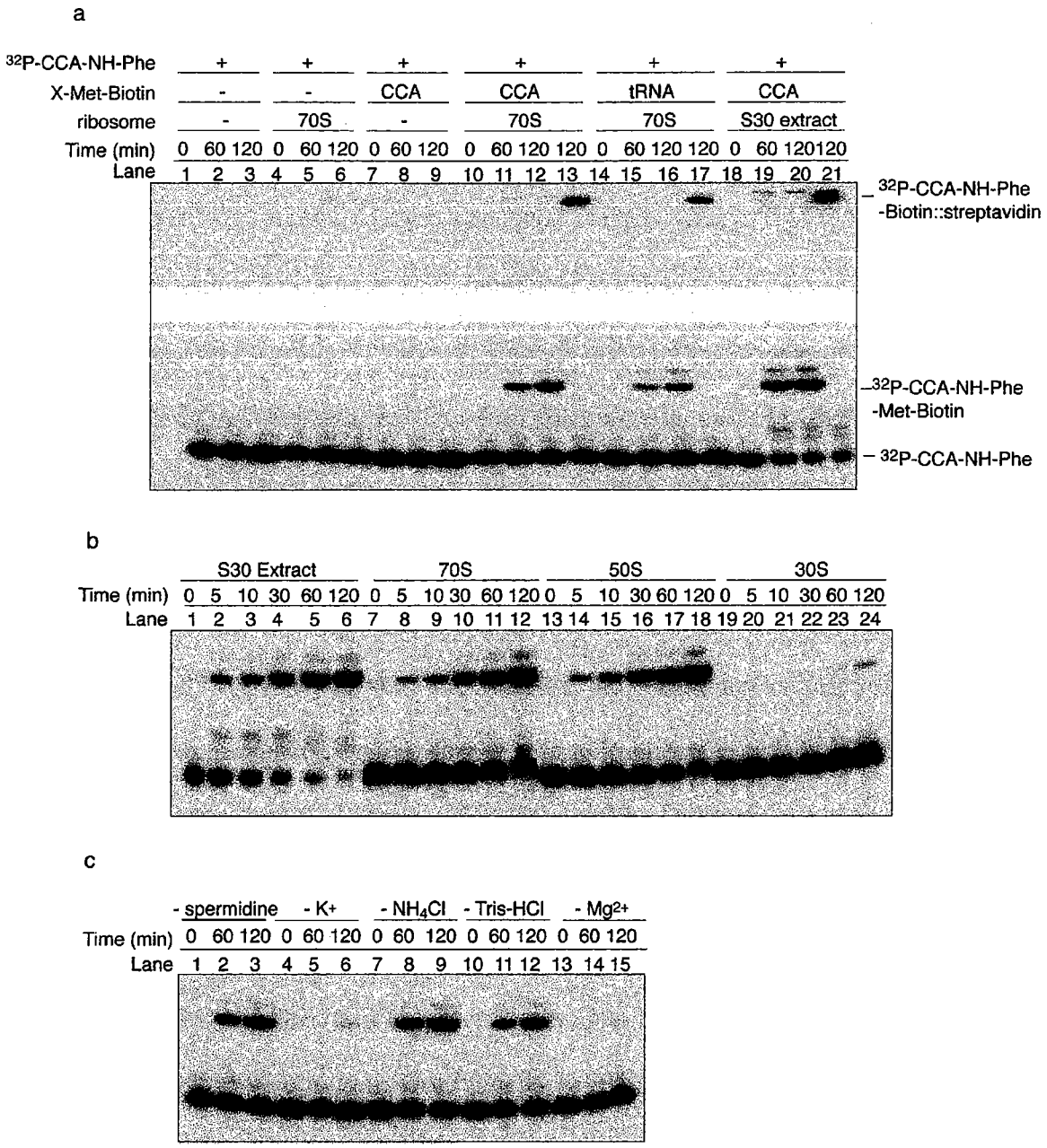

Figure 5-2. (a) Reaction validation. Two substrates, ^{32}P-CCA-*NH*-Phe and CCA-Met-Biotin, were incubated with S30 extract or 70S in the presence of 50 mM Tris•HCl (pH 7.5), 5 mM $MgCl_2$, 10 mM NH_4Cl, 100 mM KCl and 1.5 mM spermidine at 37 ^{0}C. Reactions1~3 (lanes 1-9) are negative controls. The lower band corresponds to labeled ^{32}P-CCA-*NH*-Phe; the middle band is the formed dipeptide (^{32}P-CCA-*NH*-Phe-Met-Biotin) labeled by biotin; the highest band represents ^{32}P-CCA-*NH*-Phe-Met-Biotin::streptavidin complex. (b) Peptidyltransferase activity was examined with different ribosomal components (S30 extract, 70S, 50S and 30S). (c) 50S-catalyzed peptidyltransferase activity was examined in the absence of different components (spermidine, Tris•HCl, Mg^{2+}, K^+, or NH_4Cl).

corresponds to labeled ^{32}P-CCA-*NH*-Phe; the middle band is the formed dipeptide (^{32}P-CCA-*NH*-Phe-Met-Biotin) labeled by biotin; the highest band represents ^{32}P-CCA-*NH*-Phe-Met-Biotin::streptavidin complex. When only ^{32}P-CCA-*NH*-Phe was included in the reaction (Figure 5-2a, lanes 1-3), no product was formed. When ^{32}P-CCA-*NH*-Phe was incubated with either 70S (Figure 5-2a, lanes 4-6) or CCA-Met-Biotin (Figure 5-2a, lanes 7-9), there was still no product observed. Peptide bond formation was observed only when both ^{32}P-CCA-*NH*-Phe and CCA-Met-Biotin were incubated with 70S or S30 extract (Figure 5-2a, lanes 10-12, 14-16, 18-20). Upon streptavidin incubation, the middle band shifted to the top of the gel (Figure 5-2a, lanes 13, 17, and 21), indicating that a biotin group was covalently linked to ^{32}P-CCA-*NH*-Phe via the formation of peptide bond between Phe and Met. Furthermore, we investigated which component within the ribosome was responsible for the peptidyltransferase activity by incubating these two substrates with S30 extract, 70S, 50S or 30S. As shown in Figure 5-2b, peptide bond was formed in S30 extract, 70S and 50S (Figure 5-2b, lanes 1-18), but not in 30S (Figure 5-2b, lanes 19-24). Altogether, these results suggest that peptide bond is formed between ^{32}P-CCA-*NH*-Phe and CCA-Met-Biotin upon incubation with the ribosome, and the peptidyltransferase activity resides in the large ribosomal subunit (50S).

We continued to examine buffer and salt requirements for the 50S-catalyzed peptidyltransfer reaction. Experiments were performed with ^{32}P-CCA-*NH*-Phe, CCA-Met-Biotin and 50S in the absence of different components. Without either spermidine, NH_4Cl or Tris•HCl, the peptidyltransferase activity was not affected (Figure 5-2c, lanes 1-3, 7-9, 10-12). However, both Mg^{2+} and K^+ were required for the reaction (Figure 5-2c, lanes 4-6, 13-15), indicating that divalent and monovalent metal ions play important roles

in promoting 50S-catalyzed peptidyltransfer reaction. The optimized condition for the peptidyltransferase activity was reached with 35 mM $MgCl_2$, 100 mM NH_4Cl, 1000 mM KCl in the presence of 50 mM Tris•HCl (pH 7.4). This reaction condition was used for all the next experiments except changing of metal ions or pH values for examination of divalent metal ion specificity and pH dependence.

Divalent Metal Ion Specificity

Divalent metal ions are important for the ribosomal peptidyltransferase activity (Maden & Monro, 1968; Pestka, 1972). Crystal structures also indicated the presence of Mg^{2+} nearby the peptidyltransferase catalytic center (Nissen et al., 2000). Therefore, we examined the 50S activity with six kinds of divalent metal ions (5 mM Mg^{2+}, Ca^{2+}, Mn^{2+}, Zn^{2+}, Co^{2+}, Cu^{2+}). 50S was active with Mg^{2+}, Ca^{2+}, or Mn^{2+} alone (Figure 5-3, lanes 1-15); however, Zn^{2+}, Co^{2+}, or Cu^{2+} alone was inert for the 50S-catalyzed reaction (Figure 5-3a, lanes 15-30). Mg^{2+}, Ca^{2+}, and Mn^{2+} also exhibited similar concentration dependencies that 50S activity increased with the increasing of metal ions at low concentrations but was inhibited by high concentrations of divalent metal ions (Figure 5-3b). These results agree with previous report (Maden & Monro, 1968; Pestka, 1972) that Mg^{2+}, Ca^{2+}, and Mn^{2+} play similar functions for 50S peptidyltransferase activity. Possible roles might be stabilizing the catalytic center or binding the CCA terminus of the P-site substrate to the active center (Maden & Monro, 1968). So far, we cannot totally eliminate the possibility that these divalent metal ions are directly involved in the chemical steps of peptidyltransfer reaction.

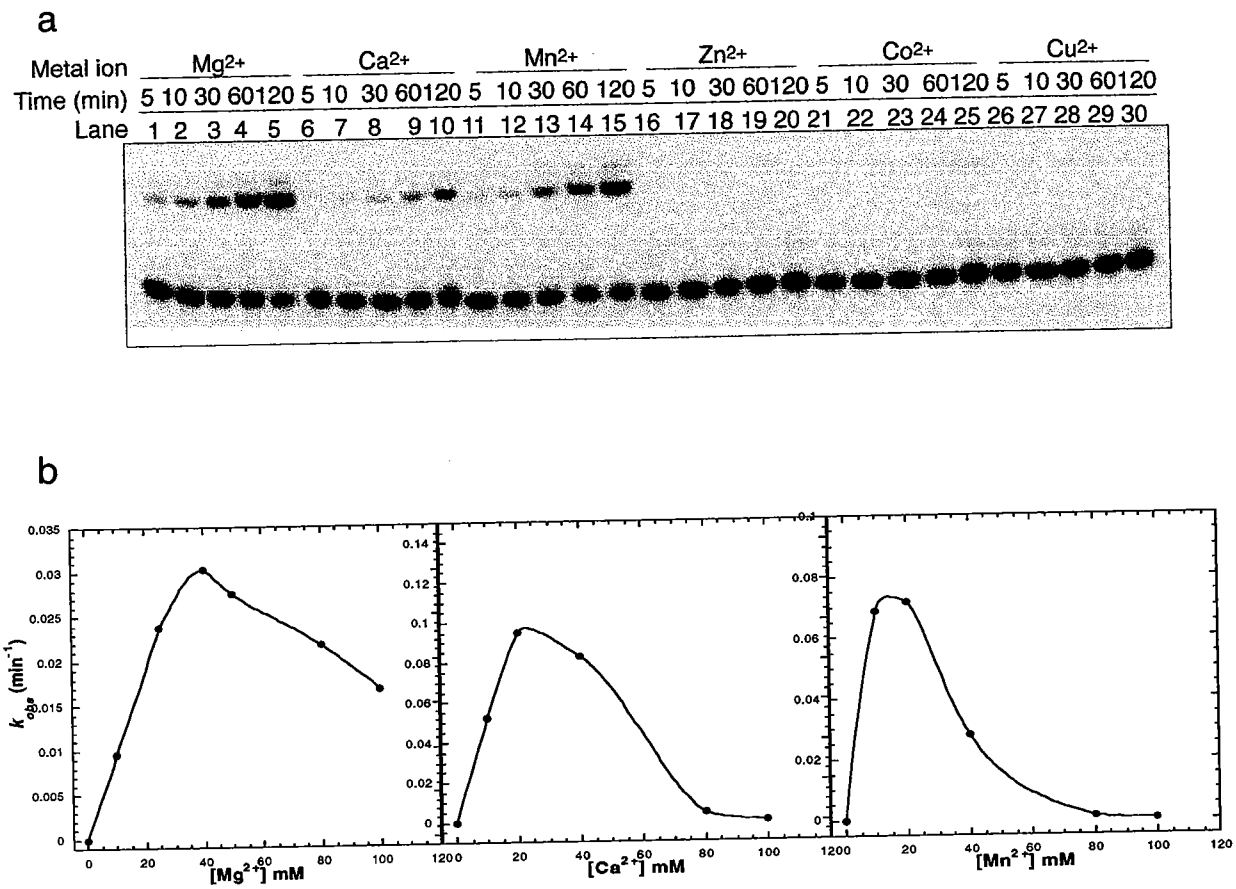

Figure 5-3. Divalent metal ion requirement in 50S catalyzed reaction. (a) Six kinds of divalent metal ions (Mg^{2+}, Ca^{2+}, Mn^{2+}, Zn^{2+}, Co^{2+}, Cu^{2+}) were tested for the peptidyltransferase activity. Reactions were performed with 1 A_{260} unit 50S subunit, 50 μM CCA-Met-Biotin, trace amount of ^{32}P-CCA-*NH*-Phe in the presence of 50 mM Tris•HCl (pH 7.5), 100 mM NH_4Cl, 1000 mM KCl and 5 mM divalent metal ion at 37 ^{0}C. (b) Metal ion concentration dependence of 50S-catalyzed peptidyltransfer reaction.

pH Dependence

To further investigate the 50S-catalyzed peptidyltransfer reaction, pH-dependence experiments were performed in the presence of different kinds of divalent metal ions (Mg^{2+}, Ca^{2+}, or Mn^{2+}) at pH range 6.42-9.54. Figure 5-4 showed the pH dependence of 50S-catalyzed peptidyltransferase reaction with Mg^{2+}, Ca^{2+}, or Mn^{2+}. All pH profiles exhibited as bell-shape curves, however, the pH values where the maximum activity reached and the slopes of the curves were different for Mg^{2+}, Ca^{2+}, and Mn^{2+}-mediated reactions. In 20 mM Mg^{2+}, the maximum activity was achieved at pH 8.07; it was pH 7.63 in 20 mM Ca^{2+} and pH 7.35 in 20 mM Mn^{2+}. This difference might reflect the different ionization ability of these divalent metals. These results suggest that Mg^{2+}, Ca^{2+}, and Mn^{2+} might play similar functions in the 50S-catalyzed peptidyltransfer reaction, but their contributions in promoting the reaction are different. Nonetheless, the similar shapes of pH-dependence profiles suggest that Mg^{2+}, Ca^{2+}, and Mn^{2+} play similar functions for 50S-catalyzed peptidyltransfer reaction but their abilities in supporting the reaction are different.

Previous studies suggested one functional group with a pK_a of 7.5 ~ 8.0 (Maden & Monro, 1968), or a pK_a of 7.3 (Pestka, 1972) involved in the peptidyltransfer reaction in the presence of Mg^{2+}. I analyzed the pH profiles by Malcolm Dixon method (Dixon, 1953; Tipton & Dixon, 1979) with two pK_a values obtained. The pK_a values were 7.3 and 8.7 for Mg^{2+}, 6.6 and 8.1 for Mn^{2+}, but the Ca^{2+} data could not be fitted using this method. One of the pK_a values (7.3) obtained in the presence of Mg^{2+} was close to the reported pK_a. However, the result also indicated the presence of a second pK_a (8.7) at high pHs. A decrease of the peptidyltransferase activity at high pHs was also detected

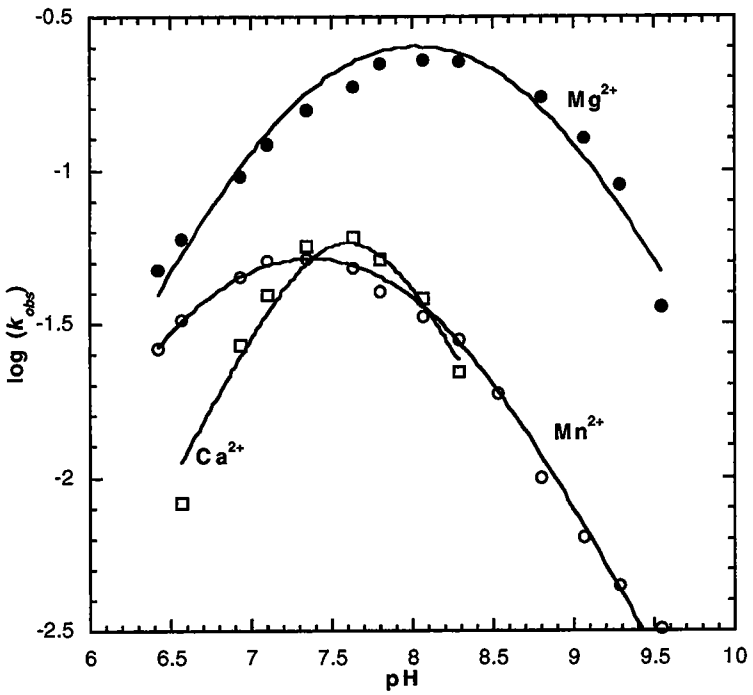

Figure 5-4. pH dependence of peptidyltransferase reaction. pH dependence experiments were performed in 50S with 20 mM Mg^{2+}, Ca^{2+}, or Mn^{2+} at different pHs (Bis•Tris propane, pH 6.4 – 9.5; MES, pH 5.5 - 6.3.

but this effect received no further investigation (Maden & Monro, 1968; Pestka, 1972). Instead, these data exhibited the pH effect on the 50S-catalyzed peptidyltransfer reaction in a broader range (pH 6.5-9.5) and displayed a bell-shape profile of pH dependence. There are several possibilities about the pH effect of the peptidyltransfer reaction. One possibility is that two ionizable groups are essential for the peptidyltransferase activity and the peptidyltransferase can be considered as a dibasic acid (Tipton & Dixon, 1979). Such groups could include the functional groups on the rRNA nucleotides, water, or the nearby metal ions. Also, it is possible that this bell-shape pH profile reflects the pH-dependent conformational flexibility within the ribosomal peptidyltransferase center (Muth et al., 2001).

P-site Substrate Specificity

An interesting question in the ribosomal peptidyltransfer reaction is how the substrates contribute to the reaction. In the new assay, CCA-Met-Biotin was used as the prototype P-site substrate and ^{32}P-CCA-*NH*-Phe was considered as the A-site substrate. Several features of the P-site substrate were examined including size of the oligonucleotide fragment (tRNA-, CCA-, CA-, AMP-Met-Biotin), configuration of the amino acid (AMP-L-Met-Biotin, AMP-D-Met-Biotin) and modification of the groups on 2', 3' positions (2'-deoxy-AMP-Met-Biotin, 3'-deoxy-AMP-Met-Biotin, 2'-methoxy-AMP-Met-Biotin). Figure 5-5 shows the chemical structures of these P-site substrate derivatives.

First, the size effect of the P-site substrate on 50S-catalyzed reaction was examined (Figure 5-6a). 50S was active with all four tested substrates (200 μM), tRNA-

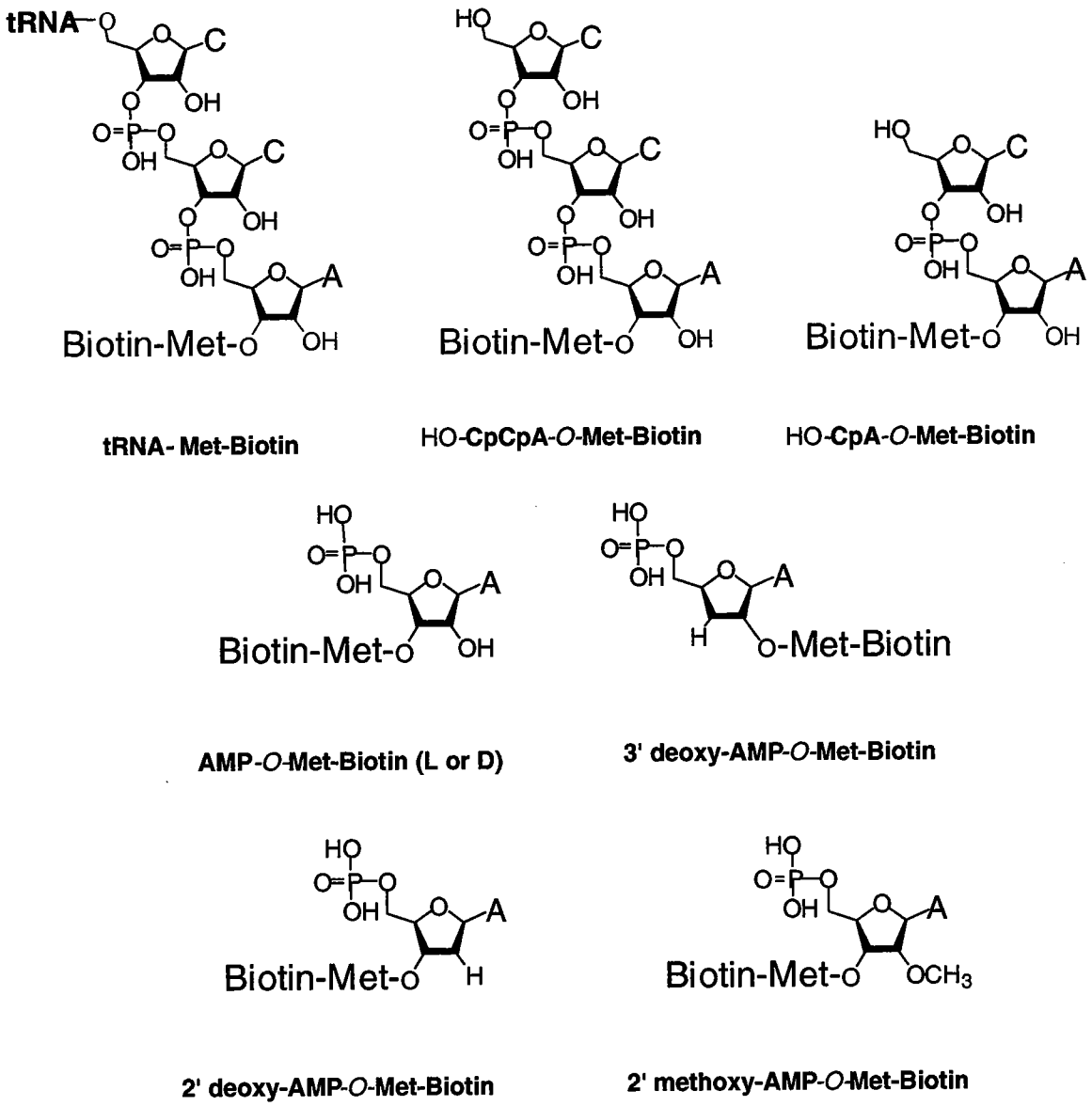

Figure 5-5. Chemical structures of eight different P-site substrates for ribosomal peptidyltransferase reaction.

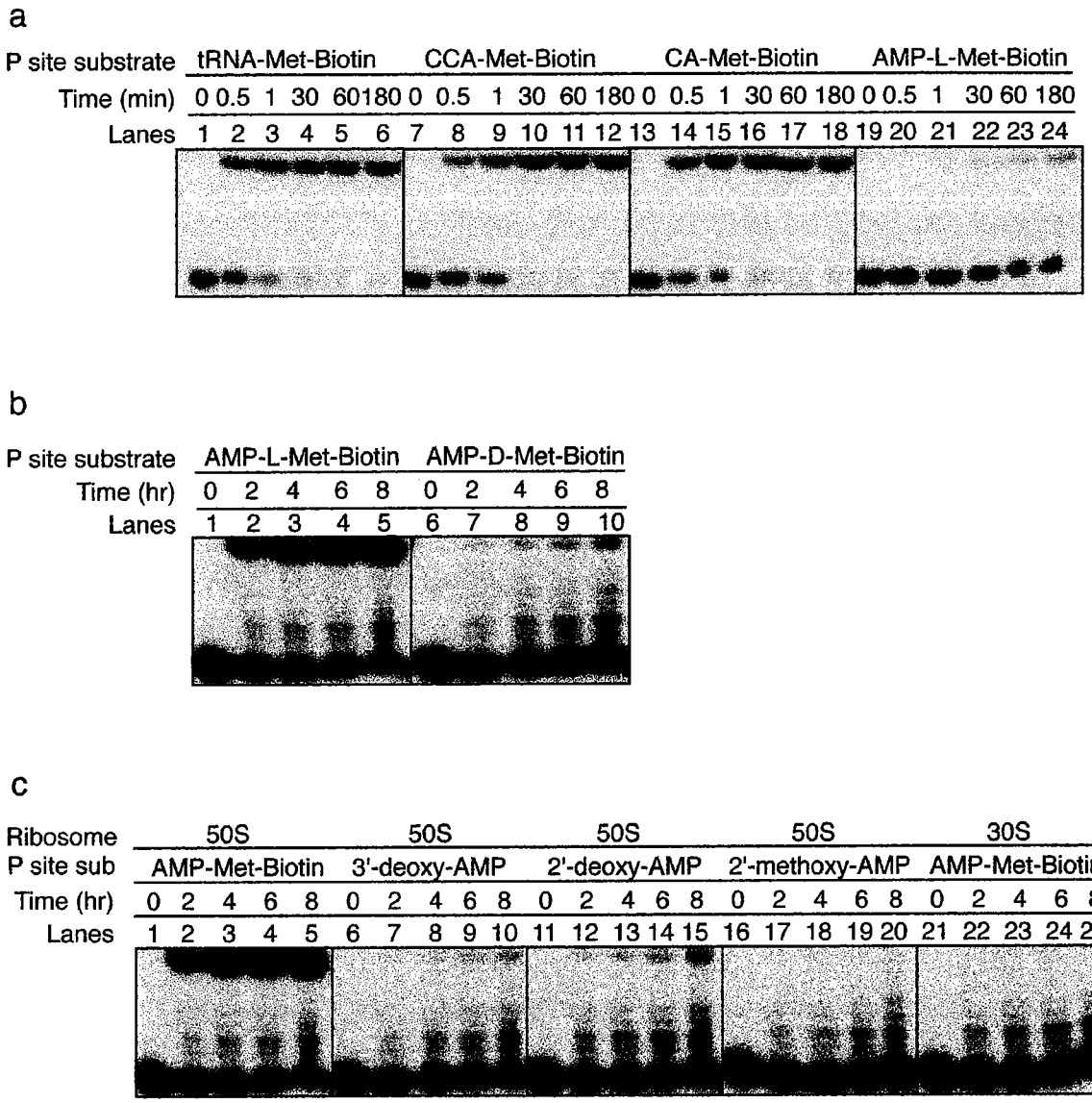

Figure 5-6. P-site substrate specificity of 50S-catalyzed peptidyltransfer reaction. (a) Size effect. Experiments were performed under standard reaction condition with 200 μM tRNA-Met-Biotin, 200 μM CCA-Met-Biotin, 200 μM CA-Met-Biotin, 200 μM AMP-L-Met-Biotin included; (b) Configuration effect. Experiments were performed under standard reaction condition with 1 mM AMP-L-Met-Biotin and 1 mM AMP-D-Met-Biotin included; (c) 2'(3') modification. Experiments were performed under standard reaction condition with 1 mM AMP-Met-Biotin, 1 mM 2' deoxy-AMP-Met-Biotin, 1 mM 3'deoxy-AMP-Met-Biotin and 1 mM 2' methoxy-AMP-Met-Biotin.

Met-Biotin, CCA-Met-Biotin, CA-Met-Biotin, and AMP-Met-Biotin but the activities were different. It was no surprise that the activity with tRNA-Met-Biotin was the highest (1.8 min^{-1}) since tRNA is the natural substrate for the ribosome (Figure 5-6a, lanes 1-6). 50S was very active with CCA-Met-Biotin (Figure 5-6a, lanes 7-12) but the activity (1.0 min^{-1}) was about half time lower than that with tRNA-Met-Biotin indicating that CCA is sufficient for interaction at the P-site but the rest of the tRNA sequence still provides extra binding with the 50S subunit. This result is consistent with an early study in which the intact F-Met-tRNA gave a reaction rate more than twice that with the CCA-Met-F (Monro et al., 1968). Monro and colleagues also indicated that CA-Met-F and Adenosine-Met-F were inactive P-site substrates but this result was challenged by later research in which both CA-Phe and A-Phe were active P-site substrates but CA-Phe was 500-fold more active than A-Phe (Quiggle & Chladek, 1980). Our results showed that 50S was very active with CA-Met-Biotin (Figure 5-6a, 13-18) and much less active with AMP-Met-Biotin (Figure 5-6a, 19-24), which agreed with Quiggle and Chaldek. Interestingly, the activity with CA-Met-Biotin was the same as that with tRNA-Met-Biotin (1.8 min^{-1}) and even higher than that with CCA-Met-Biotin (1.0 min^{-1}), suggesting that removal of the first C residue from CCA fragment doesn't affect the 50S-catalyzed peptidyltransfer reaction and CA is sufficient for interaction at the P-site. However, removal of the second C residue to AMP-Met-Biotin resulted in a 700-fold reduction of activity compared to tRNA/CA-Met-Biotin and 500-fold reduction to CCA-Met-Biotin (0.0026 min^{-1}). This dramatic activity decrease suggests that the most proximal C residue to the 3' terminal adenosine makes important contribution for interaction on the P-site perhaps by base pairing with the nearby nucleotides on the 23S rRNA (Nissen et al.,

2000). Altogether, these data imply that the 3' terminal sequence CA is sufficient for interaction on the P-site and this C residue provides important interaction with the nearby rRNA in promoting the 50S-catalyzed peptidyltransfer reaction.

Next, we investigated the configuration effect of methionine on the P-site substrate. AMP-L-Met-Biotin and AMP-D-Met-Biotin were chemically synthesized and purified by HPLC. In nature, the L-isomer amino acid is preferentially selected for protein synthesis due to preferences at several steps and resulting in a cumulative preference for the L isomer 4 orders of magnitude higher than the D isomer (Calendar & Berg, 1967; Yamane & Hopefield, 1977; Yamane et al., 1981; Lacey et al., 1988). Our result showed that 50S was very active with high concentration of AMP-L-Met-Biotin (1.0 mM, Figure 5-6b, lanes 1-5) but displayed very low yet still detectable activity with AMP-D-Met-Biotin (1.0 mM, Figure 5-6b, lanes 5-10), suggesting that the ribosome distinctively recognizes the L-methionine on the P-site rather than the D-methionine. It has been shown that the L isomers are more readily used by the ribosome but the incorporation of D isomers into peptides are still possible (Yamane et al., 1981). Our results agree that 50S preferential recognizes the L-configuration amino acid on the P-site during the step of peptide bond formation. The D-configuration amino acid could be but not efficiently utilized by the 50S even if it is pre-placed at the P-site position within the peptidyltransfer center. These results indicate that the requirement at the peptidyltransfer center is very strict, any unfavorable factor such as imperfect positioning or steric hindrance would greatly hamper peptide bond formation.

Finally, the role of the 2'-OH group on the terminal A residue in peptide bond formation was probed. Because the amino acids esterified to the ribose group of AMP

constantly migrate between the 2' and 3' positions of the ribose, we synthesized 2'-deoxy-AMP-Met-Biotin and 3'-deoxy-AMP-Met-Biotin to eliminate the possible movements of the amino acid (Figure 5-5). A control reaction was performed by incubating ^{32}P-CCA-*NH*-Phe and AMP-L-Met-Biotin in the presence of 30S subunit (Figure 5-6c, 21-25), indicating that peptide bond formation between ^{32}P-CCA-*NH*-Phe and AMP-L-Met-Biotin does not occur spontaneously in the absence of 50S subunit. 50S activity was greatly increased when AMP-Met-Biotin concentration was raised from 200 μM (Figure 5-6a, lanes 19-24) to 1.0 mM (Figure 5-6c, lanes 1-5). 50S was active with both 2'-deoxy-AMP-Met-Biotin and 3'-deoxy-AMP-Met-Biotin although the activity was still very low even after 8-hour incubation (Figure 5-6c, lanes6-10, 11-15). It is amazing that 50S is active with both 2'-deoxy-AMP-Met-Biotin and 3'-deoxy-AMP-Met-Biotin since it challenges the traditional idea that the ribosome incorporate amino acids into proteins only when they are at the 3' position (Hecht, 1977; Sprinzl & Cramer, 1979; Wagner et al., 1982; Taiji et al., 1985). The activity with 2'-deoxy-AMP-Met-Biotin was greatly decreased but still detectable, suggesting that the peptidyltransfer reaction does not require the 2'-OH group but the presence of the 2'-OH group makes important contribution to the peptidyltransfer reaction. Because removal of the 2'-OH group also changed the pK_a of the leaving group, it is possible that the dramatic activity decrease results from the change in the leaving ability of AMP. To probe this possibility, 2'-OCH_3-AMP-Met-Biotin was synthesized which has similar pK_a with 2'-OH-AMP-Met-Biotin (Figure 5-5). 50S was not active with 2'-methoxy derivative (Figure 5-6c, lanes 16-20), indicating that pK_a of the leaving group makes little contribution to the ribosomal peptidyltransfer reaction. Instead, this result suggests an important role for the

hydrogen atom in the 2'-OH group. It is very likely that this hydrogen is involved in hydrogen bonding that facilitates the peptidyltransfer reaction. The introduction of an inert methoxy group will hamper the interaction between the substrate and the ribosome thus killing the reaction.

A recent publication reported that the 2'-deoxy derivative caused the complete loss of the peptidyltransferase activity (Dorner et al., 2002), and because the 2'-OH was also observed in close vicinity of the synthesized peptide bond formation in the crystal structures (Ban et al., 2000), it was suggested that the 2'-OH group was directly involved in the catalysis of peptide bond formation (Dorner et al., 2002). Our results suggest several possible roles of 2'-OH group in the peptidyltransfer reaction. One possibility is that the 2'-OH group might be involved in catalysis by peptide bond formation. It is also possible that the 2'-OH group functions by providing tight association of AMP-Met-Biotin with the ribosome through hydrogen bonds. Further discrimination between these two possibilities may employ a series of CA-Met-Biotin derivatives with modifications at the 2' position. The presence of an extra C residue in the P-site substrate will pre-anchor the terminal A residue to the P site no matter the 2'-OH contributes to binding or not, thus it will be straightforward to examine whether the 2'-OH group is directly involved in the catalysis of peptide bond formation.

Antibiotics Inhibition Studies

Antibiotics have been very useful in probing ribosomal structure and functions. We utilized our newly developed system to examine the effects of different antibiotics specifically on peptide bond formation. Two sets of substrates were used in the

antibiotics inhibition study, CCA-Met-Biotin with CCA-*NH*-Phe and tRNA-Met-Biotin and CCA-*NH*-Phe in order to probe the difference between the whole tRNA sequence and the terminal CCA fragment in contributing to the peptidyltransfer reaction. Meanwhile, activities were compared between 70S and 50S to reveal different interactions among the antibiotics, substrates and the ribosome.

In the absence of any inhibitor, 50S activities with both substrates were higher than 70s activities (Figure 5-7a~7d), suggesting that 50S is better than 70S in catalyzing peptide bond formation between CCA-*NH*-Phe and CCA/tRNA-Met-Biotin. Activities with tRNA-Met-Biotin were slightly higher than those with CCA-Met-Biotin in both 70S and 50S-mediated peptidyltransfer reactions, confirming that the rest of the tRNA sequence provides extra interactions with the ribosome and promotes peptide bond formation other than binding from the terminal CCA sequence.

Tetracycline. It is generally assumed that tetracycline inhibits A-site aminoacyl-tRNA binding to the 30S subunit (Oehler et al., 1997; Epe et al., 1987; Goldman et al., 1983; Tritton, 1977). In our peptidyltransferase assay, CCA-*NH*-Phe serves as the A-site substrate and CCA/tRNA-Met-Biotin as the P-site substrate. Because the CCA moiety of CCA-*NH*-Phe only interact with 50S subunit and the peptidyltransferase activity solely depends on 50S, we predict that tetracycline will not inhibit peptide bond formation between CCA-*NH*-Phe and CCA/tRNA-Met-Biotin. This assumption was confirmed by the inhibition experiments (Figure 5-7). Both 70S and 50S activities in the presence of 100 μM tetracycline were the same as those obtained in no inhibitor reactions.

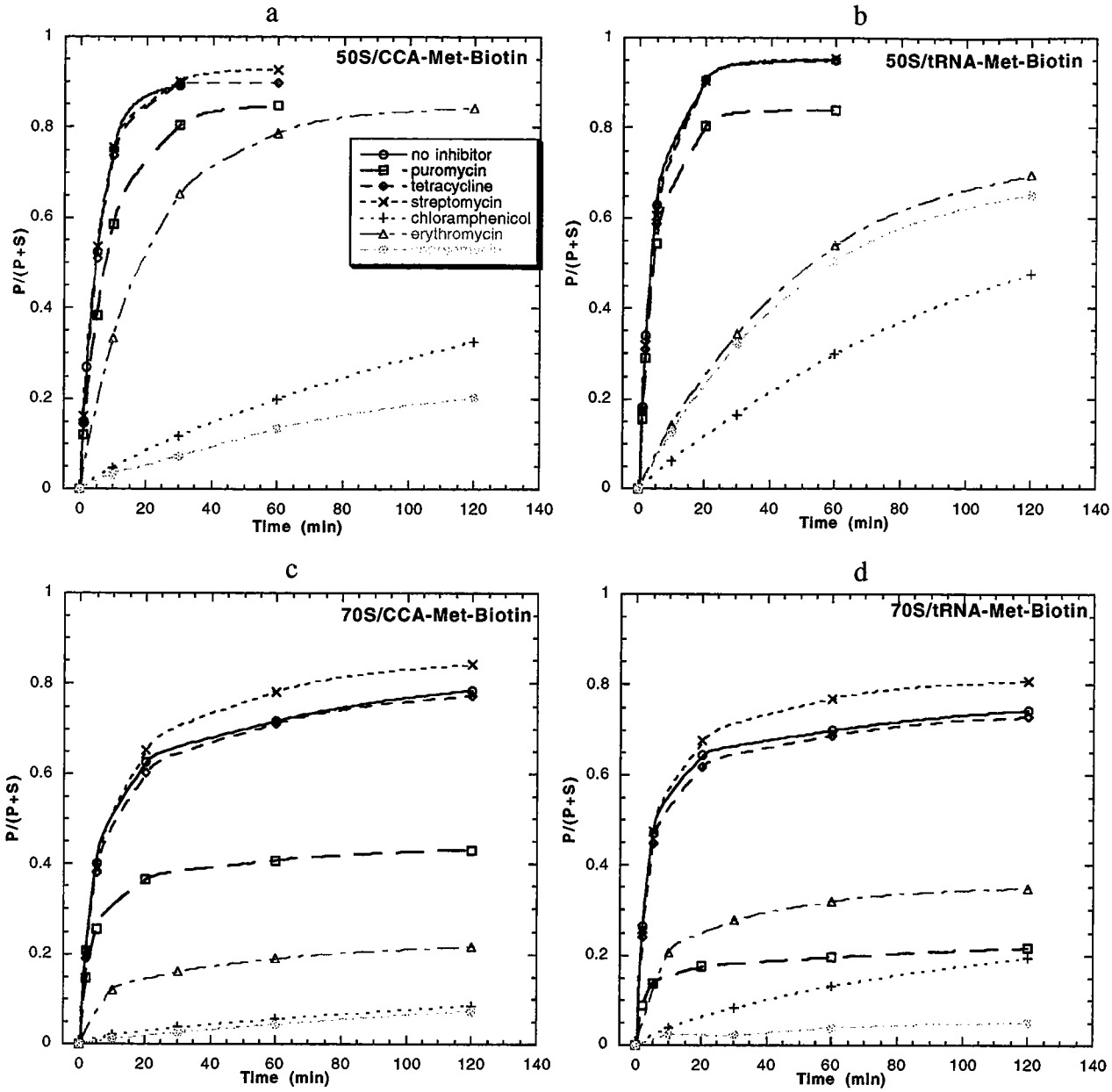

Figure 5-7. Antibiotics inhibition of 70S or 50S-catalyzed peptidyltransfer reactions. Reactions were carried out with 50S or 70S, 50 μM CCA-Met-Biotin or tRNA-Met-Biotin, trace amount of ^{32}P-CCA-*NH*-Phe (~ 5×10^{-4} μM), 100 μM antibiotics in the presence of 50 mM Tris•HCl (pH 7.5), 35 mM $MgCl_2$, 100 mM NH_4Cl and 1000 mM KCl at 37 ^{0}C. For each reaction, same amount of 50S or 70S (10 pmol) was included. (a) 50S with CCA-Met-Biotin. (b) 50S with tRNA-Met-Biotin. (c) 70S with CCA-Met-Biotin. (d) 70S with tRNA-Met-Biotin.

Streptomycin. Streptomycin affects protein synthesis by causing mRNA misreading (Vazquez, 1979), thus it did not affect peptide bond formation between CCA-*NH*-Phe and CCA/tRNA-Met-Biotin catalyzed by either 70S or 50S (Figure 5-6).

Chloramphenicol. Chloramphenicol inhibits protein synthesis by blocking A-site substrate binding on 50S (Rodriguez-Fonseca et al., 1995; Moazed & Noller, 1987; Schlunzen et al., 2001). Therefore, it will compete with CCA-*NH*-Phe in binding to 50S and specifically inhibit peptide bond formation between CCA-*NH*-Phe and CCA/tRNA-Met-Biotin. As shown in Figure 5-7, chloramphenicol strongly inhibited peptide bond formation in both 70S and 50S-mediated reactions.

Puromycin. The inhibition of puromycin to protein synthesis has been extensively studied. It is generally accepted that puromycin acts as an aminoacyl-tRNA analog to compete binding to the A site (Nathans & Neidle, 1963; Steiner et al., 1988; Kirillov et al., 1997). Puromycin could also be prematurely linked to the C-terminus of newly synthesized peptides (Allen & Zamecnik, 1962; Nathans, 1963; Traut & Monro, 1964; Zamir et al., 1966; Etsuko et al., 2000). Recently, it was suggested that puromycin might affect ribosome activity in multiple ways (Shelley & Roberts, 2002) in addition to the two modes described above. In our studies, the effects of 100 μM puromycin on 50S-mediated peptidyltransfer reactions were very small (Figure 5-7a, 5-7b); instead, puromycin significantly inhibited 70S-mediated reactions (Figure 5-7c, 5-7d). These results suggest that puromycin does not specifically inhibit peptide bond formation because 50S activity was not greatly hampered. However, puromycin might interact with other components within the ribosome or influence the general conformation of ribosome, thus inhibit peptide bond formation between CCA-*NH*-Phe and CCA/tRNA-Met-Biotin.

Sparsomycin. Sparsomycin is one of the few antibiotics that affect protein synthesis by specifically inhibiting peptide bond formation (Vazquez, 1979; Cundliffe, 1981; Tan et al., 1996; Porse et al., 1999; Monro et al., 1969). The binding site of sparsomycin is located on 50S subunits. It is likely that it inhibits peptide bond formation by the combination of two effects: interfering with A-site substrate binding (Cundliffe, 1981) and forming an inert complex to lock the P-site substrate (Monro et al., 1969). Our results showed that sparsomycin greatly inhibited 50S activity in catalyzing peptide bond formation between CCA-*NH*-Phe and CCA-Met-Biotin (Figure 5-7a); however, the inhibition effect on CCA-*NH*-Phe and tRNA-Met-Biotin in 50S was not so significant (Figure 5-7b). This phenomenon implies that the interaction between tRNA and 50S might compensate part of the inhibition effects from sparsomycin. Interestingly, the 70S activities with both sets of substrates were almost totally inhibited by 100 μM sparsomycin (Figure 5-7c, 5-7d), suggesting that in addition to its specific inhibition for peptide bond formation, sparsomycin might interact with other components within the ribosome to affect protein synthesis.

Erythromycin. Erythromycin represents one group of the macrolide antibiotics (Gale et al., 1981). It inhibits protein synthesis by two modes: destabilizing the P-site peptidyl-tRNA and blocking the peptide exit tunnel (Gale et al., 1981; Spahn & Prescott, 1996; Porse et al., 1995; Moazed & Noller, 1987). The 50S-CCA reaction was not greatly inhibited by erythromycin indicating that the direct effect of erythromycin on peptide bond formation is minor. Erythromycin inhibited 50S-tRNA reaction more than 50S-CCA reaction, suggesting that the destabilization of the P-site substrate is mostly on the rest of tRNA sequence other than the terminal CCA fragment. However,

erythromycin inhibited 70S-catalyzed reactions much more significantly than the 50S-catalyzed reaction, suggesting a general effect of erythromycin on 70S other than its influence on peptide bond formation.

Conclusion

A new assay has been successfully established for characterizing the ribosomal peptidyltransfer reaction. This assay employs utilization of two synthesized substrates: CCA-Met-Biotin (P-site) and CCA-*NH*-Phe (A-site) in specifically probing the peptidyltransfer reaction catalyzed by the ribosome or ribosomal subunit. Above results show that: (1) divalent metal ions (Mg^{2+}, Ca^{2+}, or Mn^{2+}) are required to promote 50S-catalyzed peptidyltransfer reaction; (2) the 2'-OH group on the terminal A residue of the P-site substrate makes important contribution to the 50S-catalyzed peptidyltransfer reaction; and (3) various antibiotics differentially inhibit the ribosomal peptidyltransfer reaction.

Chapter VI

Summary And Discussion

In previous chapters, I have focused on characterizing the peptidyltransferase reaction mediated by *in vitro* selected ribozymes and by the ribosome. Peptide bond formation has been readily observed in both systems. Several aspects of peptide bond formation catalyzed by the ribozyme and the ribosome have been investigated, including metal ion requirement, pH dependence, and substrate specificity. This chapter summarizes the results from these studies. The coherence between these two peptide-synthesizing systems is discussed and their potential applications are explored.

Ribozyme-mediated peptide bond formation

The R180 ribozyme is selected for catalyzing peptide bond formation using the aminoacyl-adenylate as the substrate. Peptide bond is formed between a phenylalanine tethered to the 5' end of R180 and a biotinylated methionyl-adenylate substrate (Figure 3-1). From an evolutionary point of view, because the aminoacyl-adenylate is a universal intermediate for both ribosomal and nonribosomal processes of protein biosynthesis in the modern biological systems, it might also function as a common intermediate in the ancient protein synthesis. Ribozymes have been isolated to use aminoacyl-adenylate in catalyzing various reactions (Kumar & Yarus, 2001; Illangasekare et al., 1995; Illangasekare & Yarus, 1999a; Illangasekare & Yarus, 1999b; Wiegand et al., 1997; Lohse et al., 1996). In this thesis, the isolation of the R180 ribozyme provides the

plausibility that RNA might have directed uncoded protein synthesis using the aminoacyl-adenylate as the substrate.

The R180 ribozyme is efficient in catalyzing peptide bond formation with a second-order rate constant (k_{cat}/K_m) of 19,300 $M^{-1}min^{-1}$, which is modest compared to many protein enzymes. The R180 ribozyme could accommodate a wide range of amino acids, including positively charged arginine and lysine, polar glutamine, aromatic phenylalanine and tryptophan, and aliphatic alanine, leucine, and methionine. This feature is remarkable since these amino acids are also indiscriminately recognized and utilized in the ribosomal protein synthesis. This phenomenon again favors the hypothesis that primordial RNA could have directed uncoded peptide synthesis.

The R180 ribozyme is very active in Li^+, Na^+ or K^+ in the absence of any divalent metal ions, such as Mg^{2+} and Ca^{2+}. This finding provides strong evidence that not all ribozymes require divalent metal ions to perform catalysis and agrees with recent studies that three small naturally occurring ribozymes (hammerhead, hairpin, and *Neuropora* VS) are active in high concentrations of monovalent metal ions alone. The R180 ribozyme gives the first example of *in vitro* selected ribozymes that are selected in the presence of both divalent and monovalent metal ions yet active with monovalent metal ions alone.

Investigation of pH dependence of the R180-catalyzed reaction in either Li^+ or Mg^{2+} reveals almost identical pH profiles except the activity difference, suggesting that Li^+ and Mg^{2+} function similarly in the peptide bond forming reaction. Both pH profiles exhibit linear relationship at low pHs with a slope of 1.0, suggesting that one proton transfer is involved in the rate-limiting step of peptide bond formation. Isotope replacement experiments exhibit a 10-fold decrease in activity over the entire range of

tested pHs, supporting that proton transfer may be the rate-limiting step and implying that peptide bond formation might take place via a general base catalysis mechanism. Based on these results, a mechanism is proposed for the ribozyme-catalyzed peptidyltransferase reaction (Figure 4-8). Briefly, the amino group of phenylalanine of 5'-Phe-linker-RNA acts as a nucleophile attacking the carbonyl carbon of the methionine of biotin-Met-AMP anhydride to form a tetrahedral intermediate. Deprotonation of the intermediate by a general base (base, phosphate backbone, buried water, or other groups) forms a negatively charged intermediate, resulting in the cleavage of the C-O bond to give the dipeptide product. The rate-limiting step could be the deprotonation of the forming intermediate at pH $\leq$ 8.0 with one proton transfer involved in this step. The divalent or monovalent ions may confer similar functions to stabilize the developing intermediate and/or to assist folding an active ribozyme conformation.

A previously isolated peptide-bond-forming ribozyme, the C25 ribozyme, is found that could also use the aminoacyl-5'-adenylate as its substrate in catalyzing peptide bond formation. Both R180 and C25 ribozymes exhibit no discrimination for amino acids in peptide bond formation. These facts further suggest the key role of the aminoacyl-5'-adenylate in modern and probably primordial protein synthesis and bolster the hypothesis that aminoacyl-5'-adenylate might serve as the substrate in mediating the RNA-catalyzed uncoded peptide synthesis. Our results demonstrate that these two ribozymes recognize the Biotin-Met-5'-AMP substrate distinctively. Biotin moiety of biotin-Met-5'-AMP is the major binding site for the R180 ribozyme, while AMP of biotin-Met-5'-AMP contributes most to substrate binding for the C25 ribozyme. Another

interesting feature of these two ribozymes is that besides dipeptide synthesis, both are capable of catalyzing longer peptide synthesis (tri-, tetra-, and penta-peptides) although the C25 ribozyme is more efficient than the R180 ribozyme. The C25 ribozyme could even catalyze synthesis of a seven-amino acid peptide (data not shown).

Ribosomal peptidyltransfer reaction

To gain a better understanding of the mechanism of ribosome-mediated protein synthesis, efforts were taken to establish a new assay in specifically and accurately monitoring the ribosomal peptidyltransfer reaction. The significance of the new assay is four fold: substrate analogs closely mimicking the authentic ribosomal substrates, directly monitoring peptide bond formation, high sensitivity and easy quantitation of the products.

Using this assay, the ribosomal peptidyltransfer reaction has been examined for its metal ion requirement, pH dependence and antibiotic inhibition. Peptide bond formation is stimulated by the presence of Mg^{2+}, Ca^{2+} or Mn^{2+}, which is consistent with other publications. pH dependence experiments display a bell-shape profile of 50S-catalyzed peptidyltransfer reaction, suggesting the involvement of two ionizable groups in the chemical step of the reaction or a general effect of pH on the ribosome conformation. Antibiotic inhibition studies reveal different action of the antibiotics on intact ribosome and the large ribosomal subunit, suggesting that the new system can specifically identify the peptidyltransferase inhibitors.

The emphasis has been placed on examining the P-site substrate specificity of 50S-catalyzed peptidyltransfer reaction. Eight P-site substrate derivatives have been tested for minimum requirement of P-site substrate, and importance of the 2'-OH group

on A76 of tRNA. Changing the length of the P-site substrate (tRNA-, CCA-, CA-, AMP-Met-Biotin) reveals that the CA is the minimum requirement for P-site substrate and C75 residue plays an important role in the binding but it is not necessary for the catalysis of peptide bond formation. Modifications of the 2'(3') position groups of A76 give out more interesting results. Removal of the 2'-OH group greatly reduces but does not eliminate peptide bond formation, suggesting that the presence of 2'-OH significantly promotes but is not required for the peptidyltransfer reaction. Replacement of the 2'-OH with 2'-OCH_3, however, totally kills the reaction, suggesting that it is the hydrogen atom but not the oxygen atom that makes important contribution to the formation of peptide bond. These results imply two possibilities of the role of 2'-OH in the peptidyltransfer reaction. One possibility is that 2'-OH is actively involved the catalysis by stabilizing the reaction intermediate. It is also likely that 2'-OH helps the binding of AMP-Met-Biotin to the ribosome.

Discussion

Although the ribosome is a ribozyme, the ribosomal peptidyltransferase activity has not been achieved with ribosomal RNAs alone, implying that the modern ribosome requires proteins to perform catalysis. However, from an evolutionary point of view, because RNA is the catalyst in the ribosome, it is very likely that the evolution of the ribosome might have started from an all RNA particle and the ribosomal proteins have joined at a later stage. Therefore, the attempted goal of this research has been to seek for

the catalytic RNAs that can catalyze peptide bond formation, and such ribozymes might serve as a reminiscence of ribosome catalysis in an ancient world. We have successfully isolated ribozymes by *in vitro* selection to catalyze peptide bond formation and these ribozymes can even direct tri-peptide and tetra-peptide synthesis. This achievement itself indicates that RNA can catalyze peptide bond formation in the absence of proteins and strengthens the "RNA world" hypothesis that RNAs have catalyzed all the reactions before the emergency of the DNA/protein system. In this ribozyme system, there is no template to direct peptide synthesis, thus the ribozyme catalyzes uncoded peptide synthesis using the aminoacyl-adenylate as the substrate. The catalytic activity of this ribozyme is pretty good; the ribozyme is also highly active in the presence of monovalent metal ions alone; this ribozyme could even utilize a large variety of amino acids in synthesizing peptides, and this feature makes the ribozyme like the ribosome, which recognizes various kinds of amino acids in making proteins.

In spite of all these good features about R180 catalysis, how feasible is it to use the R180 system as a model to investigate the ribosomal peptidyltransferase reaction? It is very likely that after a long time of evolution and with the appearance of the ribosomal proteins, the modern ribosomal RNA might have been far deviated from its ancestor. Therefore, it may not be realistic to explore the ribosome-catalyzed peptide bond formation in this ribozyme system. Another obvious disadvantage of the R180 system is its substrate-binding specificity. We have demonstrated that in the ribozyme system, biotin contributes most to substrate binding. It will be hard to imagine that in the primordial world, RNA would recognize biotinylated amino acids to synthesize peptides since biotin is not a populated component. Instead, it is more likely that nucleotides

might be involved in substrate binding. Unfortunately, in our ribozyme-catalyzed peptide synthesis, adenosine only serves as a good leaving group but not for substrate binding. Therefore, these limitations hamper us to use the ribozyme system as a model to investigate the ribosomal peptide bond formation. However, because we have identified multiple active families from the selection, it is likely that we may find ribozymes from other families whose substrate recognition site is not biotin, but is AMP. It is also possible that we could find such ribozymes that have similar sequences with the ribosomal RNAs. These ribozymes will then be more close to the authentic ribosome system in catalyzing peptide bond formation.

Future study of R180 catalysis may be searching for the general base in catalyzing peptide bond formation. Nucleotide Analog Interference Mapping (NAIM) will be the best tool in seeking of the functional groups on the RNA that may act as a general base. Also, deletion and mutation studies would tell us which region is directly involved in catalyzing peptide bond formation.

The R180 system still has its potential applications in other fields. First, a high percentage of the ribozyme could be converted to the product, suggesting that the ribozymes might have folded into a uniform conformation. Usually, *in vitro* selected ribozymes are not easy to fold into a uniform active conformation, which makes crystallization impractical. R180 is ideal for crystallization. Therefore, we can clearly observe how peptide bond formation occurs in the R180 crystal structures. Second, because of its high affinity to biotin, R180 might be used to substitute streptavidin for detecting the biotinylated molecules in gel-shift assay or other assays. Third, because R180 is very efficient in catalyzing peptide synthesis, we could immobilize the ribozyme

on beads or surface and use it as a peptide-synthesizing machine to make small fragment of peptides. Fourth, we may use the R180 ribozyme as the initial bait for isolating the next generation of ribozymes that can catalyze long peptide synthesis between peptidyl-ribozyme and amino acids, like the process of polyketide synthesis.

It is our ultimate goal to investigate peptide bond formation catalyzed by the ribosome. Indeed, until now, no one has been able to achieve ribosomal peptidyltransferase activity with ribosomal RNAs only. So, why is it so hard? A feasible explanation is the large size of ribosomal RNAs. The length of total 23S rRNA in the large ribosomal subunit is about 2900 nucleotides. Even domain V within 23S rRNA is about 600 nt long. It might be difficult for such long RNAs to fold into active conformation properly without the help of proteins or other factors in order to perform catalysis. However, we still need to discriminate between two possibilities of rRNA catalysis. Is there any catalytic group from rRNAs or other factors (e.g. metal ions) directly involved in catalyzing peptide bond formation, or do the rRNAs only serve as template to bring the two substrates into close proximity to form peptide bond spontaneously? It is generally accepted that metal ions function as scaffold factors in supporting the structure of the ribosome while its role in catalysis still remains elusive. A more promising candidate for catalyzing peptide bond formation is the nucleobases. Although the biggest drawback of the nucleobases in acting as an enzyme is their low pK_a values, it is proposed that such low pK_a could be raised by the environment through a charge-relay mechanism. However, subsequent studies throw doubts on this hypothesis and provide strong evidence that the nearby nucleotides might not be critically involved

in catalyzing peptide bond formation. Therefore, it seems likely that the nucleobases are not directly involved in catalysis. Instead, our study reveals important role of the functional group on the substrate in catalysis. The 2'-OH group on the terminal adenosine of the P-site substrate makes great contribution to peptide bond formation, suggesting that it may be directly involved in catalysis. But the hydroxyl group is not required since peptide bond formation is still detectable in the absence of this group. Therefore, our results, as well as other reported data, favor the hypothesis that peptide bond formation occurs spontaneously once the aminoacyl-tRNAs are perfectly positioned inside the ribosome. The contribution from the 2'-OH group in this reaction might be stabilizing the transition intermediate or involved in substrate binding.

Future study using the new established assay could examine the ribosomal peptidyltransferase activity with pCpA-Met-Biotin derivatives modified on the 2' position of adenosine. The presence of an extra C residue will stabilize the substrate position in the reaction center, thus the role of the 2'-OH group either in catalysis or substrate binding could be easily distinguished. Substitution of the 2'-OH by a fluoro group may also provide hint whether the OH group is involved in catalysis or not.

Although we still couldn't achieve ribosomal peptidyltransferase activity with ribosomal RNAs only, the newly established assay still has its potential application in other fields. One promising application could be in drug screening to identify the specific inhibitors for the peptidyltransferase reaction. The ribosome is a good target for many antibiotics. Our assay specifically monitors peptide bond formation in the ribosome. Therefore, it provides a good system to search for the designed or natural

existing compounds that can destroy the ribosome function by inhibiting peptide bond formation.

References

Allen, D. W., Zamecnik, P. C. (1962) The effect of puromycin on rabbit reticulocyte ribosomes. *Biochim. Biophys. Acta. 55*, 865-874.

Allerson, C. R.; Chen, S. L.; Verdine, G. L. A. (1997) Chemical Method for Site-Specific Modification of RNA: The Convertible Nucleoside Approach. *J. Am. Chem. Soc. 119*, 7423-7433.

Ban, N., Freeborn, B., Nissen, P., Penczek, P., Grassucci, R. A., Sweet, R., Frank, J., Moore, P. B., Steitz. T. A. (1998) A 9 A resolution X-ray crystallographic map of the large ribosomal subunit. *Cell 93*, 1105-1115.

Ban, N., Nissen, P., Hansen, J., Moore, P. B., Steitz, T. A. (2000) The complete atomic structure of the large ribosomal subunit at 2.4 A resolution. *Science 289*, 905-920.

Barta, A., Dorner, S., Polacek, N. (2001) Mechanism of ribosomal peptide bond formation. *Science 291*, 203a.

Bartel, D. P. & Szostak, J. W. (1993) Isolation of new ribozymes from a large pool of random sequences. *Science 261*, 1411-1418.

Basu, S., Rambo, R. P., Strauss-Soukup, J., Cate, J. H., Ferre-D'Anre, A. R., Strobel, S. A., Doudna, J. A. (1998) A specific monovalent metal ion integral to the AA platform of the RNA tetraloop receptor. *Nat. Struct. Biol. 3*, 993-1009.

Bayfield, M. A., Dahlberg, A. E., Schulmeister, U., Dorner, S., Barta, A. (2001) A conformational change in the ribosomal peptidyl transferase center upon active/inactive transition. *Proc. Nat. Acad. Sci. USA. 98*, 10096-10101.

Beaudry, A. A. & Joyce, G. F. (1992) Directed evolution of an RNA enzyme. *Science 257*, 635-641.

Benner, S. A., Ellington, A. D. & Tauer, A. (1989). Modern metabolism as a palimpsest of the RNA world. *Proc. Natl. Acad. Sci. USA 86*, 7054-7058.

Berg, P. (1958). The chemical synthesis of amino acyl adenylates. *J. Biol. Chem. 233*, 608-611.

Blanchard, S. C., Puglisi, J. D. (2001) Solution structure of the A loop of 23S ribosomal RNA. *Proc. Natl. Acad. Sci. USA. 98*, 3720-3725.

Bodley, J. W. (1988) in Biochemistry, (Zubay, G. ed.), pp. 928-973, *Macmillan Publishing Company*, New York.

Burgin, A.; Pace, N. (1990) Mapping the active site of ribonuclease P RNA using a substrate containing a photoaffinity agent. *EMBO J. 9*, 4111-4118.

Cadwell, R. C., Joyce, G. F. (1992) Randomization of genes by PCR mutagenesis. *PCR. Meth. Appl. 2*, 28-33.

Calendar, R. & Berg, P. (1967) D-Tyrosyl RNA: formation, hydrolysis and utilization for protein synthesis. *J. Mol. Biol. 26*, 39-54.

Cate, J. H., Yusupov, M. M., Yusupova, G. Zh., Earnest, T. N., Noller, H. F. (1999) X-ray crystal structures of 70S ribosome functional complexes. *Science 285*, 2095-2104.

Cech, T. R.; Herschlag, D. *Catalytic RNA*; Eckstein, F., Lilley, D. M. J., Eds.; Springer-Verlag :Berlin, 1996; Vol. *10*, pp 1-17.

Cech, T. R., Zaug, A. J., Grabowski, P. J. (1981) In vitro splicing of the ribosomal RNA precursor of Tetrahymena: involvement of a guanosine nucleotide in the excision of the intervening sequence. *Cell 27*, 487-496.

Chu, B. C. F.; Kramer, F. R. and Orgel, L. (1986) Synthesis of an amplifiable reporter RNA for bioassays. *Nucleic Acids Res. 14*, 5591-5603.

Chu, B. C. F. and Orgel, L. (1988) Ligation of oligonucleotides to nucleic acids or proteins via disulfide bonds. *Nucleic Acids Res. 16*, 3671-3691.

Chen, Y. and Baker, G. L. (1999) Synthesis and Properties of ABA Amphiphiles. *J. Org. Chem. 64*, 6870-6873.

Cleland, W. W. (1997) The use of pH studies to determine chemical mechanisms of enzyme-catalyzed reactions. In *Isotope effects on enzyme-catalyzed reactions*, O'Leary, M. H. and Northrop, D. B., eds. (University Park Press, Baltimore, MD).

Cohen, S. B.; Cech, T. R. (1997) Dynamics of Thermal Motions within a Large Catalytic RNA Investigated by Cross-linking with Thiol-Disulfide Interchange. *J. Am. Chem. Soc. 119*, 6259-6268.

Cook, P. F. (1991) In *Enzyme mechanism from isotope effects*. (CRC press, Inc., Boca Raton, FL).

Crick, F. H. C. (1968). The origin of the genetic code. *J. Mol. Biol. 38*, 367-379.

Cundliffe, E. (1981) Antibiotic inhibitors of ribosome function. In the *Molecular basis of antibiotic action* (Gale, E. F., Cundliffe, E., Reynolds, P. E., Richmond, M. H., Waring, M. J., eds), pp 402-545, John Wiley & Sons, London, New York, Sydney, Toronto.

Curtis, E. A., Bartel, D. P. (2001) The hammerhead cleavage reaction in monovalent cations. *RNA 7*, 546-552.

Czworkowski, J.; Odom, O.; Hardesty, B. (1991) Fluorescence study of the topology of messenger RNA bound to the 30S ribosomal subunit of Escherichia coli. *Biochemistry 30*, 4821-4830.

DeRose, V. J. (2002) Two decades of RNA catalysis. *Chem & Biol. 9*, 961-969.

Dewey, T. M.; Zyzniewski, M. C.; Eaton, B. E. (1996) The RNA world: functional diversity in a nucleoside by carboxyamidation of uridine. *Nuleosides Nucleotides 15*, 1611-1617.

Dimitrijevich, S. D.; Verheyden, J. P. H.; Moffatt, J. G. (1979) Halo sugar nucleosides 6. Synthesis of some 5'-deoxy -5'-iodo and 4',5'-unsatured purine nucleosides. *J. Org. Chem. 44*, 400-406

Dinos, G. P., Kalpasix, D. L. (2000) Kinetic studies on the interaction between a ribosomal complex active in peptide bond formation and the macrolide antibiotics tylosin and erythromycin. *Biochemistry 39*, 11621-11628.

Dorner, S., Polacek, N., Schulmeister, U., Panuschka, C., Barta, A. (2002) Molecular aspects of the ribosomal peptidyltransferase. *Transactions 30*, 1131-1137.

Doudan, J. A. & Cech, T. R. (2002) The chemical repertoire of natural ribozymes. *Nature 418*, 222-228.

Ekland, E. H., Bartel, D. P. (1996) RNA-catalyzed RNA polymerization using nucleoside triphosphates. *Nature 382*, 373-376.

Ekland, E. H., Szostak, J. W., Bartel, D. P. (1995) Structurally complex and highly active RNA ligases derived from random RNA sequences. *Science 269*, 364-370.

Ellington, A. D. & Szostak, J. W. (1990) *In vitro* selection of RNA molecules that bind specific ligands. *Nature 346*, 818-822.

Epe, B., Woolley, P., Hornig, H. (1987) Competition between tetracycline and tRNA at both P and A sites of the ribosome of Escherichia coli. *FEBS Lett. 213*, 443-447.

Fahnestock, S., Erdmann, V., Nomura, M. (1974) Reconstitution of 50S ribosomal subunits from Bacillus Stearothermophilus. *Meth. Enzymol. 30*, 554-562.

Favre, A. *Bioorganic Photochemistry: Photochemistry and the Nucleic Acids;* Morrison, H. Ed.; Wiley: New York, 1990, pp. 379-425.

Fidanza, J. A.; Ozaki, H. and McLaughlin, L. W. (1994) Related Articles Functionalization of oligonucleotides by the incorporation of thio-specific reporter groups. *Methods Mol Biol. 26*, 121-43.

Gale, E. F., Cundliffe, E., Reynolds, P. E., Richmond, M. H., Waring, M. J. (1981) *The molecular basis of antibiotic action*, John Wiley & Sons, London.

Gait, M. J.; Earnshaw, D. J.; Farrow, M. A.; *et al. RNA-protein interactions: A practical approach*; Smith, C. Ed.; Oxford Univ. Press: Oxford, 1998; pp. 1-36.

Garrett, R. A., Rodriguez-Fonseca, C. (1995) In *Ribosomal RNA: structure, evolution, processing and function in protein biosynthesis*, eds. Zimmermann, R. A. & Dahlberg, A. E. (CRC, Boca Raton, FL), pp. 327-335.

Giambattista, M. D., Engelborghs, Y., Nyssen, E., Cocito, C. (1987) Kinetics of binding of macrolides, lincosamides, and synergimycins to ribosomes. *J. Biol. Chem. 262*, 8591-8597.

Gilbert, W. (1986). The RNA world. *Nature 319*, 618-620.

Golden, B. L., Gooding, A. R., Podell, E. R., Cech, T. R. (1998) A preorganized active site in the crystal structure of the Tetrahymena ribozyme. *Science 282*, 259-264.

Goldman, R. A., Hasan, T., hall, C. C., Strycharz, W. A., Cooperman, B. S. (1983) Photoincorporation of tetracycline into Escherichia coli ribosomes. Identification of the major proteins photolabeled by native tetracycline and tetracycline photoproducts and implications for the inhibitory action of tetracycline on protein synthesis. *Biochemistry 22*, 359-368.

Goody, R. S.; Eckstein, F. (1971) Thiophosphate analogs of nucleoside di and triphosphates. *J. Am. Chem. Soc. 93*, 6252-6257.

Gottikh, B. P.; Krayevsky, A. A.; Tarussova, N. B.; Purygin, P. P. & Tsilevich, T. L. (1970). The general synthetic route to amino acid esters of nucleotides and nucleoside-5'-triphosphates and some properties of these compounds. *Tetrahydron 26*, 4419-4433.

Green R & Noller HF. (1999) Reconstitution of functional 50S ribosomes from in vitro transcripts of *Bacillus stearothermophilus* 23S rRNA. *Biochemistry. 38*, 1772-1779.

Griffin, E.; Qin, Z.; Michels, W.; Pyle, A. (1995) Group II intron ribozymes that cleave DNA and RNA linkages with similar efficiency, and lack contacts with substrate 2'-hydroxyl groups. *Chem. Biol. 2*, 761-770.

Gregory, S. T., Dahlberg, A. E. (1999) Mutations in the conserved P loop perturb the conformation of two structural elements in the peptidyl transferase center of 23S ribosomal RNA. *J. Mol. Biol. 285*, 1475-1483.

Guerrier-Takada, C., Gardiner, K., Marsh, T., pace, N., Altman, S. (1983) The RNA moiety of ribonucleases P is the catalytic subunit of the enzyme. *Cell 35*, 849-857.

Hager, A. J., Pollard, J. D. & Szostak, J. W. (1996). Ribozymes: aiming at RNA replication and protein synthesis. *Chem. & Biol. 3*, 717-725.

Hampel, A., Cowan, J. A. (1997) A unique mechanism for RNA catalysis: the role of metal cofactors in hairpin ribozyme cleavage. *Chem. Biol. 4*, 513-517.

Hampton, A.; Brox, L. W. and Bayer, M. (1969) Analogs of inosine 5'-phosphate with phosphorus-nitrogen and phosphorus-sulfur bond: Binding and kinetic studies with inosine 5'-phosphate dehydrogenase. *Biochemistry 8*, 2303-2311.

Hanna, R., Doudna, J. A. (2000) Metal ions in ribozyme folding and catalysis. Curr. Opin. *Chem. Biol. 4*, 166-170.

Harms, J., Schluenzen, F., Zarivach, R., Bashan, A., Gat, S., Agmon, I., Bartels, H., Granceschi, F., Yonath, A. (2001) High resolution structure of the large ribosomal subunit from a mesophilic eubacterium. *Cell 107*, 679-788.

Haugland, R. P. *Handbook of Fluorescent Probes and Research Chemicals*, 6th ed.; Molecular Probes, Inc., Eugene, OR, 1996; p48-59.

Hecht, S. M. (1977) Participation of isomeric tRNAs in the partial reactions of protein biosynthesis. *Tetrahedron 33*, 1671-1696.

Illangasekare, M., Sanchez, G., Nickles, T. & Yarus, M. (1995). Aminoacyl-RNA synthesis catalyzed by an RNA. *Science 267*, 643-647.

Illangasekare, M. & Yarus, M. (1999). Specific, rapid synthesis of Phe-RNA by RNA. *Proc Natl Acad Sci USA 96*, 5470-5475.

Illangasekare, M. & Yarus, M. (1999). A tiny RNA that catalyzes both aminoacyl-RNA and peptidyl-RNA synthesis. *RNA 5*, 1482-1489.

Ioannou, M., Coutsogeorgopoulos, C., Synetos, D. (1998) Kinetics of inhibition of rabbit reticulocyte peptidyltransferase by anisomycin and sparsomycin. *Mol. Pharmacology. 53*, 1089-1096.

Jaeger, L., Wright, M. C., Joyce, G. F. (1999) A complex ligase ribozyme evolved in vitro from a group I ribozyme domain. *Proc. Natl. Acad. Sci. USA. 96*, 14712-14717.

Jenne, A. & Famulok, M. (1998) A novel ribozyme with ester transferase activity. *Chemistry & Biology 5*, 23-34.

Johnston, W. K., Unrau, P. J., Lawrence, M. S., Glasner, M. E. & Bartel, D. P. (2001). RNA-catalyzed RNA polymerization: accurate and general RNA-templated primer extension. *Science 292*, 1319-1325.

Joseph, S. and Noller, H. (1996) Mapping the rRNA neighborhood of the acceptor end of tRNA in the ribosome. *EMBO J. 15*, 910-916.

Jou, R., Cowan, J. A. (1991) Ribonuclease H activation by inert transition-metal complexes. Mechanistic probes for metallocofactors: insights on the metallobiochemistry of divalent magnesium ion. *J. Am. Chem. Soc. 113*, 6685-6686.

Joyce, G. F. (1989) Amplification, mutation and selection of catalytic RNA. *Gene. 82*, 83-87.

Joyce, G. F. (2002) The antiquity of RNA-based evolution. *Nature 418*, 214-221.

Joyce, G. F. & Orgel, L. E. (1999). In *The RNA World*, (Gesteland, R. F., Cech, T. R. & Atkins, J. F. eds.), pp. 49-77, Cold Spring Harbor Laboratory Press, New York.

Khaitovich, P, Mankin, A. S., Green, R., Lancaster, L., Noller, H. F. (1999a) Characterization of functionally active subribosomal particles from Thermus aquaticus. *Proc. Natl. Acad. Sci. USA. 96*, 85-90.

Khaitovich, P., Tenson, T., Mankin, A. S., Green, R. (1999b) Peptidyl transferase activity catalyzed by protein-free 23S ribosomal RNA remains elusive. *RNA 5*, 605-608.

Kirillov, S. V., Porse, B. T., Garrett, R. A. (1999) Peptidyl transferase antibiotics perturb the relative positioning of the 3'-terminal adenosine of P/P'-site-bound tRNA and 23S rRNA in the ribosome. *RNA 5*, 1003-1013.

Kirillov, S. V., Porse, B. T., Vester, B., Woolley, P., Garrett, R. A. (1997) Movement of the 3'-end of tRNA through the peptidyl transferase centre and its inhibition by antibiotics. *FEBS Lett. 406*, 223-233.

Kleinkauf, H.; von Dohren, H. (1990). Nonribosomal biosynthesis of peptide antibiotics. Eur. *J. Biochem.192*, 1-15.

Kruger, K., Grabowski, P., Zaug, A., Sands, J., Gottschling, D., Cech, T. (1982) Self-splicing RNA: autoexcision and autocyclization of the ribosomal RNA intervening sequences of Tetrahymena. *Cell 31*, 147-157.

Kuijpers, W. H. A. and van Boeckel, C. A. A. (1993). A new strategy for the solid-phase synthesis of 5'-thiolated oligodeoxynucleotides. *Tetrahedron 49*, 10931-10944.

Kumar, R. K. & Yarus, M. (2001). RNA-catalyzed amino acid activation. *Biochemistry 40*, 6998-7004.

Lacey, J. C., Thomas, R. D., Staves, M. P., Watkins, C. L. (1991) Stereoselective formation of bis(α-aminoacyl) esters of 5'-AMP suggests a primitive peptide synthesizing system with a preference for L-amino acids. *Biochimica et Biophysicaa Acta. 1076*, 395-400.

Lacey, J. C., Jr., Hawkins, A. F., Thomas, R. D., Watkins, C. L. (1988) Differential distribution of D and L amino acids between the 2' and 3' positions of the AMP residue at the 3' terminus of transfer ribonucleic acid. *Proc. Natl. Acad. Sci. USA. 85*, 4996-5000.

Lacey, J. C., Jr., Thomas, R. D., Wicharamasinghe, N. S. M.D. & Watkins, C. L. (1990). Chemical Esterification of 5'-AMP occurs predominantly at the 2'-position. *J. Mol. Evol. 31*, 251-256.

Lee, N., Bessho, Y., Wei, K., Szostak, J. W. & Suga, H. (2000) Ribozyme-catalyzed tRNA aminoacylation. *Nature Structural Biology 7*, 28-33.

Lieberman, K. R., Dahlberg A. E. (1995) Ribosome-catalyzed peptide-bond formation. *Prog. Nucl. Acid. Res. Mol. Biol. 50*, 1-23.

Lohse, P. A. & Szostak, J. W. (1996) Ribozyme-catalyzed amino-acid transfer reactions. *Nature 381*, 442-444.

Lorsch, J. R. & Szostak, J. W. (1994) *In vitro* evolution of new ribozymes with polynucleotide kinase activity. *Nature 371*, 31-36.

Macosko, J. C.; Pio, M. S.; Tinoco, Jr., I. and Shin, Y. -K. (1999) A novel 5 displacement spin-labeling technique for electron paramagnetic resonance spectroscopy of RNA. *RNA 5*, 1158-1166.

Maden, B. E. H., Monro. R. E. (1968) Ribosome-catalyzed peptidyl transfer: effects of cations and pH value. *Euro. J. Biochem. 6*, 309-316.

Marahiel, M. A., Stachelhaus, T. & Mootz, H. D. (1997). Modular peptide synthetases involved in nonribosomal peptide synthesis. *Chem. Rev. 97*, 2651-2673.

McGinness, K. E., Joyce, G. F. (2002) RNA-catalyzed RNA ligation on an external RNA template. *Chem.. Biol. 9*, 297-307.

Milligan, J. F.; Uhlenbeck, O. C. (1989) Synthesis of small RNAs using T7 RNA polymerase. *Methods Enzymol. 180*, 51-62.

Misra, V. K., Draper, D. E. (1998) On the role of magnesium ions in RNA stability. *Biopolymers 48*, 113-135.

Miyamoto-Sato, E., Nemoto, N., Kobayashi, K., Yanagawa, H. (2000) Specific bonding of puromycin to full-length protein at the C-terminus. *Nucleic Acids Research 28*, 1176-1182.

Moazed, D., Noller, H. F. (1987) Chloramphenicol, erythromycin, carbomycin and vernamycin B protect overlapping sites in the peptidyl transferase region of 23S ribosomal RNA. *Biochimie 69*, 879-884.

Moazed, D., Noller, H. F. (1989a) Intermediate states in the movement of transfer RNA in the ribosome. *Nature 342*, 142-148.

Moazed, D., Noller, H. F. (1989b) Interaction of tRNA with 23S rRNA in the ribosomal A, P, and E sites. *Cell 57*, 585-597.

Monro, B. R. E., Cerna, J., Marcker, K. A. (1968) Ribosome-catalyzed peptidyl transfer: substrate specificity at the P-site. *Biochemistry 61*, 1042-1049.

Monro, R. E., Marcker, K. A. (1967) Ribosome-catalysed reaction of puromycin with a formylmethionine-containing oligonucleotide. *J. Mol. Biol. 25*, 347-350.

Murray, J. B., Seyhan, A. A., Walter, N. G., Burke, J. M., Scott, W. G. (1998) The hammerhead, hairpin and VS ribozymes are catalytically proficient in monovalent cations alone. *Chem. Biol. 5*, 587-595.

Musier-Forsyth, K. and Schimmel, P. (1994) Acceptor helix interactions in a class II tRNA synthetase: photoaffinity cross-linking of an RNA miniduplex substrate. *Biochemistry 35*, 1647-1650.

Muth, G. W., Chen, L., Kosek, A. B., Strobel, S. A. (2001) pH-dependent conformational flexibility with the ribosomal peptidyl transferase center. *RNA 7*, 1403-1415.

Muth, G. W., Donnelly-Ortoleva, L., Strobel, S. A. (2000) A single adenosine with a neutral pK_a in the ribosomal peptidyl transferase center. *Science 289*, 947-950.

Nakano, S., Bevilacqua, P. C. (2001) Proton inventory of the genomic HDV ribozyme in Mg^{2+}-containing solutions. *J. Am. Chem. Soc. 123*, 11333-11334.

Nakano, S., Chadalavada, D. M., Bevilacqua, P. C. (2000) General acid-base catalysis in the mechanism of a hepatitis delta virus ribozyme. *Science 287*, 1493-1497.

Nathans, D., Neidle, A. (1963) Structural requirements for puromycin inhibition of protein synthesis. *Nature 197*, 1076-1077.

Nissen, P., Hansen, J., Ban, N., Moore, P. B., Steitz, T. A. (2000) The structural basis of ribosome activity in peptide bond synthesis. *Science 289*, 920-930.

Nitta, I., Kamada, Y., Noda, H., Ueda, T., Watanabe, K. (1998) Reconstitution of peptide bond formation with Escherichia coli 23S ribosomal RNA domains. *Science 281*, 666-669.

Nitta, I., Ueda, T., Watanabe, K. (1999) Retraction. *RNA 5*, 707.

Noll, M., Hapke, B., Schreier, M. H., Noll, H. (1973) Structural dynamics of bacterial ribosomes. *J. Mol. Biol. 75*, 281-294.

Noller, H. F., Hoffarth, V., Zimniak, L. (1992) Unusual resistance of peptidyl transferase to protein extraction procedures. *Science 256*, 1416-1419.

Oehler, R., Polacek, N., Steiner, G., Barta, A. (1997) Interaction of tetracycline with RNA: photoincorporation into ribosomal RNA of Escherichia coli. *Nucleic Acids Research 25*, 1219-1224.

O'Rear, J. L., Wang, S., Feig, A. L., Beigelman, L., Uhlenbeck, O. C., Herschlag, D. (2001) Comparison of the hammerhead cleavage reactions stimulated by monovalent and divalent cations. *RNA 7*, 537-545.

Orgel, L. E. (1968) Evolution of the genetic apparatus. *J. Mol. Biol. 38*, 381-393.

Pestka, S. (1972) Peptidyl-puromycin synthesis on polyribosomes from Escherichia Coli. *Proc. Nat. Acad. Sci. USA. 69*, 624-628.

Polacek N., Gaynor M., Yassin A., and Mankin A. S. (2001) Ribosomal peptidyl transferase can withstand mutations at the putative catalytic nucleotide. *Nature 411*, 498-501.

Porse, B. T., Kirillov, S. V., Awayez, M. J., Ottenheijm, H. C. J., Garrett, A. R. (1999) Direct crosslinking of the antitumor antibiotic sparsomycin, and its derivatives, to A2602 in the peptidyl transferase center of 23S-like rRNA within ribosome-tRNA complexes. *Proc. Natl. Acad. Sci. USA. 96*, 9003-9008.

Porse, B. T., Rodriguez-Fonseca, C., Leviev, I., Garrett, R. A. (1995) Antibiotic inhibition of the movement of tRNA substrates through a peptidyl transferase cavity.*Biochem. Cell. Biol. 73*, 877-885.

Pregel, M. J., Dunn, E. J., Nagelkerke, r., Thatcher, G. R. J., Buncel, E. (1995) *Chem. Soc. Rev.* 449-455,

Pyle, A. M. (1993) Ribozymes: A distinct class of metalloenzymes. *Science 161*, 709-714.

Pyle, A. M. (1996) In *Metal ions in biological systems*, H. Sigel, ed. (Marce Dekker, New York), pp. 479-520.

Qin, P. Z. and Pyle, A. M. (1999) Site-specific labeling of RNA with fluorophores and other structural probes. *Methods: A Companion to Methods Enzymol. 18*, 60-70.

Quiggle, K., Chladek, S. (1980) The role of the cytidine residues of the tRNA 3'-terminus at the peptidyltransferase A- and P-sites. *FEBS Lett. 118*, 172-175.

Robertson, M. P. & Ellington, A. D. (1999) In vitro selection of an allosteric ribozyme that transduces analytes into amplicons. *Nature Biotechnol. 17*, 62-66.

Robertson, D. L. & Joyce, G. F. (1990) Selection *in vitro* of an RNA enzyme that specifically cleaves single-stranded DNA. *Nature 344*, 467-468.

Rodriguez-Fonseca, C., Amils, R., Garrett, R. A. (1995) Fine structure of the peptidyl transferase center on 23S-like rRNAs deduced from chemical probing of antibiotic-ribosome complex. *J. Mol. Biol. 247*, 224-235.

Rogers, J. & Joyce, G. F. (2001) The effect of cytidine on the structure and function of an RNA ligase ribozyme. *RNA 7*, 395-404.

Schimmel, P., Giege, R., Moras, D. & Yokoyama, S. (1993). An operational RNA code for amino acids and possible relationship to genetic code. *Proc. Natl. Acad. Sci. USA 90*, 8763-8768.

Schimmel, P. & Henderson, B. (1994). Possible role of aminoacyl-RNA complexes in noncoded peptide synthesis and origin of coded synthesis. *Proc. Natl. Acad. Sci. USA 91*, 11283-11286.

Schlunzen, F., Zarivach, R., Narms, J., Bashan, A., Tocilj, A., Albrecht, R., Yonath, A., Franceschi, F. (2001) Structural basis for the interaction of antibiotics with the peptidyl transferase center in eubacteria. *Nature*, *413*, 814-821.

Schmeing, T. M., Seila, A. C., Hansen, J. L., Freeborn, B., Soukup, J. K., Scaringe, S. A., Strobel, S. A., Moore, P. B., Steitz, T. A. (2002) A pre-translocational intermediate in protein synthesis observed in crystals of enzymatically active 50S subunits. *Nat. Struct. Biol. 9*, 225-230.

Seelig, B. & Jaschke, A. (1999) A small catalytic RNA motif with Diels-Alderase activity. *Chemistry & Biology 6*, 167-176.

Seelig, B. & Jaschke, A. (1999) Ternary conjugates of guanosine monophosphoate as initiator nucleotides for the enzymatic synthesis of 5'-modified RNAs. *Bioconjugate Chem. 10*, 371-378.

Sengle, G.; Jenne, A.; Arora, P. S.; Seelig, B.; Nowick, J. S.; Jaschke, A.; Famulok, M. (2000) Synthesis, incorporation efficiency, and stability of disulfide bridged functional groups at RNA 5'-Ends. *Bioorg. & Med. Chem. 8*, 1317-1329

Shan, S., Yoshida, A., Sun, S., Piccirilli, J. A., Herschlag, D. (1999) Three metal ions at the active site of the Tetrahymena group I ribozyme. *Proc. Natl. Acad. Sci. USA. 96*, 12299-12304.

Smith, J. D., Traut, R. R., Blackburn, G. M., Monro, R. E. (1965) Action of puromycin in polyadenylic acid-directed polylysine synthesis. *J. Mol. Biol. 13*, 617-628.

Sontheimer, E. J.; Steitz, J. A. (1993) The U5 and U6 small nuclear RNAs as active site components of the spliceosome. *Science 262*, 1989-1996.

Sontheimer, E. J.; Sun, S.; Piccirilli, J. A. (1997) Metal ion catalysis during splicing of premessenger RNA. *Nature 388*, 801-805.

Spahn, C. M. T., Prescott, C. D. (1996) Throwing a spanner in the works: antibiotics and the translation apparatus. *J. Mol. Med. 74*, 423-439.

Sprinzl, M. & Cramer, F. (1979) The -C-C-A end of tRNA and its role in protein biosynthesisProg. *Nucleic Acid Res. Mol. Biol. 22*, 1-69.

Stachelhaus, T., Mootz, H. D., Bergendahl, V., Marahiel, M. A. (1998) Peptide bond formation in nonribosomal peptide biosynthesis. *J. Biol. Chem. 273*, 22773-22781.

Starck, S. R., Roberts, R. W. (2002) Puromycin oligonucleotides reveal steric restrictions for ribosome entry and multiple modes of translation inhibition. *RNA 8*, 890-903.

Steiner, G., Kuechler, E., Barta. A. (1988) Photo-affinity labeling at the peptidyl transferase center reveals two different positions for the A- and P-sites in domain V of 23S rRNA. *EMBO. J. 7*, 3949-3955.

Stemmer, W. P. C. (1994) DNA shuffling by random fragmentation and reassembly: In vitro recombination for molecular evolution. *Proc. Natl. Acad. Sci. USA. 91*, 10747-10751.

Strobel, S. A. (1998) Ribozyme chemogenetics. *Biopolymers 48*, 65-81.

Stobel, S. A., Ortoleva-Donnelly, L. (1999) A hydrogen-bonding triad stabilizes the chemical transition state of a group I ribozyme. *Chem. Biol. 6*, 153-165.

Strobel, S. A.; Shetty, K. (1997) Defining the chemical groups essential for Tetrahymena group I intron function by nucleotide analog interference mapping. *Proc. Natl. Acad. Sci. USA 94*, 2903-2908.

Suga, H., Cowan, J. A., Szostak, J. W. (1998) Unusual metal ion catalysis in an acyl-transferase ribozyme. *Biochemistry 37*, 10118-10125.

Sun, L., Cui, Z., Gottlieb, R. L., & Zhang, B. (2002). A selected ribozyme catalyzing diverse dipeptide synthesis. *Chemistry & Biology 9*, 619-628.

Sun, L., Li, C., Cui, Z., & Zhang, B. Ribozyme catalysis of peptide bond formation: pH and metal ion dependence. In preparation.

Sun, S.; Tang, X.-Q.; Merchant, A.; Anjaneyulu, P. S. R.; Piccirilli, J. A. (1996) Efficient Synthesis of 5'-(Thioalkyl)uridines *via* Ring Opening of-Ureidomethylene Thiolactones. *J. Org. Chem. 61*, 5708-5709.

Taiji, M., Yokoyama, S., Miyazawa, T. (1985) Slow transacylation of peptidyladenosine allows analysis of the 2'/3'-isomer specificity of peptidyltransferase. *Biochemistry 24*, 5776-5780.

Takagi, Y., Warashina, M., Stec, W. J., Yoshinari, K., Taira, K. (2001) Recent advances in the elucidation of the mechanisms of action of ribozymes. *Nucleic Acids Research 29*, 1815-1834.

Tan, G. T., DeBlasio, A., Mankin, A. S. (1996) Mutations in the peptidyl transferase center of 23S rRNA reveal the site of action of sparsomycin, a universal inhibitor of translation. *J. Mol. Biol. 261*, 222-230.

Tarasow, T. M., Tarasow, S. L. & Eaton, B. E. (1997) RNA-catalyzed carbon-carbon bond formation. *Nature 389*, 54-57.

Thompson, J., Kim, D. F., O'Connor, M., Lieberman, K. R., Bayfield, M. A., Gregory, s. T., Green, R., Noller, N. F., Dahlberg, A. E. (2001) Analysis of mutations at residues A2451 and G2447 of 23S rRNA in the peptidyltransferase active site of the 50S ribosomal subunit. *Proc. Nat. Acad. Sci. USA. 98*, 9002-9007.

Thomson, J. B.; Tuschl, T.; Eckstein, F. *Catalytic RNA*; Eckstein, F., Lilley, D. M. J., Eds.; Springer-Verlag: Berlin, 1996; Vol. *10*, pp 173-196.

Tipton, K. F., Dixon, H. B. F. (1976) Effects of pH on enzymes. *Meth. Enzymol. 63*, 183-234.

Traut, R. R., Monro, R. E. (1964) *J. Mol. Biol. 10*, 63-72.

Triman, K. L. (1999) Mutational analysis of 23S ribosomal RNA structure and function in Escherichia Coli. *Adv. Gene. 41*, 157-195.

Tritton, T. R. (1977) Ribosome-tetracycline interactions. *Biochemistry 16*, 4133-4138.

Tsang, J. & Joyce, G. F. (1994) Evolution optimization of the catalytic properties of a DNA-cleaving ribozyme. *Biochemistry 33*, 5966-5973.

Tuerk, C. & Gold, L. (1990) Systematic evolution of ligands by exponential enrichment: RNA ligands to bacteriophage T4 DNA polymerase. *Science 249*, 505-510.

Uhlmann, E.; Peyman, A. (1990) Antisense oligonucleotides: a new therapeutic principle. *Chem. Rev.*, *90*, 543-584.

Unrau, P. J. & Bartel, D. P. (1998) RNA-catalysed nucleotide synthesis. *Nature 395*, 260-263.

Valadkhan, S. Manley, J. L. (2001) Splicing-related catalysis by protein-free snRNAs. *Nature 685*, 701-707.

Vazquez, D. (1979) *Inhibitors of protein biosynthesis*. Springer-Verlag, Berlin, Heidelberg, New York.

Von. Dohren, H., Keller, U., Vater, J. & Zocher, R. (1997). Multifunctional peptide synthetases *Chem. Rev. 97*, 2675-2705.

Wagner, T., Cramer, F. & Sprinzl, M. (1982) Activity of the 2' and 3' isomers of aminoacyl transfer ribonucleic acid in the in vitro peptide elongation on Escherichia coli ribosomes. *Biochemistry 21*, 1521-1529.

Waldrop, M. M. (1992) Finding RNA makes proteins gives 'RNA World" a big boost. *Science 256*, 1396-1394.

Weber, A. L. & Orgel, L. E. (1980) Poly(U)-directed peptide bond formation from the 2'(3')-glycyl esters of adenosine derivatives. *J. Mol. Evol. 16*, 1-10.

Wecker, M., Smith, D. & Gold, L. (1996) *In vitro* selection of a novel catalytic RNA: characterization of a sulfur alkylation reaction and interaction with a small peptide. *RNA 2*, 982-994.

Weinstein, L. B., Jones, B. C., Cosstick, R., Cech, T. R. (1997) A second catalytic metal ion in group I ribozyme. *Nature 388*, 805-808.

Wickramasinghe, N. S. M. D. & Lacey, J. C., Jr. (1992). Mixed anhydrides are also formed in the esterification of 5'-AMP with N-acetylaminoacyl imidazolides: implications regarding the origin of protein synthesis. *Orig. Life Evol. Biosph. 22*, 361-368.

Wiegand, T. W., Jassen, R. C. & Eaton, B. E. (1997). Selection of RNA amide synthases. *Chem. & Biol 4*, 675-683.

Wilson, C. & Szostak, J. W. (1995) *In vitro* evolution of a self-alkylating ribozyme. *Nature 374*, 777-782.

Woese, C. R. (1967). In *The Genetic Code: The molecular basis for genetic expression*, pp. 179-195, Harper & Row, New York.

Wower, J., Rosen, K. V., Hixson, S. S., Zimmermann, R. A. (1994) Recombinant photoreactive tRNA molecules as probes for cross-linking studies. *Biochimie 76*, 1235-1246.

Wower, J., Wower, I. K., Kirillov, S. V., Rosen, K. V., Hixson, S. S., Zimmermann, R. A. (1995) Peptidyl transferase and beyond. *Biochem. Cell. Biol. 73*, 1041-1047.

Xiong, L., Polacek, N., Sander, P., Bottger, E. C., Mankin, A. (2001) pK_a of adenine 2451 in the ribosomal peptidyl transferase center remains elusive. *RNA 7*, 1365-1369.

Yamane, T., Hopfield, J. (1977) Experimental evidence for kinetic proofreading in the aminoacylation of tRNA by synthetase. *Proc. Natl. Acad. Sci. USA. 74*, 2246-2250.

Yamane, T., Miller, D. L., Hopfield, J. J. (1981) Discrimination between D- and L-Tyrosyl transfer ribonucleic acid in peptide chain elongation. *Biochemistry 20*, 7059-7064.

Yarus, M. (1999). Boundaries for an RNA world. *Curr. Opin. Chem. Biol. 3*, 260-267.

Young, K. J., Gill, F., Grasby, J. A. (1997) Metal ions play a passive role in the hairpin ribozyme catalysed reaction. *Nucleic Acids Research 25*, 3760-3766.

Yusupov, M. M., Yusupova, G. Zh., Baucom, A., Lieberman, K., Earnest, T. N., Cate, H. D., Noller, H. F. (2001) Crystal structure of the ribosome at 5.5 A resolution. *Sciencexpress*, March 29.

Zamir, A., Leder, P., Elson, D. (1996) *Proc. Natl. Acad. Sci. USA. 56*, 1794-1801.

Zhang, B. & Cech, T. R. (1997). Peptide bond formation by in vitro selected ribozymes. *Nature 390*, 96-100.

Zhang, B. & Cech, T. R. (1998). Peptidyl-transferase ribozymes: trans reactions, structural characterization and ribosomal RNA-like features. *Chemistry & Biology 5*, 539-553.

Zhang, B., Cui, Z., Sun, L. (2001) Synthesis of 5'-deoxy-5'-thioguanosine-5'-monophosphorothioate and its incorporation into RNA 5'-termini. *Organic letters 3 (2)*, 275-278.

Zhang, B., Zhang, L., Sun, L., Cui, Z. (2002) Synthesis of pCpCpA-3'-NH-phynylalanine as a ribosomal substrate. *Organic Letters 4 (21)*, 3615-3618.

Zhang, L., Sun, L., Cui, Z., Gottlieb, R. L., & Zhang, B. (2001). 5'-Sulfhydryl-modified RNA: initiator synthesis, in vitro transcription, and enzymatic incorporation. *Bioconjugate Chem 12*, 939-948.

Zuker, M., Mathews, D.H. & Turner, D.H. (1999). *A Practical Guide In RNA Biochemistry and Biotechnology*, (Barciszewski J., Clark, B.F.C., eds.), pp. 11-43, NATO ASI Series, Kluwer Academic Publishers.